Prague Medical REPORT

(Sborník lékařský)

Multidisciplinary Biomedical Journal
of the First Faculty of Medicine,
Charles University

Vol. 123 (2022) No. 3

Reviews

Factors Affecting Drug Exposure after Inhalation / *Nováková A., Šíma M., Slanař O.* page 129

Clinical Outcomes of Routine Awake Prone Positioning in COVID-19 Patients: A Systematic Review and Meta-analysis of Randomized Controlled Trials / *Chong W. H., Saha B. K., Tan C. K.* page 140

Primary Scientific Studies

Disturbance in Serum Levels of IL-17 and TGF-β1 and in Gene Expression of ROR-γt and FOX-P3 Is Associated with Pathogenicity of Systematic Lupus Erythematosus / *Ali H. N., Alubaidi G. T., Gorial F. I., Jasim I. A.* page 166

Impact of Hemorrhagic Stroke on Molar Bite Force: A Prospective Study / *da Silva G. P., Verri E. D., Palinkas M., Gonçalves C. R., Gonçalves P. N., Lopes R. F. T., Gomes G. G. C., Regalo I. H., Siéssere S., Regalo S. C. H.* page 181

A New Mystery: Phantosmia after COVID-19 Infection / *Erdogan B. A., Eldahshan A.* page 188

Case Reports

Rare Location of a Dermoid Cyst in the Parotid Gland: A Case Report / *Vavro M., Horák S., Dvoranová B., Čierna Z., Babál P., Kobzová D., Hirjak D., Czakó L.* page 193

Primary Epithelioid Angiomyolipoma of Adrenal Gland: Case Report and Literature Review / *Cicek M., Kazan H. O., Atis R. G., Yildirim A.* page 199

Instructions to Authors page 206

D
C
E
Fig. 7.
B
C
A
Fig. 6.
B
A
Fig. 8.
C
B
A
Fig. 2.
B
D
A
E
D
E
Fig. 9.
A

Prague Medical Report (Prague Med Rep) is indexed and abstracted by Index-medicus, MEDLINE, PubMed, EuroPub, CNKI, DOAJ, EBSCO, and Scopus.

Abstracts and full-texts of published papers can be retrieved from the World Wide Web (https://pmr.lf1.cuni.cz).

Engraving overleaf: Laurentius Heister, Institutiones chirurgicae, Amsterdam 1750.
Illustration provided by the Institute for History of Medicine and Foreign Languages.

Factors Affecting Drug Exposure after Inhalation

Anežka Nováková, Martin Šíma, Ondřej Slanař
Institute of Pharmacology, First Faculty of Medicine, Charles University and General University Hospital in Prague, Prague, Czech Republic

Received May 23, 2022; Accepted August 2, 2022.

Key words: Pharmacokinetics – Physicochemical properties – Pulmonary metabolism – Pulmonary clearance – Drug delivery – Respiratory system

Abstract: Administration of drugs by inhalation is mainly used to treat lung diseases and is being investigated as a possible route for systemic drug delivery. It offers several benefits, but it is also fraught with many difficulties. The lung is a complex organ with complicated physiology and specific pharmacokinetic processes. Therefore, the exposure and subsequently efficacy of a drug after inhalation is affected by a number of factors. In this review, we summarize the main variables that may affect drug fate after inhalation delivery, such as physicochemical properties of the drug, pulmonary clearance and metabolism, pathophysiological factors and inhalation device. Factors that have impact on pharmacokinetic processes need to be considered during development as their correct setting can lead to new effective inhaled drugs.

This study was supported by the Charles University Cooperatio Program (research area PHAR) and grant No. SVV 260 523. A. N. wishes to acknowledge the support provided by Pharmaceutical Applied Research Centre (The PARC) for her scientific work.

Mailing Address: Mgr. Anežka Nováková, Institute of Pharmacology, First Faculty of Medicine, Charles University and General University Hospital in Prague, Albertov 4, 128 00 Prague 2, Czech Republic; Phone: +420 224 968 163; e-mail: anezka.novakova@lf1.cuni.cz

https://doi.org/10.14712/23362936.2022.13
© 2022 The Authors. This is an open-access article distributed under the terms of the Creative Commons Attribution License (http://creativecommons.org/licenses/by/4.0).

Introduction

Inhalation route is a way how to deliver a drug for various pulmonary diseases directly to the main place of its effect in the lungs. It has a long tradition, especially for local delivery, but in the meantime it has been also extended for systemic drug delivery. The first and still the most common use of inhaled drugs is the treatment of asthma and chronic obstructive pulmonary disease with beta-sympathomimetics, anticholinergics and corticosteroids. The inhalation delivery may be advantageous for macromolecule drugs that would otherwise have to be injected because the lungs are naturally permeable not only for small molecules but also for peptides and proteins. Inhalation has been tested for systemic exposure of insulin since many years. It has even reached the market in the US and provides patients an option for a needle-free treatment. However, many more drugs such as vaccines, chemotherapy or gene therapy have been tested (Chow et al., 2007).

Inhalation is preferred route of drug administration for local treatment of pulmonary diseases. The drug is delivered directly to the site of action. High drug concentration in the lung is also ensured by avoiding first-pass metabolism of the liver and low enzymatic activity in the lungs. This allows the use of lower dose of the drug and reduces its systemic adverse effects (Rau, 2005; Eedara et al., 2021). Inhalation is well tolerated and usually easy to administer.

One of possible advantages of inhalation delivery is rapid onset of action. Therefore, it is used to treat an acute exacerbation and may also be beneficial for systemic treatment due to highly permeable and perfused epithelium (Hou et al., 2015). This could represent a clear benefit for the treatment of pain (Macleod et al., 2012; Mercadante et al., 2019), migraine (Aurora et al., 2011), nausea and vomiting (Merritt et al., 2002) or epileptic seizures (French et al., 2017).

Like other routes of administration, inhalation has its own limits. One of them is the characteristics of the drug and drug formulation (Borghardt et al., 2018). Aerodynamic particle size has a major effect on deposition and subsequent absorption in the respiratory tract (Heyder, 2004). Other key factors that affect pulmonary administration are lung condition and inhalation device (Borghardt et al., 2018). In patients with lung disease, deposition is thought to be worse due to pathophysiological modification. This may affect the expected kinetic processes. Change in ventilation parameters and breathing patterns may cause incorrect inhalation from an inhaler (Wang et al., 2014). The limit may also be the patient handling the inhalation device.

Due to complexity of pulmonary administration, there are many factors that affect the efficacy of inhaled drugs. Their overview is limited, although administration by inhalation is relatively often studied. Therefore, this review focuses on the main influencing factors such as drug properties (physical and physicochemical properties), pulmonary characteristics (clearance, metabolism and pathophysiology) and inhalation device.

Literature search

The search was done till February 2022 in PubMed and Web of Science databases. The key words used for the searches were pulmonary delivery, pharmacokinetics, drug formulation, inhalation, absorption, mucociliary clearance and lung diseases in various combinations. The publications found were then evaluated in terms of relevance to the purpose of this review.

Pharmacokinetic processes after inhalation

Deposition

Drug formulations are deposited in different parts of the lungs depending on their particle size. The particles larger than 5 μm are deposited in the mouth, throat and upper airways. They are swallowed and subsequently absorbed in the gastrointestinal tract instead of reaching the lungs. The best particle size for achieving the lower airways is 1–5 μm for adults (Prime et al., 1997; Hassan and Lau, 2010). For children, it is assumed that the particle size should be different. It is not generally known how large it should be (Laube et al., 2011; Deng et al., 2018). The particles smaller than 0.5 μm may not deposit at all (Pilcer and Amighi, 2010) as they may be breathed out of the body. After deposition, the particles are cleared from lungs, absorbed or degraded.

Clearance

Multiple processes take place in the lungs due to their complex structure. There are diverse clearance mechanisms in different parts of the lungs such as mucociliary, macrophage and metabolic clearance. Mucocilliary clearance is the key factor for drug particles elimination from the upper airways while macrophages degrade the most of drug in the lower airways (Borghardt et al., 2015). These are physiological mechanisms that remove deposits of various mostly insoluble particles. Clearance processes nevertheless eliminate dissolved drug as well.

Mucociliary clearance is the first line defense mechanism of the mucous layer, the airways and the cilia (Munkholm and Mortensen, 2014). Insoluble particles are trapped and transferred to the mouth by the cilia waving cells, and then are swallowed into the gastrointestinal tract. This mechanism is more common and faster for larger particles, in general they are completely removed within 24 h (Edwards et al., 1997).

Macrophages play an important role in the immune response. They removed insoluble or slowly dissolving particles from the alveolar region and transported them to the cilia mucus. The ability of macrophage phagocytosis is dependent of aerodynamic particle size (optimally 1–3 μm) (Edwards et al., 1997) and surface charge. Macrophages have negatively charged surface, so the particles with a charged surface are thought to be more susceptible to phagocytosis. Soluble and hydrophilic particles have the ability to avoid macrophages (Patel et al., 2015; Liu et al., 2020). Perhaps because they dissolve faster than they are captured by macrophages. The

particles that macrophages do not recognize can deposit in the alveoli for years (Edwards et al., 1997). However, macrophages may be the delivery target of some inhaled drugs. For example, for the treatment of infectious diseases (Rojanarat et al., 2012; Zhang et al., 2018).

Absorption

The absorption rate depends on the dissolution rate (Borghardt et al., 2015) and on the hydrophilicity of the drug (Dugas et al., 2013). Drug absorption is more rapid from the alveolar space than from the tracheo-bronchial region due to higher perfusion and thinner airway wall (Brown and Schanker, 1983; Mobley and Hochhaus, 2001; Chillistone and Hardman, 2017). Absorption half-life of small lipophilic molecules from the alveoli is about 1 to 2 minutes, and they are absorbed by passive diffusion through epithelial cell membrane. Small hydrophilic molecules have absorption half-life approximately 65 minutes, and they are most likely to be transported via tight junctions or specific transporters (Patton et al., 2004, 2010; Bacle et al., 2021). The macromolecules are usually absorbed via tight junctions and transcytosis. Transport by endocytic vesicles is promoted by cationic charge of the compounds. In general, the absorption time of the drug is dependent on the molecular weight. Small peptides and proteins are usually absorbed faster compared to subcutaneous administration and with increasing size the absorption gets slower (Patton et al., 2004, 2010; Bacle et al., 2021).

Metabolism

Metabolic processes take place in the lung as in other tissues in the organism. Drug metabolism enzymes are the same as in the intestine or the liver but their expression is generally less in the lungs. Therefore, considerably lower doses may be administered compared to the oral route to achieve similar systemic exposure (Taylor, 1990; Upton and Doolette, 1999).

The most relevant metabolizing enzymes in the lungs are CYP1A1, CYP1B1, CYP2E1 and CYP2B6 (Borghardt et al., 2018; Pasqua et al., 2022). CYP1A1 and 1B1 are mostly elevated in smokers (Kim et al., 2004). Their substrates are e.g. theophylline or zolmitriptan that have been studied for inhaled delivery. CYP2E1 metabolizes anesthetics such as isoflurane, enflurane and halothane, one of the most common used for the administration of inhaled drugs (Guengerich, 2020). Lungs further contain several other drug metabolizing enzymes as aldehyde oxidases, glucuronosyltransferases, hydrolases, esterases, and peptidases (Pasqua et al., 2022). Carboxylesterases have been shown to rapidly hydrolyse mycophenolate mofetil to the active molecule after pulmonary administration (Dugas et al., 2013). Small natural peptides (< 3,000 D) can be very strongly enzymatically hydrolyzed by peptidase. Therapeutic peptides should be chemical modified to be resistant to peptidases (Patton et al., 2004). As the expression of drug metabolizing enzymes is relatively low, drug metabolism is expected to be minor after inhalation.

Although the impact of active drug transporters on drug distribution after pulmonary delivery could be envisaged (Endter et al., 2007; Patton et al., 2010), the real impact seems to be limited as several studies demonstrated high bioavailability of substrates of MDR1 from rat and mice lungs (Tronde et al., 2003a; Manford et al., 2008). It suggests a minor role of P-glycoprotein in absorption from the lungs.

Physicochemical properties

The Lipinski's Rule of Five is a widely accepted method to predict ADME (absorption, distribution, metabolism, and excretion) properties of oral drug candidates. There are only a few studies that compared bioavailability of inhaled drugs on the market with the Lipinski's rule. Inhaled drugs on the market correlate with the Rule probably as they were first administered orally (Choy and Prausnitz, 2011). However, optimal physicochemical property for delivery of inhaled compounds have not been defined, yet (Ritchie et al., 2009; Strong et al., 2018).

The physicochemical properties of the drug do not appear to be as a significant factor for lung delivery as after oral administration. Systemic absorption has been described for drugs that did not comply with the Lipinski's Rule and cannot be delivered by conventional route (Uchenna Agu et al., 2001; Ritchie et al., 2009; Siekmeier and Scheuch, 2009). This group includes macromolecules or proteins such as insulin, as well as heparin or interleukin-2 (Siekmeier and Scheuch, 2009; Shute et al., 2018; Dixon et al., 2021).

Pulmonary epithelium is permeable to molecules with high molecular polar surface area unlike the intestinal epithelium and blood-brain barrier (Tronde et al., 2003b). The degree of ionization can affect absorption and transport to the systemic circulation. It is assumed that charged molecules may interact with protein and lipid structures at the delivery site and this may slow down or diminish the rate of absorption. Mucins that are negatively charged can capture the drugs with a positive charge, while negatively charged particles easily penetrate (Sigurdsson et al., 2013; Bacle et al., 2021). The ability to penetrate also depends on the lipophilicity of the particle. Hydrophilic particles diffuse faster through lipophilic mucus compared to hydrophobic molecules. Lipophilicity is even thought to have a greater influence on mucus diffusion compared to charge (Leal et al., 2017; Liu et al., 2020). The mucus layer can form certain specific binding interaction with the trapped particles due to cationic or other selectivity of epithelial channels and thus form a barrier to the passage of the particles (Sigurdsson et al., 2013; Tamai, 2013).

The dissolution rate has main impact on the effectiveness of pulmonary clearance. Inhaled drugs should avoid these clearance mechanisms to ensure their effect (Edwards et al., 1997). Drugs are therefore formulated as liquid or aerosol particles that dissolve much faster than they are mechanically removed by mucus or recognized by macrophages. Thus, these mechanisms appear to be negligible for inhaled drugs (Patton and Byron, 2007; Borghardt et al., 2018).

Inhalation devices and drug formulation

Inhalation devices, excipients, a drug composition and handling with the device by patient may affect the efficiency of the drug. The most often used devices for inhalation delivery are dry powder inhalation system (DPI), metered-dose inhalation system (MDI) and nebulizer systems.

The deposition of the particles is influenced mainly by the physical properties of the aerosol (size, density, shape, hygroscopicity) and by respiratory physiology such as anatomy and breathing pattern (Yeh et al., 1976; Prime et al., 1997; Braakhuis et al., 2014). Humidity of the environment or even due to exhalation into the device may disrupt the formulation of the hygroscopic drugs and can reduce their efficiency. Hygroscopic aerosol is absorbing the water after inhalation which can cause a particle size growing and different deposition patterns (Ferron et al., 1989).

Each inhaler device class has specific drug load capacity, advantages and disadvantages that can affect administration of the drug or compliance with the therapy. An issue of DPI device is inhalation flow. Each DPI has its own minimum and optimal inhalation flow, most often around 30–60 l/min. Thus, the powder disperses into fine particles suitable for inhalation (Hassan and Lau, 2010). The disadvantage of nebulizers is a long time of inhalation connected with a cleaning time after inhalation and low proportion of drug delivery (Pilcer and Amighi, 2010). MDI devices have the most difficult handling technique. The coordination between breath (deep and hard) and manual coordination may be for many patients challenging. Moreover, even within each class of inhalation devices the individual device properties are unique, subsequently the performance in drug delivery differs and therefore different inhalers are not automatically interchangeable (Edsbäcker et al., 2008; Cazzola et al., 2016). However, detailed review of inhalation device characteristics and performance have not been included in this review.

Lung diseases

Lung diseases may have an impact on the fate of inhaled drugs for each process (deposition, absorption and clearance) through a number of interacting mechanisms. Obstructive lung disease (e.g. COPD [chronic obstructive pulmonary disease], asthma, cystic fibrosis) affects the airways. Restrictive lung disease (e.g. pulmonary edema, lung cancers, pulmonary embolus) causes the restriction in lung expansion, which may be caused by involvement the alveoli, blood vessels and/or interstitium. However, lung diseases can affect several different parts at the same time.

Lung diseases usually alters the deposition and subsequently absorption of inhaled particles. Obstructive lung diseases increase the deposition of particles on diseased lung lesions due to changes in airway diameter and ventilation conditions (Darquenne, 2012). Systemic absorption is reduced due to less deposition in the alveoli. Overall, this may be beneficial for local treatment (Borghardt et al., 2016), however disadvantageous for systemic drug delivery. Pulmonary vascular disease (emphysema, pulmonary fibrosis, pulmonary embolus) decreases systemic drug

absorption due to dysfunction of air-blood transfer. Loss or damage of functional surface area and blood vessel damage lead to impaired lung perfusion and thus reduced drug absorption. However, chronic airway inflammation and pulmonary edema may increase systemic absorption due to loss of integrity and increased permeability of barriers, which facilitates drug penetration (Patton et al., 2010; Wang et al., 2014).

The mechanism of clearance may also be affected by lung disease. Phagocytosis of alveolar macrophage is decreased in patients with COPD and cystic fibrosis, probably due to inflammatory agents. Mucociliary clearance is impaired in almost all pulmonary disease due to mucus changes (Houtmeyers et al., 1999; Munkholm and Mortensen, 2014), the effect of inflammation mediators and cilia changes. Changes in clearance mechanisms may not have a major impact on the drug efficacy, their dysfunction consequently can alter the deposition patterns of the drug (Apiou-Sbirlea et al., 2010) and even impede the drug from reaching its target.

Interspecies comparison

Since various animal models are used to study the development of inhaled medicinal products, anatomical and physiological differences should be considered. Overall, they can affect all pharmacokinetics processes. Data from the U.S. Food and Drug

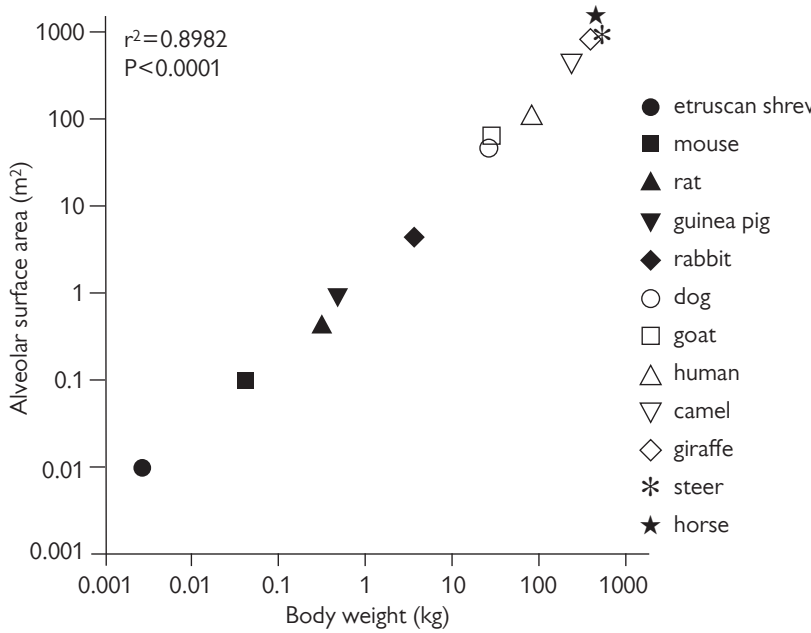

Figure 1 – Allometric plots for alveolar surface area with body weight. On log/log scale, the size of alveolar surface area within a species increases in proportion to body weight. Data obtained from Wirkes et al. (2010).

Administration (2005) are used to convert doses between species. They are based on dose normalization to body surface area, which correlates with biological parameters such as basal metabolism, and thus cover especially elimination phase of pharmacokinetic processes. This is accurate for conversion after administration by the conventional routes (e.g. intraperitoneal), however, more specific routes of administration such as inhalation may be affected by much more factors (e.g. breath rate, alveolar surface area). No dose conversion after inhalation between human and other species has been suggested yet. We compared alveolar surface area and body weight of different mammals (Wirkes et al., 2010) to find a correlation between them that could predict drug absorption. Figure 1 shows on a logarithmic scale allometric relationship of the alveolar surface area within a species to body weight. Based on this observation, we suggest that usually used body weight-normalized dose conversion between species sufficient and no other adjustments are required. However, dose estimation requires careful consideration of all available information and there is currently no uniform and universal approach. Inhalation in particular is complex (different morphological structures, breathing patterns, etc.) and needs to be further investigated.

Conclusion

Inhalation is route of choice for administration of drugs in the treatment of lung diseases such as asthma and chronic obstructive pulmonary disease. Determining the physicochemical and physical properties of the drug, drug formulation and inhalation device can help to optimize the kinetic processes of the drug. The pulmonary kinetic and absorption processes are highly complex. Lung diseases may change the structure of the lungs, their clearance mechanism, perfusion and affect breathing patterns. We observed strong correlation between alveolar surface area and body weight. Based on this observation, traditionally used allometric scaling for conversion of doses between animals and humans can be used without needs of further adjustments.

References

Apiou-Sbirlea, G., Katz, I. M., Martonen, T. B. (2010) The effect of simulated airway diseases and affected flow distributions on aerosol deposition. *Respir. Care* **55**, 707–718.

Aurora, S. K., Silberstein, S. D., Kori, S. H., Tepper, S. J., Borland, S. W., Wang, M., Dodick, D. W. (2011) MAP0004, orally inhaled DHE: A randomized, controlled study in the acute treatment of migraine. *Headache* **51**, 507–517.

Bacle, A., Bouzillé, G., Bruyère, A., Cuggia, M., Fardel, O., Le Corre, P. (2021) Drivers of absolute systemic bioavailability after oral pulmonary inhalation in humans. *Eur. J. Pharm. Biopharm*. **164**, 36–53.

Borghardt, J. M., Weber, B., Staab, A., Kloft, C. (2015) Pharmacometric models for characterizing the pharmacokinetics of orally inhaled drugs. *AAPS J*. **17**, 853–870.

Borghardt, J. M., Weber, B., Staab, A., Kunz, C., Kloft, C. (2016) Model-based evaluation of pulmonary pharmacokinetics in asthmatic and COPD patients after oral olodaterol inhalation. *Br. J. Clin. Pharmacol*. **82**, 739–753.

Borghardt, J. M., Kloft, C., Sharma, A. (2018) Inhaled therapy in respiratory disease: The complex interplay of pulmonary kinetic processes. *Can. Respir. J.* **2018**, e2732017.

Braakhuis, H. M., Park, M. V., Gosens, I., De Jong, W. H., Cassee, F. R. (2014) Physicochemical characteristics of nanomaterials that affect pulmonary inflammation. *Part. Fibre Toxicol*. **11**, 18.

Brown, R. A., Schanker, L. S. (1983) Absorption of aerosolized drugs from the rat lung. *Drug Metab. Dispos*. **11**, 355–360.

Cazzola, M., Ora, J., Di Paolo, A., Puxeddu, E., Calzetta, L., Rogliani, P. (2016) Onset of action of budesonide/formoterol Spiromax® compared with budesonide/formoterol Turbuhaler® in patients with COPD. *Pulm. Pharmacol. Ther*. **39**, 48–53.

Chillistone, S., Hardman, J. G. (2017) Factors affecting drug absorption and distribution. *Anaesthesia and Intensive Care Medicine* **18**, 335–339.

Chow, A. H. L., Tong, H. H. Y., Chattopadhyay, P., Shekunov, B. Y. (2007) Particle engineering for pulmonary drug delivery. *Pharm. Res*. **24**, 411–437.

Choy, Y. B., Prausnitz, M. R. (2011) The Rule of Five for non-oral routes of drug delivery: Ophthalmic, inhalation and transdermal. *Pharm. Res*. **28**, 943–948.

Darquenne, C. (2012) Aerosol deposition in health and disease. *J. Aerosol Med. Pulm. Drug Deliv*. **25**, 140–147.

Deng, Q., Ou, C., Chen, J., Xiang, Y. (2018) Particle deposition in tracheobronchial airways of an infant, child and adult. *Sci. Total Environ*. **612**, 339–346.

Dixon, B., Smith, R. J., Campbell, D. J., Moran, J. L., Doig, G. S., Rechnitzer, T., MacIsaac, C. M., Simpson, N., van Haren, F. M. P., Ghosh, A. N., Gupta, S., Broadfield, E. J. C., Crozier, T. M. E., French, C., Santamaria, J. D. (2021) Nebulised heparin for patients with or at risk of acute respiratory distress syndrome: A multicentre, randomised, double-blind, placebo-controlled phase 3 trial. *Lancet Respir. Med*. **9**, 360–372.

Dugas, H. L., Peters, J. I., Williams, R. O. (2013) Nebulization of mycophenolate mofetil inhalation suspension in rats: Comparison with oral and pulmonary administration of Cellcept®. *Int. J. Pharm*. **441**, 19–29.

Edsbäcker, S., Wollmer, P., Selroos, O., Borgström, L., Olsson, B., Ingelf, J. (2008) Do airway clearance mechanisms influence the local and systemic effects of inhaled corticosteroids? *Pulm. Pharmacol. Ther*. **21**, 247–258.

Edwards, D. A., Hanes, J., Caponetti, G., Hrkach, J., Ben-Jebria, A., Eskew, M. L., Mintzes, J., Deaver, D., Lotan, N., Langer, R. (1997) Large porous particles for pulmonary drug delivery. *Science* **276**, 1868–1872.

Eedara, B. B., Alabsi, W., Encinas-Basurto, D., Polt, R., Ledford, J. G., Mansour, H. M. (2021) Inhalation delivery for the treatment and prevention of COVID-19 infection. *Pharmaceutics* **13**, 1077.

Endter, S., Becker, U., Daum, N., Huwer, H., Lehr, C.-M., Gumbleton, M., Ehrhardt, C. (2007) P-glycoprotein (MDR1) functional activity in human alveolar epithelial cell monolayers. *Cell Tissue Res*. **328**, 77–84.

Ferron, G. A., Oberdörster, G., Henneberg, R. (1989) Estimation of the deposition of aerosolized drugs in the human respiratory tract due to hygroscopic growth. *J. Aerosol Med*. **2**, 271–284.

French, J., Friedman, D., Wechsler, R., DiVentura, B., Gelfand, M., Pollard, J., Huie, K., Vazquez, B., Gong, L., Cassella, J., Kamemoto, E. (2017) Inhaled alprazolam, a potential rescue medication, works rapidly in patients with photosensitive epilepsy (P6.236). *Neurology* **88**, (16 Supplement).

Guengerich, F. P. (2020) Cytochrome P450 2E1 and its roles in disease. *Chem. Biol. Interact*. **322**, 109056.

Hassan, M., Lau, R. (2010) Effect of particle formulation on dry powder inhalation efficiency. *Curr. Pharm. Des*. **16**, 2377–2387.

Heyder, J. (2004) Deposition of inhaled particles in the human respiratory tract and consequences for regional targeting in respiratory drug delivery. *Proc. Am. Thorac. Soc*. **1**, 315–320.

Hou, S., Wu, J., Li, X., Shu, H. (2015) Practical, regulatory and clinical considerations for development of inhalation drug products. *Asian J. Pharm. Sci*. **10**, 490–500.

Houtmeyers, E., Gosselink, G., Gayan-Ramirez, G., Decramer, M. (1999) Regulation of mucociliary clearance in health and disease. *Eur. Respir. J.* **13**, 1177–1188.

Kim, J. H., Sherman, M. E., Curriero, F. C., Guengerich, F. P., Strickland, P. T., Sutter, T. R. (2004) Expression of cytochromes P450 1A1 and 1B1 in human lung from smokers, non-smokers, and ex-smokers. *Toxicol. Appl. Pharmacol*. **199**, 210–219.

Laube, B. L., Janssens, H. M., de Jongh, F. H. C., Devadason, S. G., Dhand, R., Diot, P., Everard, M. L., Horvath, I., Navalesi, P., Voshaar, T., Chrystyn, H. (2011) What the pulmonary specialist should know about the new inhalation therapies. *Eur. Respir. J.* **37**, 1308–1417.

Leal, J., Smyth, H. D. C., Ghosh, D. (2017) Physicochemical properties of mucus and their impact on transmucosal drug delivery. *Int. J. Pharm*. **532**, 555–572.

Liu, Q., Guan, J., Qin, L., Zhang, X., Mao, S. (2020) Physicochemical properties affecting the fate of nanoparticles in pulmonary drug delivery. *Drug Discov. Today* **25**, 150–159.

Macleod, D. B., Habib, A. S., Ikeda, K., Spyker, D. A., Cassella, J. V., Ho, K. Y., Gan, T. J. (2012) Inhaled fentanyl aerosol in healthy volunteers: Pharmacokinetics and pharmacodynamics. *Anesth. Analg*. **115**, 1071–1077.

Manford, F., Riffo-Vasquez, Y., Spina, D., Page, C. P., Hutt, A. J., Moore, V., Johansson, F., Forbes, B. (2008) Lack of difference in pulmonary absorption of digoxin, a P-glycoprotein substrate, in mdr1a-deficient and mdr1a-competent mice. *J. Pharm. Pharmacol*. **60**, 1305–1310.

Mercadante, S., Voza, A., Serra, S., Ruggiano, G., Carpinteri, G., Gangitano, G., Intelligente, F., Bonafede, E., Sblendido, A., Farina, A., Soldi, A., Fabbri, A.; MEDITA Study Group (2019) Analgesic efficacy, practicality and safety of inhaled methoxyflurane versus standard analgesic treatment for acute trauma pain in the emergency setting: A randomised, open-label, active-controlled, multicentre trial in Italy (MEDITA). *Adv. Ther*. **36**, 3030–3046.

Merritt, B. A., Okyere, C. P., Jasinski, D. M. (2002) Isopropyl alcohol inhalation: Alternative treatment of postoperative nausea and vomiting. *Nurs. Res*. **51**, 125–128.

Mobley, C., Hochhaus, G. (2001) Methods used to assess pulmonary deposition and absorption of drugs. *Drug Discov. Today* **6**, 367–375.

Munkholm, M., Mortensen, J. (2014) Mucociliary clearance: Pathophysiological aspects. *Clin. Physiol. Funct. Imaging* **34**, 171–177.

Pasqua, E., Hamblin, N., Edwards, C., Baker-Glenn, C., Hurley, C. (2022) Developing inhaled drugs for respiratory diseases: A medicinal chemistry perspective. *Drug Discov. Today* **27**, 134–150.

Patel, B., Gupta, N., Ahsan, F. (2015) Particle engineering to enhance or lessen particle uptake by alveolar macrophages and to influence the therapeutic outcome. *Eur. J. Pharm. Biopharm*. **89**, 163–174.

Patton, J., Byron, P. (2007) Inhaling medicines: Delivering drugs to the body through the lungs. *Nat. Rev. Drug Discov*. **6**, 67–74.

Patton, J. S., Fishburn, C. S., Weers, J. G. (2004) The lungs as a portal of entry for systemic drug delivery. *Proc. Am. Thorac. Soc*. **1**, 338–344.

Patton, J. S., Brain, J. D., Davies, L. A., Fiegel, J., Gumbleton, M., Kim, K.-J., Sakagami, M., Vanbever, R., Ehrhardt, C. (2010) The particle has landed – Characterizing the fate of inhaled pharmaceuticals. *J. Aerosol Med. Pulm. Drug Deliv*. **23**, S71–S87 (Suppl. 2).

Pilcer, G., Amighi, K. (2010) Formulation strategy and use of excipients in pulmonary drug delivery. *Int. J. Pharm*. **392**, 1–19.

Prime, D., Atkins, P. J., Slater, A., Sumby, B. (1997) Review of dry powder inhalers. *Adv. Drug Deliv. Rev*. **26**, 51–58.

Rau, J. L. (2005) The inhalation of drugs: Advantages and problems. *Respir. Care* **50**, 367–382.

Ritchie, T. J., Luscombe, C. N., Macdonald, S. J. F. (2009) Analysis of the calculated physicochemical properties of respiratory drugs: Can we design for inhaled drugs yet? *J. Chem. Inf. Model*. **49**, 1025–1032.

Rojanarat, W., Nakpheng, T., Thawithong, E., Yanyium, N., Srichana, T. (2012) Inhaled pyrazinamide proliposome for targeting alveolar macrophages. *Drug Deliv*. **19**, 334–345.

Shute, J. K., Calzetta, L., Cardaci, V., di Toro, S., Page, C. P., Cazzola, M. (2018) Inhaled nebulised unfractionated heparin improves lung function in moderate to very severe COPD: A pilot study. *Pulm. Pharmacol. Ther*. **48**, 88–96.

Siekmeier, R., Scheuch, G. (2009) Systemic treatment by inhalation of macromolecules – Principles, problems, and examples. *J. Physiol. Pharmacol*. **59**, 53–79 (Suppl. 6).

Sigurdsson, H. H., Kirch, J., Lehr, C.-M. (2013) Mucus as a barrier to lipophilic drugs. *Int. J. Pharm*. **453**, 56–64.

Strong, P., Ito, K., Murray, J., Rapeport, G. (2018) Current approaches to the discovery of novel inhaled medicines. *Drug Discov. Today* **23**, 1705–1717.

Tamai, I. (2013) Pharmacological and pathophysiological roles of carnitine/organic cation transporters (OCTNs: SLC22A4, SLC22A5 and Slc22a21). *Biopharm. Drug Dispos*. **34**, 29–44.

Taylor, G. (1990) The absorption and metabolism of xenobiotics in the lung. *Adv. Drug Deliv. Rev*. **5**, 37–61.

Tronde, A., Nordén, B., Jeppsson, A.-B., Brunmark, P., Nilsson, E., Lennernäs, H., Bengtsson, U. H. (2003a) Drug absorption from the isolated perfused rat lung – Correlations with drug physicochemical properties and epithelial permeability. *J. Drug Target*. **11**, 61–74.

Tronde, A., Nordén, B., Marchner, H., Wendel, A., Lennernäs, H., Bengtsson, U. H. (2003b) Pulmonary absorption rate and bioavailability of drugs *in vivo* in rats: Structure-absorption relationships and physicochemical profiling of inhaled drugs. *J. Pharm. Sci*. **92**, 1216–1233.

Uchenna Agu, R., Ikechukwu Ugwoke, M., Armand, M., Kinget, R., Verbeke, N. (2001) The lung as a route for systemic delivery of therapeutic proteins and peptides. *Respir. Res*. **2**, 198.

Upton, R. N., Doolette, D. J. (1999) Kinetic aspects of drug disposition in the lungs. *Clin. Exp. Pharmacol. Physiol*. **26**, 381–391.

U.S. Food and Drug Administration (2005) *Guidance for Industry: Estimating the Maximum Safe Starting Dose in Initial Clinical Trials for Therapeutics in Adult Healthy Volunteers*.

Wang, Y.-B., Watts, A. B., Peters, J. I., Williams, R. O. (2014) The impact of pulmonary diseases on the fate of inhaled medicines – A review. *Int. J. Pharm*. **461**, 112–128.

Wirkes, A., Jung, K., Ochs, M., Mühlfeld, C. (2010) Allometry of the mammalian intracellular pulmonary surfactant system. *J. Appl. Physiol*. **109**, 1662–1669.

Yeh, H. C., Phalen, R. F., Raabe, O. G. (1976) Factors influencing the deposition of inhaled particles. *Environ. Health Perspect*. **15**, 147–156.

Zhang, J., Leifer, F., Rose, S., Chun, D. Y., Thaisz, J., Herr, T., Nashed, M., Joseph, J., Perkins, W. R., DiPetrillo, K. (2018) Amikacin liposome inhalation suspension (ALIS) penetrates non-tuberculous mycobacterial biofilms and enhances amikacin uptake into macrophages. *Front. Microbiol*. **9**, 915.

 Prague Medical Report / Vol. 123 (2022) No. 3, p. 140–165

Clinical Outcomes of Routine Awake Prone Positioning in COVID-19 Patients: A Systematic Review and Meta-analysis of Randomized Controlled Trials

Woon Hean Chong[1], Biplab K. Saha[2], Chee Keat Tan[1]
[1]Department of Intensive Care Medicine, Ng Teng Fong General Hospital, National University Health System, Singapore;
[2]Department of Pulmonary and Critical Care, Ozarks Medical Center, West Plains, USA

Received March 15, 2022; Accepted August 2, 2022.

Key words: COVID-19 – Awake prone positioning – Prone positioning – Proning – Meta-analysis

Abstract: Before coronavirus disease 2019 (COVID-19) emerged, proning had been demonstrated to improve oxygenation in those with acute hypoxic respiratory failure and be performed in non-intensive care settings. This benefit was further exemplified by the COVID-19 pandemic, leading to awake prone positioning (APP). We assessed the efficacy of routine APP versus standard care in preventing death and invasive mechanical ventilation (IMV) in non-intubated hypoxic COVID-19 patients. PubMed, Cochrane Library, Scopus, and medRxiv databases were used from January 1st, 2020, to January 15th, 2022, to identify randomized controlled trials (RCTs). Routine APP group were encouraged to be self-prone, whereas the standard care group received care according to local clinical practice and allowed APP crossover as rescue therapy. We included eight COVID-19 RCTs assessing 809 APP vs. 822 standard care patients. APP group had less IMV requirement (26.5% vs. 30.9%; OR – odds ratio 0.77; P=0.03) than the standard care group, with subgroup analysis showing greater benefit (32.5% vs. 39.1%; OR 0.75; P=0.02) for those mainly requiring oxygen support of non-invasive mechanical ventilation (NIMV) and high-flow nasal cannula (HFNC). The time to IMV initiation was similar (mean 8.3 vs. 10.0 days; P=0.66) for patients requiring NIMV and HFNC. Patients mainly

Mailing Address: Woon Hean Chong, MD., Department of Intensive Care Medicine, Ng Teng Fong General Hospital, National University Health System, 1 Jurong East Street 21, Singapore, 609606, Singapore;
e-mail: keenanchong15@gmail.com

https://doi.org/10.14712/23362936.2022.14
© 2022 The Authors. This is an open-access article distributed under the terms of the Creative Commons Attribution License (http://creativecommons.org/licenses/by/4.0).

receiving supplemental oxygen and non-rebreather masks had improved oxygenation parameters, although not statistically significant. Other outcomes involving all-cause hospital mortality, hospital and ICU (intensive care unit) length of stay, and adverse events were comparable. APP appeared to be an important modality for reducing IMV requirements, especially in those requiring NIMV and HFNC.

Introduction

Before coronavirus disease 2019 (COVID-19), prone positioning was widely adopted as a standard practice due to improvements in oxygenation and reduction in mortality among invasive mechanical ventilation (IMV) patients with moderate to severe acute respiratory distress syndrome (ARDS). These benefits continued to be exemplified when combined with neuromuscular blockade and low-tidal volume ventilation (Guérin et al., 2013; Munshi et al., 2017). Similarly, among awake (non-ventilated) ARDS patients, prone positioning was shown to avert IMV requirements and was particularly useful in settings where intensive care resources were scarce (Ding et al., 2020). During the COVID-19 pandemic, many critically ill COVID-19 patients would develop hypoxic respiratory failure, resulting in IMV (Grasselli et al., 2020; COVID-ICU Group on behalf of the REVA Network and the COVID-ICU Investigators, 2021). The significant morbidity and mortality observed among critically ill COVID-19 patients requiring non-invasive mechanical ventilation (NIMV), high-flow nasal cannula (HFNC), and IMV lead to the implementation of prone positioning protocols across various medical institutions (Bentley et al., 2020; Ng et al., 2020; Venus et al., 2020; Touchon et al., 2021). Prone positioning has been demonstrated to improve oxygenation parameters involving partial pressure of arterial oxygen (PaO_2), partial pressure of arterial oxygen to fraction of inspired oxygen (PaO_2/FiO_2) ratio, and peripheral blood oxygen saturation to FiO_2 (SpO_2/FiO_2) ratio in critically ill COVID-19 patients requiring IMV (Sud et al., 2010; Beitler et al., 2014; Lee et al., 2014; Bloomfield et al., 2015; Park et al., 2015; Munshi et al., 2017; Shelhamer et al., 2021). The mechanisms by which prone positioning improves oxygenation in non-ventilated COVID-19 patients were thought to be similar to those requiring IMV. Our meta-analysis aimed to assess the clinical outcomes of routine awake prone positioning (APP) versus standard care in COVID-19 patients by analysing the current evidence from randomized controlled trials (RCTs).

Methods

This systematic review was conducted and presented in accordance with Preferred Reporting Items for Systematic Reviews and Meta-Analyses (PRISMA) guidelines. Ethical approval and informed consent were not required for this study as it was a systematic review of previously published studies. The protocol for this review was registered and published in the International Prospective Register of Systematic Reviews (PROSPERO) under reference number CRD42022304024.

Search criteria and selection

A literature search was performed through PubMed, Cochrane Library, Scopus, and medRxiv databases for articles published from January 1st, 2020, to January 15th, 2022, using the keywords, title/abstracts, and Medical Subjects Headings (MeSH) terms: ("coronavirus disease 2019" OR "coronavirus 2019" OR "COVID-19") AND ("prone position" OR "awake prone positioning" OR "awake prone"). Moreover, to detect additional studies, any cited references were reviewed to identify relevant literature that met our inclusion criteria.

Inclusion criteria

We included studies: 1) containing non-intubated hospitalized COVID-19 adults (age > 18 years) patients with acute hypoxic respiratory failure requiring oxygen therapy; 2) RCTs containing comparative data describing the clinical outcomes of patients receiving routine APP versus standard care; 3) suspected or proven COVID-19 pneumonia (infiltrate on chest imaging) in which the diagnosis of COVID-19 was made by reverse transcriptase-polymerase chain reaction (RT-PCR) in all cases from respiratory tract that included nasopharyngeal swabs or lower respiratory tract specimens (sputum, endotracheal aspirate – ETA, and bronchoalveolar lavage – BAL); and 4) published in peer-reviewed and non-peer-reviewed journals. Patients randomized in the routine APP group were encouraged to be self-prone for as long as possible at the beginning of the trial before returning to the supine position as necessary. In contrast, patients in the standard care group received care according to clinical practice at respective hospitals and were allowed to crossover to prone positioning (neither encouraged nor disallowed) as a form of rescue therapy for acute hypoxic respiratory failure at the treating clinician's discretion.

Exclusion criteria

We excluded: 1) systematic reviews, literature reviews, editorials, conference abstracts, opinion articles, meta-analyses, observational studies, case reports, or series; 2) non-adult (< 18 years of age), non-consentable, and pregnant patients; 3) patients with contraindications for awake proning or require the immediate need for IMV before randomization; and 4) studies published in languages other than English if no translated version of the manuscript was available. Contraindications for awake proning were recent abdominal or thoracic surgery/trauma, facial/pelvic/spinal fractures, pneumothorax, brain injury without intracranial pressure monitoring, Glasgow Coma Scale (GCS) less than 15, and life-threatening cardiac arrhythmias.

Data collection and synthesis

Two researchers (W.H.C. and B.K.S.) independently screened the titles and abstracts, and reviewed the full texts of articles to identify RCTs that compare the clinical outcomes of COVID-19 patients receiving routine APP versus standard care. Any disagreements were resolved by discussion with a third researcher (C.K.T.).

The extracted data from full texts of included studies was added into a standardized Excel (Microsoft Corporation) form. The following information was summarized in Tables 1 and 2 for each group of patients receiving routine APP and standard care and reported as means and standard deviations (SDs) for continuous variables. When continuous variables were described by the median and interquartile range (IQR) instead of mean and SD, the following formula was used for approximations: mean = (median + IQR)/3 and SD = IQR/1.35 (Wan et al., 2014). For studies that reported PaO_2/FiO_2 ratio without a corresponding SpO_2/FiO_2, we derived a conversion based on $SpO_2/FiO_2 = 64 + 0.84 \times (PaO_2/FiO_2)$ (Rice et al., 2007). Mortality was defined as all-cause in-hospital mortality. If in-hospital mortality was not described among the included studies, but ICU (intensive care unit) mortality was, we accepted the ICU mortality rate as the most suitable replacement. We used the lengthiest interval of mortality to determine the in-hospital mortality rate for studies that comprehensively described mortality at different intervals of 28-day, 30-day, 60-day, 90-day, or 180-day.

Outcomes

The primary outcomes assessed were all-cause in-hospital mortality and IMV requirement in COVID-19 patients receiving routine awake prone positioning versus standard care. The secondary outcomes were changes in SpO_2/FiO_2 ratio, time to IMV initiation, hospital and ICU LOS (length of stay), and adverse events. Adverse events were defined as skin breakdown or pressure sore/ulcer, vomiting, and invasive line dislodgement involving an arterial or central venous catheter.

Quality assessment

Two researchers (W.H.C. and B.K.S.) performed quality assessments and the risk of bias for each RCTs using the Cochrane Collaboration's Risk of Bias Tool in Table 3 (Higgins et al., 2021). The Cochrane Collaboration's Risk of Bias Tool determines the quality of RCTs based on the assessment for random sequence generation, allocation concealment, blinding of participants and personnel, blinding of outcome assessment, incomplete outcome data, selective reporting, and other bias. We considered a study's overall risk of bias to be high if any domain was judged to be at high risk of bias, except blinding of the participants and personnel, and blinding of outcome assessment. By the design and intervention of all RCTs, it was not possible for blinding between the APP (intervention) and standard care (control) groups to occur. Therefore, we accepted standardization of care according to clinical practice at respective hospitals to mitigate performance and detection bias.

Statistical analysis

A meta-analysis was performed for the primary and secondary outcomes using the Review Manager (RevMan) software, Version 5.4, The Cochrane Collaboration, 2020. Using DerSimonian and Laird's random-effects model, pooled odds ratios

Table 1 – Clinical characteristics of eight RCTs comparing routine APP versus standard care

Author	Ehrmann et al. (2021)	Fralick et al. (2022)	Gad (2021)	Jayakumar et al. (2021)	Johnson et al. (2021)	Kharat et al. (2021)	Rosén et al. (2021)	Taylor et al. (2021)
Study design	Multi-center, RCT	Multi-center, RCT	Single-center, RCT	Multi-center, RCT	Single-center, RCT	Multi-center, RCT	Multi-center, RCT	Single-center, RCT
Country	Canada, France, Ireland, Mexico, USA, Spain	Canada, USA	Egypt	India	USA	Switzerland	Sweden	USA
Recruitment date	April 2, 2020 – January 26, 2021	May 2020 – May 2021	June 2020 – September 2020	N/A	April 29, 2020 – August 6, 2020	April 6, 2020 – April 25, 2020	October 7, 2020 – February 7, 2021	June 1, 2020 – August 31, 2020
Inclusion criteria	1) Adults proven or suspected COVID-19 pneumonia 2) HFNC and SpO_2:FiO2 < 315 or PaO_2:FiO_2 < 300 mm Hg	1) Adults proven or suspected COVID-19 pneumonia 2) Supplemental oxygen up to 50% FiO_2 3) Within 48 hours of hospitalization	1) Adults proven or suspected COVID-19 pneumonia 2) Supplemental oxygen 5–10 LPM and SpO_2 < 90%, RR > 24 bpm	1) Adults proven or suspected COVID-19 pneumonia 2) Supplemental oxygen > 4 LPM and SpO_2 > 92% or PaO_2/FiO_2 100–300 mm Hg and $PaCO_2$ < 45 mm Hg 3) < 0.1 mcg/kg/min of norepinephrine	1) Adults proven or suspected COVID-19 pneumonia	1) Adults proven or suspected COVID-19 pneumonia 2) Supplemental oxygen 1–6 LPM and SpO_2 90–92%	1) Adults proven or suspected COVID-19 pneumonia 2) HFNC and NIMV	1) Adults proven or suspected COVID-19 pneumonia 2) SpO_2 < 93% in room air or supplemental oxygen > 3 LPM 3) Within 7 days of illness onset
Exclusion criteria	Pregnant, BMI > 40 kg/m^2, hemodynamically unstable, IMV, or awake proning contraindication	IMV, awake proning contraindication, dementia, delirium	IMV, RR > 40 bpm, SBP < 100 mm Hg, awake proning and NIMV contraindication	Pregnant, GCS < 15, IMV, awake proning contraindication	Pregnant, IMV, unable to change position without assistance or provide consent, incarcerated	Pregnant, unable to prone, terminally ill, recovered ARDS	Pregnant, IMV or previous IMV, hemodynamic instability, non-consentable, do-not-intubate	Awake proning contraindication

Author	**Ehrmann et al. (2021)**	**Fralick et al. (2022)**	**Gad (2021)**	**Jayakumar et al. (2021)**	**Johnson et al. (2021)**	**Kharat et al. (2021)**	**Rosén et al. (2021)**	**Taylor et al. (2021)**
Awake proning (N)	564	126	15	30	15	10	36	13
Proning duration/daily, mean ± SD (H)	5.6 ± 4.4	6.8 ± 8.4	N/A	2.0 ± 0.7	1.6 ± 2.2	4.9 ± 3.6	8.0 ± 4.6	N/A
Clinical characteristics								
Age, mean ± SD (Y)	61.5 ± 13.3	57.5 ± 17.0	49.6 ± 17.8	54.8 ± 11.1	52.3 ± 18.5	54.0 ± 14.0	64.3 ± 15.6	50.6 ± 8.9
Male gender, N (%)	380 (67.3)	82 (65.1)	9 (60.0)	25 (83.3)	8 (53.3)	6 (60.0)	23 (63.8)	7 (53.8)
BMI, mean ± SD (kg/m^2)	29.7 ± 6.6	N/A	N/A	28.2 ± 5.7	33.3 ± 8.8	29.7 ± 5.3	27.6 ± 3.7	33.0 ± 11.1
SpO_2:FiO_2 admission, mean ± SD	147.9 ± 43.9	300.0 ± 55.6	170.8 ± 111.3	233.3 ± 163.8	N/A	314.3 ± 42.2	152.0 ± 31.9	N/A
Initial O_2 support								
Supplemental oxygen or NRM, N (%)	0 (0)	118 (93.7)	15 (100)	26 (86.6)	5 (33.3)	17 (100)	0 (0)	13 (100)
NIMV, N (%)	0 (0)	0 (0)	0 (0)	2 (6.7)	0 (0)	0 (0)	5 (13.9)	0 (0)
HFNC, N (%)	564 (100)	5 (3.9)	0 (0)	1 (3.3)	0 (0)	0 (0)	31 (86.1)	0 (0)
Standard care, (N)	557	122	15	30	15	17	39	27
Proning duration/daily, mean ± SD (H)	0.3 ± 1.2	0.7 ± 1.5	N/A	1.0 ± 1.5	0	0.1 ± 0.5	4.5 ± 4.9	N/A

Author	Ehrmann et al. (2021)	Fralick et al. (2022)	Gad (2021)	Jayakumar et al. (2021)	Johnson et al. (2021)	Kharat et al. (2021)	Rosén et al. (2021)	Taylor et al. (2021)
Clinical characteristics								
Age, mean ± SD (Y)	60.7 ± 14.0	53.3 ± 13.3	43.3 ± 13.3	57.3 ± 12.1	62.0 ± 19.3	60.0 ± 11.0	63.3 ± 11.1	60.6 ± 8.1
Male gender, N (%)	366 (65.7)	78 (63.9)	8 (5.3)	25 (83.3)	8 (53.3)	11 (64.7)	32 (82.1)	20 (74.1)
BMI, mean ± SD (kg/m^2)	29.7 ± 6.6	N/A	N/A	25.8 ± 2.6	28.9 ± 6.3	27.3 ± 4.2	29.6 ± 4.4	31.6 ± 7.4
SpO_2:FiO_2 admission, mean ± SD	148.6 ± 43.1	303.7 ± 53.3	127.7 ± 112.5	219.9 ± 125.9	N/A	342.3 ± 62.9	156.0 ± 74.3	N/A
Initial O_2 support								
Supplemental oxygen or NRM, N (%)	0 (0)	119 (97.5)	0 (0)	30 (100)	6 (40.0)	10 (100)	0 (0)	25 (92.6)
NIMV, N (%)	0 (0)	0 (0)	15 (100)	0 (0)	0 (0)	0 (0)	10 (25.6)	1 (3.7)
HFNC, N (%)	557 (100)	2 (1.6)	0 (0)	0 (0)	0 (0)	0 (0)	29 (74.4)	0 (0)

APP – awake prone positioning; ARDS – acute respiratory distress syndrome; BMI – body mass index; bpm – breaths per minute; COVID-19 – coronavirus disease 2019; D – days; FiO_2 – fraction of inspired oxygen; GCS – Glasgow Coma Scale; H – hours; HFNC – high-flow nasal cannula; ICU – intensive care unit; IMV – invasive mechanical ventilation; LPM – litters per minute; N – numbers; N/A – non-available; NIMV – non-invasive mechanical ventilation; NRM – non-rebreather mask; O_2 – oxygen; $PaCO_2$ – partial pressure of carbon dioxide; PaO_2 – partial pressure of arterial oxygen; RCT – randomized controlled trial; RR – respiratory rate; SBP – systolic blood pressure; SD – standard deviation; SpO_2 – ratio of peripheral arterial oxygen saturation; Y – years

Table 2 – Clinical outcomes of eight RCTs comparing routine APP versus standard care

Author	Ehrmann et al. (2021)	Fralick et al. (2022)	Gad (2021)	Jayakumar et al. (2021)	Johnson et al. (2021)	Kharat et al. (2021)	Rosén et al. (2021)	Taylor et al. (2021)
Awake proning (N)	564	126	15	30	15	10	36	13
Outcomes								
In-hospital mortality, N (%)	117 (20.7)	1 (0.8)	3 (20.0)	3 (10.0)	2 (13.3)	N/A	6 (16.7)	0 (0)
IMV, N (%)	185 (32.8)	6 (4.8)	3 (20.0)	4 (13.3)	2 (13.3)	N/A	12 (33.3)	0 (0)
Hospital LOS, mean ± SD (D)	16.4 ± 10.5	5.7 ± 4.4	28.0 ± 5.0	N/A	N/A	N/A	16.3 ± 8.1	5.3 ± 3.7
ICU LOS, mean ± SD (D)	12.4 ± 9.0	N/A	8.0 ± 3.0	11.5 ± 6.9	4.7 ± 4.0	N/A	7.3 ± 6.7	0 (0)
Time to IMV, mean ± SD (D)	2.3 ± 2.7	N/A	20.0 ± 5.0	N/A	N/A	N/A	2.7 ± 2.9	N/A
Change in SpO_2/FiO_2 ratio, mean ± SD	N/A	53.3 ± 108.1	N/A	–3.3 ± 26.2	131.3 ± 72.3	60.7 ± 53.4	N/A	N/A
Adverse events								
Pressure sore, N (%)	8 (1.4)	N/A	N/A	N/A	N/A	N/A	2 (5.6)	0 (0)
Vomiting, N (%)	15 (2.7)	2 (1.6)	N/A	N/A	N/A	N/A	1 (2.8)	0 (0)
Line dislodgement, N (%)	26 (4.6)	N/A	N/A	N/A	N/A	N/A	0 (0)	1 (7.7)

Author	Ehrmann et al. (2021)	Fralick et al. (2022)	Gad (2021)	Jayakumar et al. (2021)	Johnson et al. (2021)	Kharat et al. (2021)	Rosén et al. (2021)	Taylor et al. (2021)
Standard care (N)	557	122	15	30	15	17	39	27
Outcomes								
In-hospital mortality, N (%)	132 (23.6)	1 (0.8)	3 (20.0)	2 (6.7)	0 (0)	N/A	3 (7.7)	0 (0)
IMV, N (%)	223 (40.0)	5 (4.1)	3 (20.0)	4 (13.3)	1 (6.7)	N/A	13 (33.3)	0 (0)
Hospital LOS, mean ± SD (D)	16.5 ± 9.7	5.0 ± 3.7	26.0 ± 5.0	N/A	N/A	N/A	19.6 ± 14.1	8.3 ± 7.4
ICU LOS, mean ± SD (D)	12.4 ± 8.4	N/A	7.0 ± 2.0	9.9 ± 5.7	4.6 ± 1.4	N/A	12.0 ± 14.1	0 (0)
Time to IMV, mean ± SD (D)	2.0 ± 2.1	N/A	25.0 ± 8.0	N/A	N/A	N/A	3.0 ± 3.7	N/A
Change in SpO_2/FiO_2 ratio, mean ± SD	N/A	61.0 ± 99.3	N/A	–11.7 ± 22.6	79.3 ± 22.7	0.0 ± 31.9	N/A	N/A
Adverse events								
Pressure sore, N (%)	10 (1.8)	N/A	N/A	N/A	N/A	N/A	9 (23.1)	0 (0)
Vomiting, N (%)	18 (3.2)	1 (0.8)	N/A	N/A	N/A	N/A	0 (0)	0 (0)
Line dislodgement, N (%)	17 (3.1)	N/A	N/A	N/A	N/A	N/A	0 (0)	0 (0)

APP – awake prone positioning; D – days; FiO_2 – fraction of inspired oxygen; ICU – intensive care unit; IMV – invasive mechanical ventilation; LOS – length of stay; N – numbers; N/A – non-available; RCT – randomized controlled trial; SD – standard deviation; SpO_2 – ratio of peripheral arterial oxygen saturation

(ORs), mean difference (MDs), and 95% confidence intervals (CIs) were calculated, and extracted outcomes were pooled by weighted averages (DerSimonian and Laird, 1986). The random-effects model was preferred over the fixed-effects model as we suspected that clinical heterogeneity might be present due to the variability across the included studies regarding differences in criteria for escalation of oxygen therapy and IMV initiation, patient population characteristics, and clinical practices. Furthermore, we aimed to assess the mean distribution of results across the eight RCTs with various sample sizes without disregarding the results of small studies and giving extra weightage to results from larger studies. Dichotomous outcomes were assessed using Mantel-Haenszel statistical method as part of the random-effects model and measured in ORs and their 95% CIs. Continuous outcomes were evaluated by the inverse variance statistical method as part of the random-effects model and measured in MDs. The inverse variance method accounts for differing sample sizes of individual studies by weighting studies by the variance of their estimates, such that small studies with large variance have less weighting, and large studies with small variance have more weighting. Statistical heterogeneity among studies was assessed by the I^2 statistic. High heterogeneity was classified as I^2 statistics of 50% and greater, and low was with I^2 statistics of less than 50% (Higgins et al., 2003). A P-value of < 0.05 was considered statistically significant. Subgroup analysis was performed by comparing RCTs involving COVID-19 patients predominantly using NIMV and HFNC versus those using supplemental oxygen and NRM (non-rebreather mask) to determine the impact of NIMV and HFNC on primary outcomes of mortality and IMV.

Results

Study selection and characteristics

Two thousand five hundred thirty-four articles were identified through searched databases. Eight eligible RCTs were included in this meta-analysis after removing duplicates and those not meeting the inclusion criteria (Figure 1). A total of 1,631 COVID-19 patients were included, of which 809 patients received APP, and the remainder received standard of care. The study and clinical characteristics were summarized in Tables 1 and 2. The risk of bias for our primary outcome was low across most studies except for two RCTs as summarized in Table 3 (Gad, 2021; Johnson et al., 2021). Five RCTs assessed patients mainly receiving supplemental oxygen and non-rebreather mask as initial oxygen support (Jayakumar et al., 2021; Johnson et al., 2021; Kharat et al., 2021; Taylor et al., 2021; Fralick et al., 2022), whereas three RCTs by Ehrmann et al. (2021), Gad (2021), and Rosén et al. (2021), assessed patients mainly receiving NIMV and HFNC.

All-cause in-hospital mortality and IMV

The overall all-cause in-hospital mortality was similar (16.5% vs. 17.5%; OR 0.90; P=0.45) between COVID-19 patients in the routine APP group versus the standard

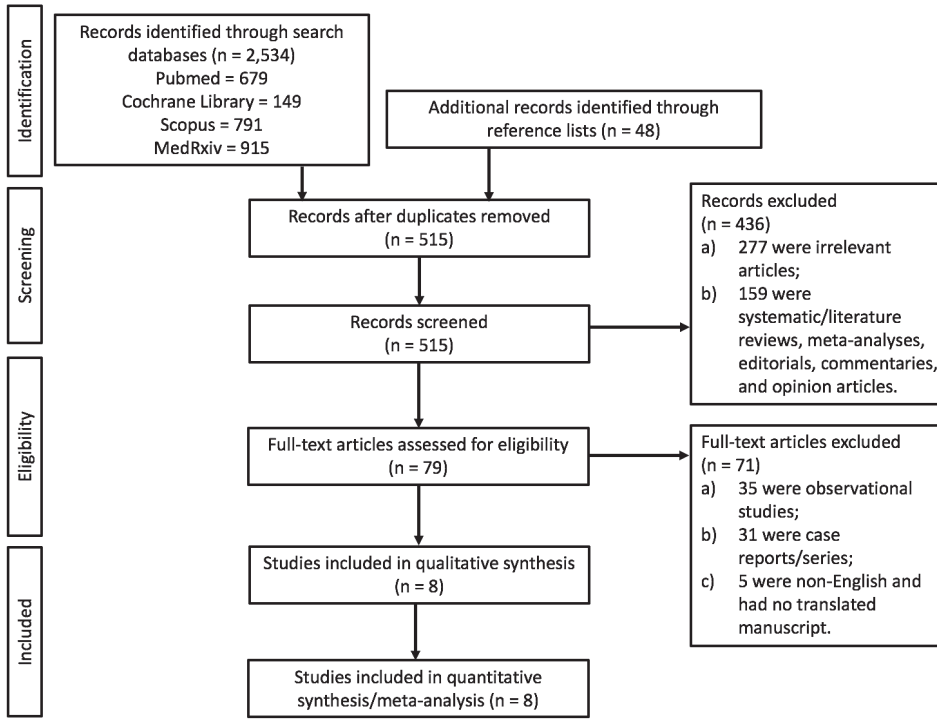

Figure 1 – Flow diagram of study selection.

care group (Figure 2). The mortality rate remained unchanged (3.2% vs. 1.5%; OR 1.79; P=0.41) in the four RCTs, mainly receiving supplemental oxygen and NRM as initial oxygen support (Jayakumar et al., 2021; Johnson et al., 2021; Taylor et al., 2021; Fralick et al., 2022). For the three RCTs assessing patients mainly receiving NIMV and HFNC as initial oxygen support, the mortality rate was equal (20.5% vs. 22.6%; OR 0.88; P=0.35) (Ehrmann et al., 2021; Gad, 2021; Rosén et al., 2021).

The overall IMV requirement was lower (26.5% vs. 30.9%; OR 0.77; P=0.03) in the routine APP group than in the standard care group (Figure 3). Although patients mainly receiving NIMV and HFNC in the routine APP group benefited from lower (32.5% vs. 39.1%; OR 0.75; P=0.02) IMV requirements than the standard care group, a similar outcome was not seen for those mainly receiving supplemental oxygen and NRM. The time to IMV initiation for patients mainly receiving NIMV and HFNC was comparable between the routine APP and standard care groups (Figure 4). Indications for IMV were described in two RCTs with COVID-19 patient deterioration involving respiratory rate > 40 breaths per minute, respiratory muscle fatigue, respiratory acidosis with pH < 7.25, copious tracheal secretions, respiratory distress with PaO_2/FiO_2 ratio < 100 mm Hg or SpO_2 < 90% at 100% FiO_2 for at

Table 3 – Results of the Cochrane Collaboration's Risk of Bias Tool for the eight randomized controlled trials

Randomized controlled trials	Random sequence generation (selection bias)	Allocation concealment (selection bias)	Blinding of participants and personnel (performance bias)	Blinding of outcome assessment (detection bias)	Incomplete outcome data (attrition bias)	Selective reporting (reporting bias)	Other bias
Ehrmann et al. (2021)	+	+	–	–	+	+	+
Fralick et al. (2022)	+	+	–	–	+	+	+
Gad (2021)	+	+	–	–	–	+	–
Jayakumar et al. (2021)	+	+	–	–	+	+	+
Johnson et al. (2021)	–	–	–	–	+	+	+
Kharat et al. (2021)	+	?	–	–	+	+	+
Rosén et al. (2021)	+	+	–	–	+	+	+
Taylor et al. (2021)	+	?	–	–	+	+	+

"+" risk of bias low; "–" risk of bias high; "?" unknown risk of bias

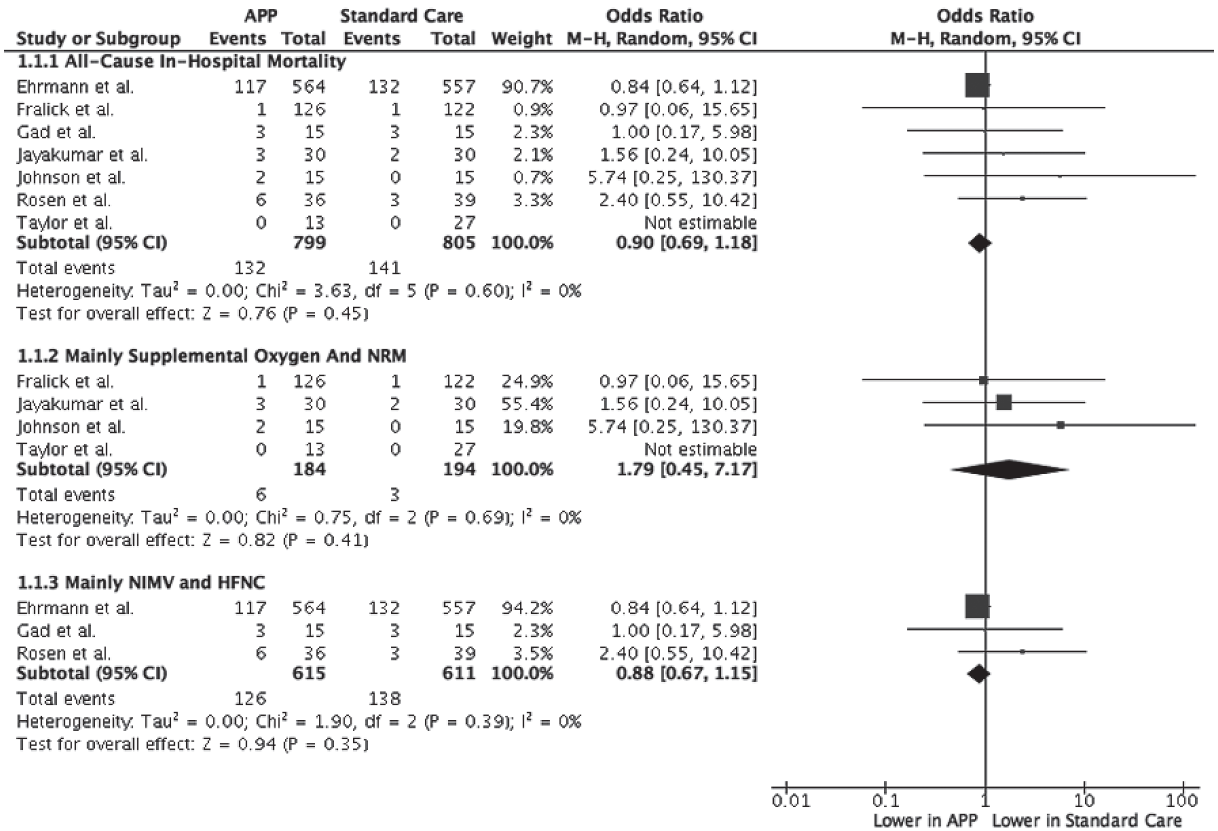

Figure 2 – Forrest plot of COVID-19 patients divided into routine APP versus standard care. Outcomes of overall all-cause in-hospital mortality was assessed. Sensitivity analysis was also performed for overall mortality dividing RCTs into patients mainly requiring supplemental oxygen and NRM, and patients mainly requiring NIMV and HFNC. The odds ratio was calculated by the Mantel-Haenszel method with a random-effects model (APP – awake prone positioning; CI – confidence interval; HFNC – high-flow nasal cannula; M-H – Mantel-Haenszel; NIMV – non-invasive mechanical ventilation; NRM – non-rebreather mask; RCTs – randomized controlled trials).

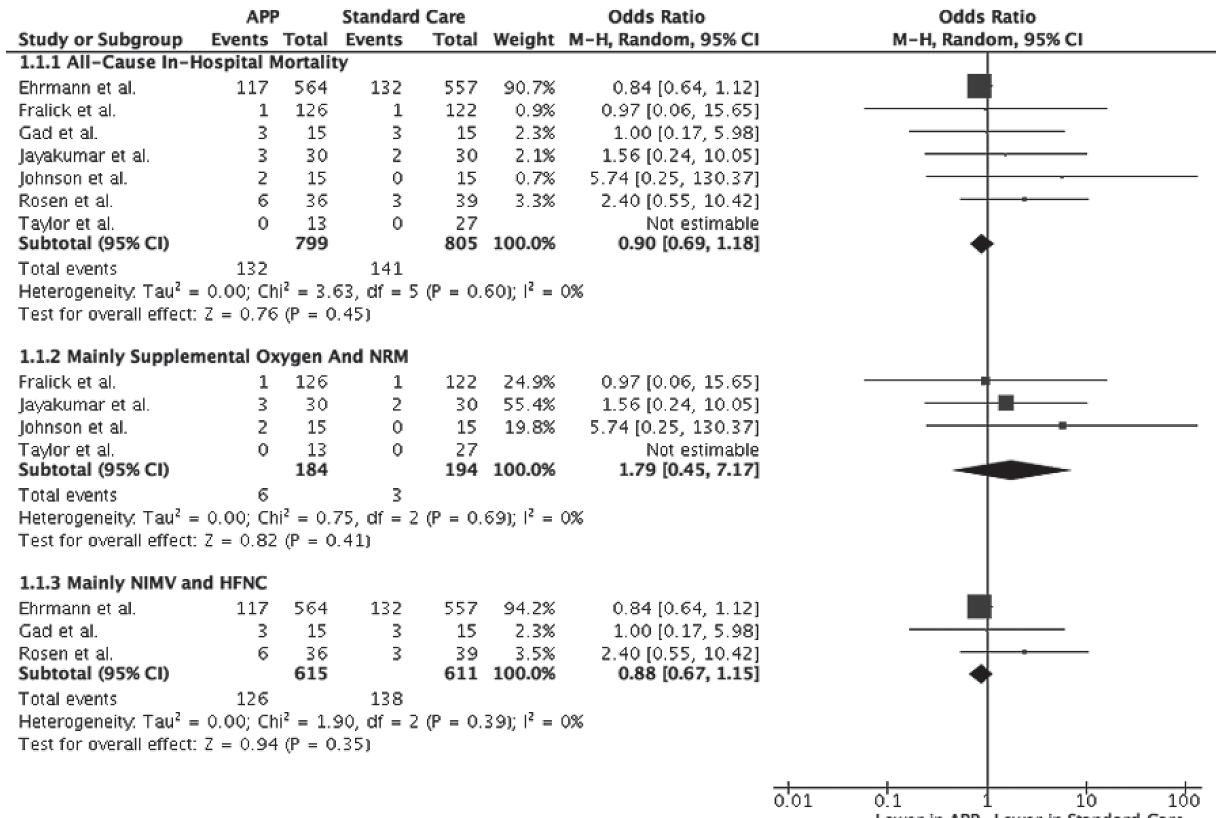

Figure 3 – Forrest plot of COVID-19 patients divided into routine APP versus standard care. Outcomes of IMV requirement was assessed. Sensitivity analysis was also performed for overall IMV requirement dividing RCTs into patients mainly requiring supplemental oxygen and NRM, and patients mainly requiring NIMV and HFNC (APP – awake prone positioning; CI – confidence interval; HFNC – high-flow nasal cannula; IMV – invasive mechanical ventilation; M-H – Mantel-Haenszel; NIMV – non-invasive mechanical ventilation; NRM – non-rebreather mask; RCTs – randomized controlled trials).

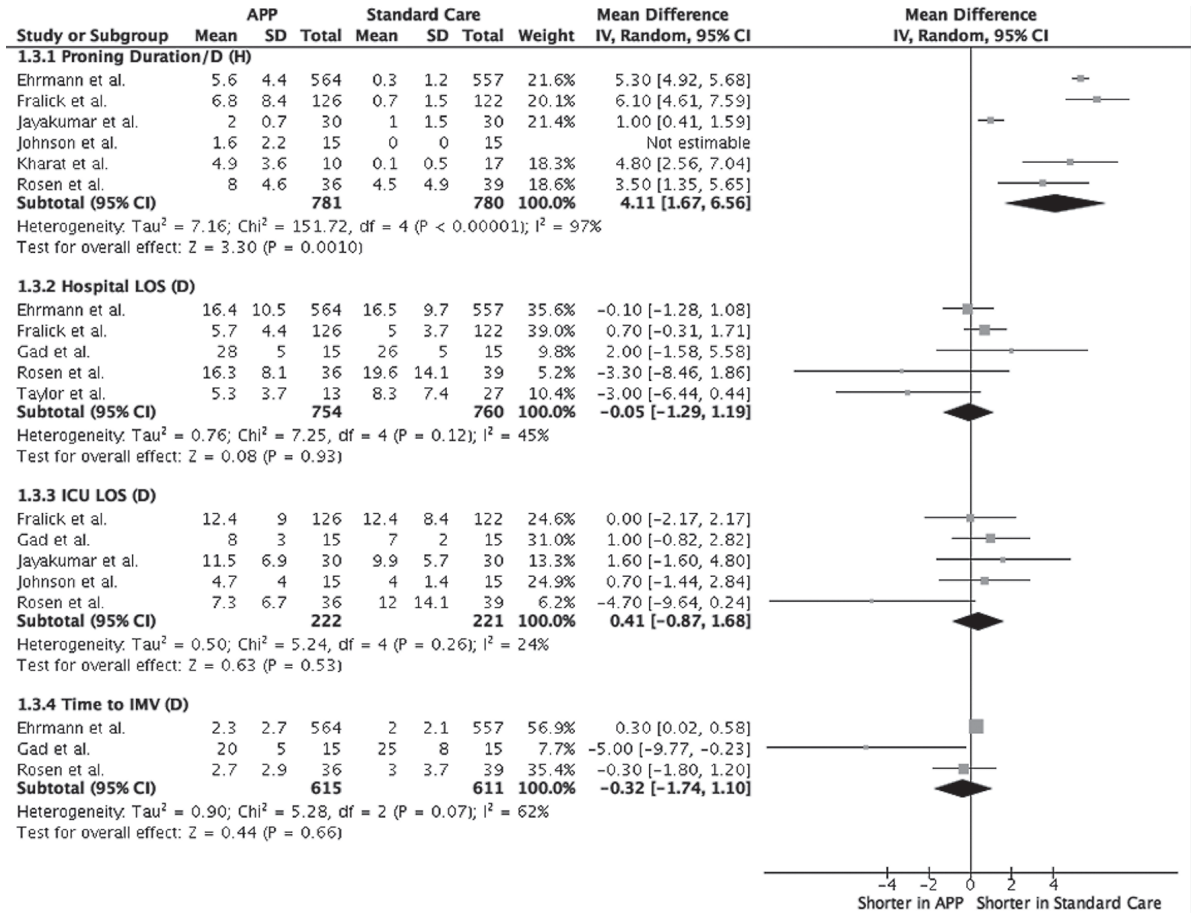

Figure 4 – Forrest plot of COVID-19 patients divided into routine APP versus standard care. Outcomes of proning duration daily, hospital and ICU LOS, and time to IMV were assessed. Mean differences were calculated by the inverse variance statistical method with a random-effects model (APP – awake prone positioning; CI – confidence interval; D – days; ICU – intensive care unit; IMV – invasive mechanical ventilation; IV – inverse variance; LOS – length of stay; SD – standard deviation).

Figure 5 – Forrest plot of COVID-19 patients divided into routine APP versus standard care. Outcome of SpO_2/FiO_2 change on supplemental oxygen and NRM was assessed (APP – awake prone positioning; CI – confidence interval; NRM – non-rebreather mask; SD – standard deviation).

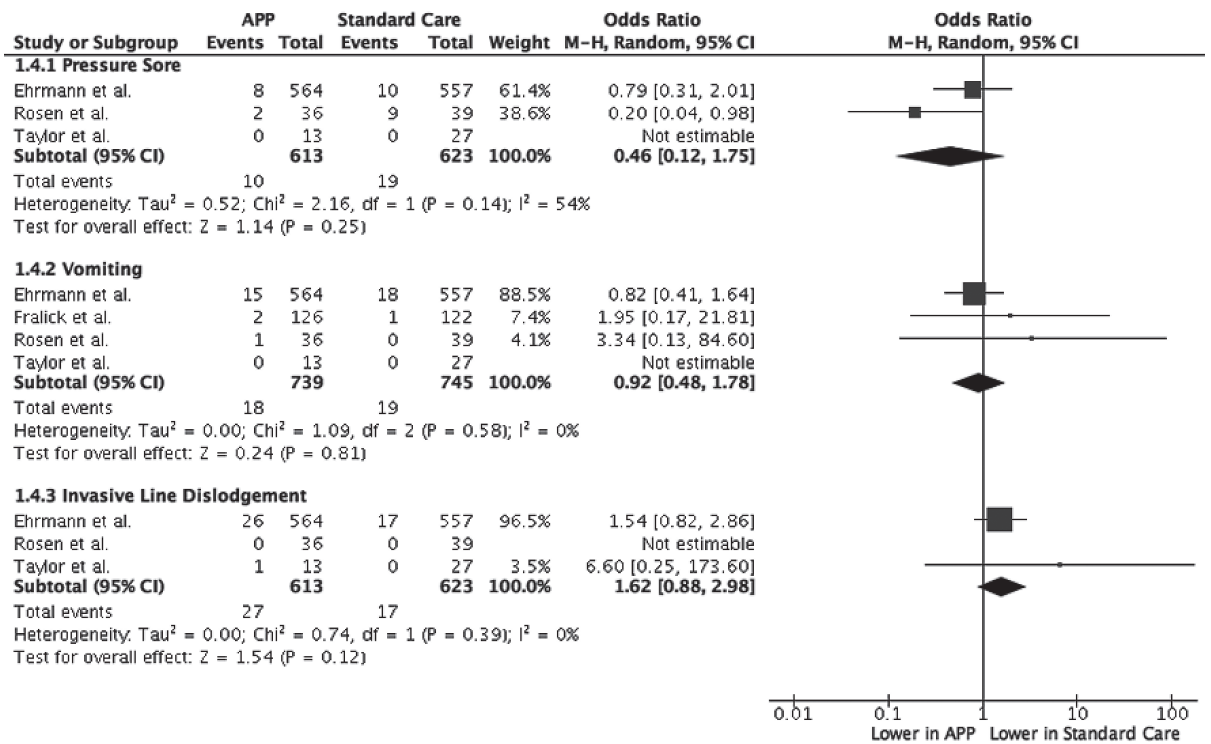

Figure 6 – Forrest plot of COVID-19 patients divided into routine APP versus standard care. Adverse events involving pressure sore, vomiting, and invasive line dislodgement were assessed (APP – awake prone positioning; CI – confidence interval; M-H – Mantel-Haenszel).

least 5 minutes, altered mental status, and hypotension or shock (Ehrmann et al., 2021; Gad, 2021).

Hospital and ICU LOS, change in SpO_2/FiO_2 ratio

In the six RCTs, the total duration of proning daily was significantly longer (mean 4.8 vs. 1.1 hours; MD 4.11; P=0.001) in the routine APP group than in the standard care group (Figure 4) (Ehrmann et al., 2021; Jayakumar et al., 2021; Johnson et al., 2021; Kharat et al., 2021; Rosén et al., 2021; Fralick et al., 2022). Five RCTs demonstrated that the routine APP and standard care groups had comparable hospital LOS (Figure 4) (Ehrmann et al., 2021; Gad, 2021; Rosén et al., 2021; Taylor et al., 2021; Fralick et al., 2022). Similarly, the ICU LOS differed between the two groups according to five RCTs (Figure 4) (Gad, 2021; Jayakumar et al., 2021; Johnson et al., 2021; Rosén et al., 2021; Fralick et al., 2022). Among the four RCTs assessing patients mainly receiving supplemental oxygen and NRM, the change in SpO_2/FiO_2 ratio was higher (mean 80.6 vs. 42.8; MD 24.30; P=0.09) in the routine APP group than the standard care group, but statistical difference was not achieved (Figure 5) (Jayakumar et al., 2021; Johnson et al., 2021; Kharat et al., 2021; Fralick et al., 2022).

Adverse events

Four RCTs assessing patients receiving routine APP versus standard care found no difference in the incidence of vomiting (Figure 6) (Ehrmann et al., 2021; Rosén et al., 2021; Taylor et al., 2021; Fralick et al., 2022). The incidence of other adverse events involving pressure sores and invasive line dislodgements were similar in both groups (Figure 6) as described in three RCTs (Ehrmann et al., 2021; Rosén et al., 2021; Taylor et al., 2021).

Discussion

APP has emerged as an important and effective adjunct therapy in managing COVID-19 patients with acute hypoxic respiratory failure due to the known physiological benefits in gaseous exchange, prevention in respiratory support escalation, good safety profile, and ease of implementation, even in non-intensive care and resource-limited setting. While prone positioning benefited critically ill patients with IMV requirements, our meta-analysis of RCTs demonstrated that routine APP in non-intubated COVID-19 patients would reduce overall IMV requirement, especially in those requiring HFNC and NIMV oxygen support. The lack of blinding and IMV indications might influence the decision-making of treating clinicians by having a lower threshold for initiating IMV in the standard care group, mainly requiring HFNC and NIMV. Though, the time to IMV initiation for patients requiring HFNC and NIMV was similar between the routine APP and standard care groups. Despite the lack of statistical difference, the improvement in SpO_2/FiO_2 ratio in patients, mainly requiring supplemental oxygen and NRM, might create a false perception of clinical improvement and lead to the potential harm caused by delayed

IMV initiation. However, no difference in all-cause in-hospital mortality, hospital and ICU LOS, and incidence of adverse events (pressure sores, vomiting, invasive line dislodgements) were observed in both groups. These findings suggested that the clinicians treated COVID-19 patients correctly and appropriately identified those that did not require IMV. Our pragmatic results supported the notion that routine APP was a valuable tool for managing acute hypoxic respiratory failure considering recent findings of comparable mortality rate and IMV duration in critically ill COVID-19 patients receiving early versus late intubation (Papoutsi et al., 2021).

Several meta-analyses published to date comparing the outcomes of APP versus standard of care in COVID-19 patients suffer from the same limitations as the majority of studies included were observational studies, lack a control group, unmeasured confounding variables, variable sample sizes, and susceptible to selection and publication bias (Ponnapa Reddy et al., 2021; Fazzini et al., 2022; Pavlov et al., 2022; Schmid et al., 2022). Furthermore, many of these studies were performed during the first and second pandemic wave, where rapid data collection and dissemination was prioritized. Hence, the reported outcomes might not be accurate and reflective of current clinical outcomes, considering the rapid advancement of COVID-19 therapies. The effectiveness of APP remains to be established in RCTs, likely due to multiple implementation barriers such as adoption, feasibility, and tolerability. Although APP is a more cost-effective therapy than IMV and extracorporeal membrane oxygenation (ECMO) for managing ARDS, APP is perceived as a labor-intensive intervention and often deferred due to the desire to minimize staff exposure and use of personal protective equipment (Poor et al., 2020; Weatherald et al., 2021). Our meta-analysis was restricted to eight RCTs, and the huge weightage of the RCT by Ehrmann et al. (2021) might have influenced the outcomes of our meta-analysis. However, the outcomes would likely not be different as Ehrmann et al. (2021) conducted a meta-trial of six RCTs to achieve a large sample size to overcome known barriers to performing a RCT. These barriers would have been further exacerbated during the ongoing pandemic in which clinicians and research staffs were relocated to meet the increasing demands of the overwhelmed healthcare setting. Other important clinical outcomes such as mortality, IMV requirement, ICU and hospital LOS, and adverse events were assessed because APP might provide a false sense of reassurance leading to potentially delayed escalation of respiratory support and IMV initiation. We also included RCTs from the grey literature of medRxiv to reduce publication bias and used mortality from the longest follow-up period to avoid missing important data contributed by the delayed clinical decompensation from the atypical COVID-19 phenotype (Chong et al., 2021, 2022). The prolonged duration of patient enrolment as the RCTs were conducted between April 2020 and May 2021 would increase the generalizability due to the rapid advancement in COVID-19 therapies and the increase in APP experience gained among healthcare providers from previous waves of the ongoing pandemic.

There are several possible reasons for the similarity in outcomes of all-cause in-hospital mortality, hospital and ICU LOS observed in COVID-19 patients receiving APP versus standard care. 1) Crossover with the use of APP as part of rescue therapy at the discretion of the treating clinician due to the known physiological benefit in the standard care group; and 2) the mean daily duration of APP was 4.8 hours compared to 1.1 hours in the standard care group might not be significant enough to demonstrate any difference in outcomes (Ehrmann et al., 2021; Jayakumar et al., 2021; Rosén et al., 2021; Fralick et al., 2022). Prone positioning when applied for a longer period (12 hours or more) has been demonstrated to improve oxygenation and mortality in non-COVID-19 patients on IMV (Beitler et al., 2014; Lee et al., 2014; Bloomfield et al., 2015; Park et al., 2015; Munshi et al., 2017). Possibly because of the physiological benefit of prone positioning to facilitate lung recruitment, improve compliance and promote ventilation-perfusion homogeneity is a time-dependent event. However, similar to multiple studies and meta-analyses assessing the benefits of prone positioning in non-COVID-19 patients with ARDS, the exact threshold of minimum daily duration and cumulative hours in which prone positioning will confer benefit remains unknown (Sud et al., 2010; Abroug et al., 2011; Park et al., 2015; Munshi et al., 2017). Although the mean daily duration of proning was recorded in our meta-analysis, the number of APP sessions and patients adhering to APP remain uncertain. Furthermore, the mean daily duration of proning was highly variable across different RCTs (Table 1), which might be explained by the crossover from standard care to the APP group and poor patient compliance to APP due to discomfort ranging from musculoskeletal discomfort, vomiting, coughing, and anxiety, despite repeated encouragements (Touchon et al., 2021). Considering that IMV patients are often heavily sedated and paralyzed to tolerate prone positioning, these explain the difficulty of achieving a similar prone positioning duration in non-IMV patients. Nevertheless, poor tolerance and adherence to APP likely reflect real-world challenges for critically ill COVID-19 patients with underlying acute hypoxic respiratory failure, multi-organ dysfunction, and a lack of high nursing-to-patient ratio to reinforce APP.

Despite the known benefit of prone positioning, there remains a lack of evidence guiding the timing of APP initiation for COVID-19 patients to achieve optimal outcomes. Early initiation (within two days of ICU admission) of prone positioning was associated with lower mortality among mechanically ventilated COVID-19 patients with moderate to severe ARDS (Mathews et al., 2021). A prospective study observed that APP COVID-19 responders (more remarkable improvement in oxygenation parameters) were those who had shorter time from hospital admission to receiving APP (mean 2.7 vs. 4.6 days) when the duration and number of APP sessions were similar (Coppo et al., 2020). A RCT that compared outcomes among 125 COVID-19 patients receiving early APP (less than 24 hours) compared to delayed APP with HFNC showed improved oxygenation parameters and 28-day mortality (Kaur et al., 2021). However, patients in the early APP had a longer daily

duration of APP (mean 5.1 vs. 3 hours) than the delayed group.

In our meta-analysis, COVID-19 patients predominantly receiving NIMV and HFNC during APP had reduced need for IMV requirements, although the time to IMV initiation, mortality, and hospital/ICU LOS were similar. The rate of escalation and the number of days free from HFNC and NIMV were not assessed in RCTs requiring supplemental oxygen and NRM. Only one RCT demonstrated no difference in mortality and IMV requirement among COVID-19 patients receiving APP combined with NRM versus those solely receiving NIMV in the standard care group (Gad, 2021). There remains a lack of studies comparing the outcomes of COVID-19 patients receiving either HFNC or NIMV during APP. Multiple prospective observational COVID-19 studies assessing APP as an adjunctive to HFNC compared to HFNC alone showed conflicting results in mortality rate and IMV requirement despite increasing oxygenation parameters in the APP group (Ferrando et al., 2020; Esperatti et al., 2022). Other small retrospective studies revealed a reduction in respiratory rate and increased oxygenation parameters among COVID-19 patients receiving NIMV with APP than those receiving NIMV alone (Winearls et al., 2020; Chiumello et al., 2021). A small retrospective observational study involving 48 COVID-19 patients receiving APP revealed that patients managed by NIMV alone had a lower mortality rate than those who transitioned from NIMV to HFNC (Hallifax et al., 2020). However, it was possible that COVID-19 patients who were transitioned from NIMV to HFNC had poor tolerance and demonstrated clinical decompensation with failure to respond to existing oxygen support. Historically, HFNC was favoured over NIMV in critically ill non-COVID-19 patients with ARDS as HFNC provided a lower level of positive pressure compared to high levels of positive pressure delivered by NIMV that may lead to patient self-induced lung injury (P-SILI) in a spontaneous breathing patient, regardless of prone positioning status (Walkey and Wiener, 2013; Spinelli et al., 2020). Therefore, current evidence supporting the use of HFNC over NIMV is limited to observational non-COVID-19 ARDS studies in which HFNC was not demonstrated to be superior over NIMV in improving gaseous exchange during APP, although clinical outcomes such as mortality were not examined (Ding et al., 2020; Pérez-Nieto et al., 2020).

Prone positioning for patients requiring IMV is associated with an increased risk of dislodgement of invasive lines that arise when turning, and pressure sores from prolonged static positioning frequently in those receiving IMV, sedation, and NMB (Venus et al., 2020). Multiple meta-analyses of non-COVID-19 patients requiring IMV showed a similar incidence of line dislodgements but increased in pressures sores during prone positioning compared to supine (Sud et al., 2010; Abroug et al., 2011; Lee et al., 2014; Bloomfield et al., 2015; Park et al., 2015; Munshi et al., 2017). However, the risks of pressure sores may be mitigated in an awake patient who can change position independently for comfort. In our meta-analysis, adverse events involving pressure sores, vomiting, and invasive line dislodgements were low (less than 5%), and there was no difference between the routine APP and standard

care groups. The lack of difference in pressure sore incidence is vital as pressure sore has been associated with higher morbidity and mortality among critically ill non-COVID-19 patients and constitutes a significant burden to the healthcare system (Labeau et al., 2021).

There were several limitations to our meta-analysis. 1) The included RCTs were diverse based on the inclusion criteria employed, unclear ARDS severity, time to APP initiation from hospital admission, missing IMV indication (only discussed in two RCTs) (Ehrmann et al., 2021; Gad, 2021), and associated-COVID-19 therapy provided. The use of a random-effect model might have resulted in wider CIs and a more conservative treatment effect; 2) As more than three-quarters of the studies were conducted in Europe and the USA, there was a lack of generalizability toward other populations of different demographics; 3) The exclusion of non-English studies might preclude the extrapolation of our results towards low- and middle-income countries that were equally burdened by COVID-19; 4) Because of the nature of APP intervention, blinding of the patients and treating clinicians will not be feasible leading to increased risk of bias; 5) Other essential clinical data that might affect the efficacy of the intervention, management, and outcomes such as the number of cycles of APP, severity and duration of illness before randomization, and existing do-not-intubate status were not well-described. Clinical outcomes that have important implications for patient care, such as changes in respiratory rate and oxygenation parameters after proning, and time to the escalation of oxygen requirement, were inconsistently assessed that might be used as a marker for P-SILI development (Venus et al., 2020); and 6) Publication bias was not assessed due to the low number of RCTs included, although RCT from grey literature of medRxiv was included (Fralick et al., 2022). Future trials should ideally minimize crossover from supine to APP, improve compliance to longer APP duration, compare the utility of different forms of respiratory support during APP, and assess the clinical benefit of specific interventions and devices for APP comfort and adherence are required.

Conclusion

When applied in an optimal manner and to the targeted COVID-19 population, APP is associated with a reduction in IMV requirement, especially in patients requiring NIMV and HFNC, and improvement in SpO_2/FiO_2 ratio in patients requiring supplemental oxygen and NRM. Current evidence cannot determine the optimal timing of initiation, duration, and frequency of APP sessions for COVID-19 patients.

References

Abroug, F., Ouanes-Besbes, L., Dachraoui, F., Ouanes, I., Brochard, L. (2011) An updated study-level meta-analysis of randomised controlled trials on proning in ARDS and acute lung injury. *Crit. Care* **15(1)**, R6.

Beitler, J. R., Shaefi, S., Montesi, S. B., Devlin, A., Loring, S. H., Talmor, D., Malhotra, A. (2014) Prone positioning reduces mortality from acute respiratory distress syndrome in the low tidal volume era: A meta-analysis. *Intensive Care Med*. **40(3)**, 332–341.

Bentley, S. K., Iavicoli, L., Cherkas, D., Lane, R., Wang, E., Atienza, M., Fairweather, P., Kessler, S. (2020)

Guidance and patient instructions for proning and repositioning of awake, nonintubated COVID-19 patients. *Acad. Emerg. Med*. **27(8)**, 787–791.

Bloomfield, R., Noble, D. W., Sudlow, A. (2015) Prone position for acute respiratory failure in adults. *Cochrane Database Syst. Rev*. **11**, CD008095.

Chiumello, D., Chiodaroli, E., Coppola, S., Cappio Borlino, S., Granata, C., Pitimada, M., Wendel Garcia, P. D. (2021) Awake prone position reduces work of breathing in patients with COVID-19 ARDS supported by CPAP. *Ann. Intensive Care* **11(1)**, 179.

Chong, W. H., Saha, B. K., Chopra, A. (2021) Does COVID-19 pneumonia signify secondary organizing pneumonia?: A narrative review comparing the similarities between these two distinct entities. *Heart Lung* **50(5)**, 667–674.

Chong, W. H., Saha, B. K., Medarov, B. I. (2022) Clinical characteristics between survivors and nonsurvivors of COVID-19 patients requiring extracorporeal membrane oxygenation (ECMO) support: A systematic review and meta-analysis. *J. Intensive Care Med*. **37(3)**, 304–318.

Coppo, A., Bellani, G., Winterton, D., Di Pierro, M., Soria, A., Faverio, P., Cairo, M., Mori, S., Messinesi, G., Contro, E., Bonfanti, P., Benini, A., Valsecchi, M. G., Antolini, L., Foti, G. (2020) Feasibility and physiological effects of prone positioning in non-intubated patients with acute respiratory failure due to COVID-19 (PRON-COVID): A prospective cohort study. *Lancet Respir. Med*. **8(8)**, 765–774.

COVID-ICU Group on behalf of the REVA Network and the COVID-ICU Investigators (2021) Clinical characteristics and day-90 outcomes of 4244 critically ill adults with COVID-19: A prospective cohort study. *Intensive Care Med*. **47(1)**, 60–73.

DerSimonian, R., Laird, N. (1986) Meta-analysis in clinical trials. *Control. Clin. Trials* **7(3)**, 177–188.

Ding, L., Wang, L., Ma, W., He, H. (2020) Efficacy and safety of early prone positioning combined with HFNC or NIV in moderate to severe ARDS: A multi-center prospective cohort study. *Crit. Care* **24(1)**, 28.

Ehrmann, S., Li, J., Ibarra-Estrada, M., Perez, Y., Pavlov, I., McNicholas, B., Roca, O., Mirza, S., Vines, D., Garcia-Salcido, R., Aguirre-Avalos, G., Trump, M. W., Nay, M.-A., Dellamonica, J., Nseir, S., Mogri, I., Cosgrave, D., Jayaraman, D., Masclans, J. R., Laffey, J. G., Tavernier, E.; for the Awake Prone Positioning Meta-Trial Group (2021) Awake prone positioning for COVID-19 acute hypoxaemic respiratory failure: A randomised, controlled, multinational, open-label meta-trial. *Lancet Respir. Med*. **9(12)**, 1387–1395.

Esperatti, M., Busico, M., Fuentes, N. A., Gallardo, A., Osatnik, J., Vitali, A., Wasinger, E. G., Olmos, M., Quintana, J., Saavedra, S. N., Lagazio, A. I., Andrada, F. J., Kakisu, H., Romano, N. E., Matarrese, A., Mogadouro, M. A., Mast, G., Moreno, C. N., Niquin, G. D. R., Barbaresi, V., Cruz, A. B., Ferreyro, B. L., Torres, A.; Argentine Collaborative Group on High Flow and Prone Positioning (2022) Impact of exposure time in awake prone positioning on clinical outcomes of patients with COVID-19-related acute respiratory failure treated with high-flow nasal oxygen: A multicenter cohort study. *Crit. Care* **26(1)**, 16.

Fazzini, B., Page, A., Pearse, R., Puthucheary, Z. (2022) Prone positioning for non-intubated spontaneously breathing patients with acute hypoxaemic respiratory failure: A systematic review and meta-analysis. *Br. J. Anaesth*. **128(2)**, 352–362.

Ferrando, C., Mellado-Artigas, R., Gea, A., Arruti, E., Aldecoa, C., Adalia, R., Ramasco, F., Monedero, P., Maseda, E., Tamayo, G., Hernández-Sanz, M. L., Mercadal, J., Martín-Grande, A., Kacmarek, R. M., Villar, J., Suárez-Sipmann, F.; COVID-19 Spanish ICU Network (2020) Awake prone positioning does not reduce the risk of intubation in COVID-19 treated with high-flow nasal oxygen therapy: A multicenter, adjusted cohort study. *Crit. Care* **24(1)**, 597.

Fralick, M., Colacci, M., Munshi, L., Venus, K., Fidler, L., Hussein, H., Britto, K., Fowler, R., Da Costa, B., Dhalla, I., Dunbar-Yaffe, R., Branfield Day, L., MacMillan, T., Zipursky, J., Carpenter, T., Tang, T., Cooke, A., Hensel, R., Bregger, M., Gordon, A., Worndl, E., Go, S., Mandelzweig, K., Castellucci, L. A.,

Tamming, D., Razak, F., Verma, A. A.; COVID Prone Study Investigators (2022) Prone positioning of patients with moderate hypoxia due to covid-19: A multicenter pragmatic randomized trial (COVID-PRONE). *BMJ* **376**, e068585.

Gad, G. S. (2021) Awake prone positioning versus non invasive ventilation for COVID-19 patients with acute hypoxemic respiratory failure. *Egypt. J. Anaesth*. **37(1)**, 85–90.

Grasselli, G., Zangrillo, A., Zanella, A., Antonelli, M., Cabrini, L., Castelli, A., Cereda, D., Coluccello, A., Foti, G., Fumagalli, R., Iotti, G., Latronico, N., Lorini, L., Merler, S., Natalini, G., Piatti, A., Ranieri, M. V., Scandroglio, A. M., Storti, E., Cecconi, M., Pesenti, A.; COVID-19 Lombardy ICU Network (2020) Baseline characteristics and outcomes of 1591 patients infected with SARS-CoV-2 admitted to ICUs of the Lombardy region, Italy. *JAMA* **323(16)**, 1574–1581.

Guérin, C., Reignier, J., Richard, J.-C., Beuret, P., Gacouin, A., Boulain, T., Mercier, E., Badet, M., Mercat, A., Baudin, O., Clavel, M., Chatellier, D., Jaber, S., Rosselli, S., Mancebo, J., Sirodot, M., Hilbert, G., Bengler, C., Richecoeur, J., Gainnier, M., Bayle, F., Bourdin, G., Leray, V., Girard, R., Baboi, L., Ayzac, L.; PROSEVA Study Group (2013) Prone positioning in severe acute respiratory distress syndrome. *N. Engl. J. Med*. **368(23)**, 2159–2168.

Hallifax, R. J., Porter, B. M., Elder, P. J., Evans, S. B., Turnbull, C. D., Hynes, G., Lardner, R., Archer, K., Bettinson, H. V., Nickol, A. H., Flight, W. G., Chapman, S. J., Hardinge, M., Hoyles, R. K., Saunders, P., Sykes, A., Wrightson, J. M., Moore, A., Ho, L.-P., Fraser, E., Pavord, I. D., Talbot, N. P., Bafadhel, M., Petousi, N., Rahman, N. M.; Oxford Respiratory Group (2020) Successful awake proning is associated with improved clinical outcomes in patients with COVID-19: Single-centre high-dependency unit experience. *BMJ Open Respir. Res*. **7(1)**, e000678.

Higgins, J. P. T., Thompson, S. G., Deeks, J. J., Altman, D. G. (2003) Measuring inconsistency in meta-analyses. *BMJ* **327(7414)**, 557–560.

Higgins, J., Thomas, J., Chandler, J., Cumpston, M., Li, T., Page, M., Welch, V. (2021) *Cochrane Handbook for Systematic Reviews of Interventions*. Available at: www.training.cochrane.org/handbook

Jayakumar, D., Ramachandran Dnb, P., Rabindrarajan Dnb, E., Vijayaraghavan Md, B. K. T., Ramakrishnan Ab, N., Venkataraman Ab, R. (2021) Standard care versus awake prone position in adult nonintubated patients with acute hypoxemic respiratory failure secondary to COVID-19 infection – A multicenter feasibility randomized controlled trial. *J. Intensive Care Med*. **36(8)**, 918–924.

Johnson, S. A., Horton, D. J., Fuller, M. J., Yee, J., Aliyev, N., Boltax, J. P., Chambers, J. H., Lanspa, M. J. (2021) Patient-directed prone positioning in awake patients with COVID-19 requiring hospitalization (PAPR). *Ann. Am. Thorac. Soc*. **18(8)**, 1424–1426.

Kaur, R., Vines, D. L., Mirza, S., Elshafei, A., Jackson, J. A., Harnois, L. J., Weiss, T., Scott, J. B., Trump, M. W., Mogri, I., Cerda, F., Alolaiwat, A. A., Miller, A. R., Klein, A. M., Oetting, T. W., Morris, L., Heckart, S., Capouch, L., He, H., Li, J. (2021) Early versus late awake prone positioning in non-intubated patients with COVID-19. *Crit. Care* **25(1)**, 340.

Kharat, A., Dupuis-Lozeron, E., Cantero, C., Marti, C., Grosgurin, O., Lolachi, S., Lador, F., Plojoux, J., Janssens, J.-P., Soccal, P. M., Adler, D. (2021) Self-proning in COVID-19 patients on low-flow oxygen therapy: A cluster randomised controlled trial. *ERJ Open Res*. **7(1)**, 00692–02020.

Labeau, S. O., Afonso, E., Benbenishty, J., Blackwood, B., Boulanger, C., Brett, S. J., Calvino-Gunther, S., Chaboyer, W., Coyer, F., Deschepper, M., François, G., Honore, P. M., Jankovic, R., Khanna, A. K., Llaurado-Serra, M., Lin, F., Rose, L., Rubulotta, F., Saager, L., Williams, G., Blot, S. I.; DecubICUs Study Team; European Society of Intensive Care Medicine (ESICM) Trials Group Collaborators (2021) Prevalence, associated factors and outcomes of pressure injuries in adult intensive care unit patients: The DecubICUs study. *Intensive Care Med*. **47(2)**, 160–169.

Lee, J. M., Bae, W., Lee, Y. J., Cho, Y.-J. (2014) The efficacy and safety of prone positional ventilation in acute

respiratory distress syndrome: Updated study-level meta-analysis of 11 randomized controlled trials. *Crit. Care Med*. **42(5)**, 1252–1262.

Mathews, K. S., Soh, H., Shaefi, S., Wang, W., Bose, S., Coca, S., Gupta, S., Hayek, S. S., Srivastava, A., Brenner, S. K., Radbel, J., Green, A., Sutherland, A., Leonberg-Yoo, A., Shehata, A., Schenck, E. J., Short, S. A. P., Hernán, M. A., Chan, L., Leaf, D. E.; STOP-COVID Investigators (2021) Prone positioning and survival in mechanically ventilated patients with coronavirus disease 2019-related respiratory failure. *Crit. Care Med*. **49(7)**, 1026–1037.

Munshi, L., Del Sorbo, L., Adhikari, N. K. J., Hodgson, C. L., Wunsch, H., Meade, M. O., Uleryk, E., Mancebo, J., Pesenti, A., Ranieri, V. M., Fan, E. (2017) Prone position for acute respiratory distress syndrome. A systematic review and meta-analysis. *Ann. Am. Thorac. Soc*. **14**, S280–S288 (Suppl. 4).

Ng, Z., Tay, W. C., Ho, C. H. B. (2020) Awake prone positioning for non-intubated oxygen dependent COVID-19 pneumonia patients. *Eur. Respir. J*. **56(1)**, 2001198.

Papoutsi, E., Giannakoulis, V. G., Xourgia, E., Routsi, C., Kotanidou, A., Siempos, I. I. (2021) Effect of timing of intubation on clinical outcomes of critically ill patients with COVID-19: A systematic review and meta-analysis of non-randomized cohort studies. *Crit. Care* **25(1)**, 121.

Park, S. Y., Kim, H. J., Yoo, K. H., Park, Y. B., Kim, S. W., Lee, S. J., Kim, E. K., Kim, J. H., Kim, Y. H., Moon, J.-Y., Min, K. H., Park, S. S., Lee, J., Lee, C.-H., Park, J., Byun, M. K., Lee, S. W., Rlee, C., Jung, J. Y., Sim, Y. S. (2015) The efficacy and safety of prone positioning in adults patients with acute respiratory distress syndrome: A meta-analysis of randomized controlled trials. *J. Thorac. Dis*. **7(3)**, 356–367.

Pavlov, I., He, H., McNicholas, B., Perez, Y., Tavernier, E., Trump, M. W., Jackson, J. A., Zhang, W., Rubin, D. S., Spiegel, T., Hung, A., Estrada, M. Á. I., Roca, O., Vines, D. L., Cosgrave, D., Mirza, S., Laffey, J. G., Rice, T. W., Ehrmann, S., Li, J. (2022) Awake prone positioning in non-intubated patients with acute hypoxemic respiratory failure due to COVID-19. *Respir. Care* **67(1)**, 102–114.

Pérez-Nieto, O. R., Guerrero-Gutiérrez, M. A., Deloya-Tomas, E., Ñamendys-Silva, S. A. (2020) Prone positioning combined with high-flow nasal cannula in severe noninfectious ARDS. *Crit. Care* **24(1)**, 114.

Ponnapa Reddy, M., Subramaniam, A., Afroz, A., Billah, B., Lim, Z. J., Zubarev, A., Blecher, G., Tiruvoipati, R., Ramanathan, K., Wong, S. N., Brodie, D., Fan, E., Shekar, K. (2021) Prone positioning of nonintubated patients with coronavirus disease 2019 – A systematic review and meta-analysis. *Crit. Care Med*. **49(10)**, e1001–e1014.

Poor, A. D., Acquah, S. O., Wells, C. M., Sevillano, M. V., Strother, C. G., Oldenburg, G. G., Hsieh, S. J. (2020) Implementing automated prone ventilation for acute respiratory distress syndrome via simulation-based training. *Am. J. Crit. Care* **29(3)**, e52–e59.

Rice, T. W., Wheeler, A. P., Bernard, G. R., Hayden, D. L., Schoenfeld, D. A., Ware, L. B.; National Institutes of Health, National Heart, Lung, and Blood Institute ARDS Network (2007) Comparison of the SpO_2/FiO_2 ratio and the PaO_2/FiO_2 ratio in patients with acute lung injury or ARDS. *Chest* **132(2)**, 410–417.

Rosén, J., von Oelreich, E., Fors, D., Jonsson Fagerlund, M., Taxbro, K., Skorup, P., Eby, L., Campoccia Jalde, F., Johansson, N., Bergström, G., Frykholm, P.; PROFLO Study Group (2021) Awake prone positioning in patients with hypoxemic respiratory failure due to COVID-19: The PROFLO multicenter randomized clinical trial. *Crit. Care* **25(1)**, 209.

Schmid, B., Griesel, M., Fischer, A.-L., Romero, C. S., Metzendorf, M.-I., Weibel, S., Fichtner, F. (2022) Awake prone positioning, high-flow nasal oxygen and non-invasive ventilation as non-invasive respiratory strategies in COVID-19 acute respiratory failure: A systematic review and meta-analysis. *J. Clin. Med*. **11(2)**, 391.

Shelhamer, M. C., Wesson, P. D., Solari, I. L., Jensen, D. L., Steele, W. A., Dimitrov, V. G., Kelly, J. D., Aziz, S., Gutierrez, V. P., Vittinghoff, E., Chung, K. K., Menon, V. P., Ambris, H. A., Baxi, S. M. (2021) Prone

positioning in moderate to severe acute respiratory distress syndrome due to COVID-19: A cohort study and analysis of physiology. *J. Intensive Care Med*. **36(2)**, 241–252.

Spinelli, E., Mauri, T., Beitler, J. R., Pesenti, A., Brodie, D. (2020) Respiratory drive in the acute respiratory distress syndrome: Pathophysiology, monitoring, and therapeutic interventions. *Intensive Care Med*. **46(4)**, 606–618.

Sud, S., Friedrich, J. O., Taccone, P., Polli, F., Adhikari, N. K. J., Latini, R., Pesenti, A., Guérin, C., Mancebo, J., Curley, M. A. Q., Fernandez, R., Chan, M.-C., Beuret, P., Voggenreiter, G., Sud, M., Tognoni, G., Gattinoni, L. (2010) Prone ventilation reduces mortality in patients with acute respiratory failure and severe hypoxemia: Systematic review and meta-analysis. *Intensive Care Med*. **36(4)**, 585–599.

Taylor, S. P., Bundy, H., Smith, W. M., Skavroneck, S., Taylor, B., Kowalkowski, M. A. (2021) Awake prone positioning strategy for nonintubated hypoxic patients with COVID-19: A pilot trial with embedded implementation evaluation. *Ann. Am. Thorac. Soc*. **18(8)**, 1360–1368.

Touchon, F., Trigui, Y., Prud'homme, E., Lefebvre, L., Giraud, A., Dols, A.-M., Martinez, S., Bernardi, M., Begne, C., Granier, P., Chanez, P., Forel, J.-M., Papazian, L., Elharrar, X. (2021) Awake prone positioning for hypoxaemic respiratory failure: Past, COVID-19 and perspectives. *Eur. Respir. Rev*. **30(160)**, 210022.

Venus, K., Munshi, L., Fralick, M. (2020) Prone positioning for patients with hypoxic respiratory failure related to COVID-19. *CMAJ* **192(47)**, E1532–E1537.

Walkey, A. J., Wiener, R. S. (2013) Use of noninvasive ventilation in patients with acute respiratory failure, 2000–2009: A population-based study. *Ann. Am. Thorac. Soc*. **10(1)**, 10–17.

Wan, X., Wang, W., Liu, J., Tong, T. (2014) Estimating the sample mean and standard deviation from the sample size, median, range and/or interquartile range. *BMC Med. Res. Methodol*. **14**, 135.

Weatherald, J., Solverson, K., Zuege, D. J., Loroff, N., Fiest, K. M., Parhar, K. K. S. (2021) Awake prone positioning for COVID-19 hypoxemic respiratory failure: A rapid review. *J. Crit. Care* **61**, 63–70.

Winearls, S., Swingwood, E. L., Hardaker, C. L., Smith, A. M., Easton, F. M., Millington, K. J., Hall, R. S., Smith, A., Curtis, K. J. (2020) Early conscious prone positioning in patients with COVID-19 receiving continuous positive airway pressure: A retrospective analysis. *BMJ Open Respir. Res*. **7(1)**, e000711.

 Prague Medical Report / Vol. 123 (2022) No. 3, p. 166–180

Disturbance in Serum Levels of IL-17 and TGF-β1 and in Gene Expression of ROR-γt and FOX-P3 Is Associated with Pathogenicity of Systematic Lupus Erythematosus

Hanaa N. Ali[1], Ghassaq T. Alubaidi[2], Faiq I. Gorial[3], Ilham A. Jasim[2]
[1]Microbiology Unit, Emam Ali Hospital, Baghdad, Iraq;
[2]Medical Research Unit, College of Medicine, Al-Nahrain University, Baghdad, Iraq;
[3]Rheumatology Unit, Department of Medicine, College of Medicine, University of Baghdad, Baghdad, Iraq

Received December 27, 2021; Accepted August 2, 2022.

Key words: SLE – IL-17 – TGF-β1 – IL-17/TGF-β1 – ROR-γt/FOX-P3

Abstract: To investigate the disturbance in serum levels of interleukin-17 (IL-17) and transforming growth factor-beta1 (TGF-β1) and gene expression of retinoic acid-related orphan receptor-gamma t (ROR-γt) and forkhead box-P3 (FOX-P3) in patients with systemic lupus erythematosus (SLE) and to study their association with disease pathogenicity and activity. Newly diagnosed active patients with SLE (n=88) and healthy volunteers (n=70) were included. Serum IL-17 and TGF-β1 were measured using enzyme-linked immunosorbent assay. Gene-expression profiles of ROR-γt and FOX-P3 were screened using real-time polymerase chain reaction. The IL-17/TGF-β1 and ROR-γt/FOX-P3 levels were also calculated. The mean age of the patients was 30.96±8.25 years; they were 82 women and 6 men. Of the patients, 11.4% manifested mild disease while 88.6% had severe disease. The serum level of TGF-β1 was significantly lower (70.2±34.9 vs. 200.23±124.77 pg/ml), while both IL-17 (614.7±317.5 vs. 279.76±110.65 pg/ml) and IL-17/TGF-β1 (18.5±30.1 vs. 1.66±0.9) levels were significantly higher, in patients than in controls ($p<0.0001$). The gene-expression level of FOX-P3 (0.6±0.8 vs. 13.68±39.35) was reported to be lower, while ROR-γt (3.9±3.5 vs. 1.99±2.09) and ROR-γt/FOX-P3 (18.6±21.1 vs. 7.63±17.19) levels were significantly higher, in patients than in controls ($p<0.0001$). Disturbance in serum levels of IL-17 and TGF-β1 in T helper-17 and T-regulatory

Mailing Address: Dr. Ghassaq T. Alubaidi, Medical Research Unit, Faculty of Medicine, Al-Nahrain University, Alkadhmiyia Street 60, 10006 Baghdad, Iraq; e-mail: ghasaqtariq119@gmail.com

https://doi.org/10.14712/23362936.2022.15
© 2022 The Authors. This is an open-access article distributed under the terms of the Creative Commons Attribution License (http://creativecommons.org/licenses/by/4.0).

cells proliferation was highlighted through an imbalance in the gene expression of FOX-P3 and ROR-γt, as both are signature genes for the two cell types, respectively. These findings underscore the critical role of IL-17 and TGF-β1 in SLE development, rendering them potential targets for developing novel immunotherapeutic strategies.

Introduction

Systemic lupus erythematosus (SLE) is a chronic, debilitating, systemic autoimmune disease. Excessive innate immune response contributes to SLE pathogenicity through tissue damage due to extensive production of proinflammatory cytokines, as well as by activation of autoreactive T- and B-cells, which in turn leads to autoantibody production, immune complex deposition, and organ failure (Schinocca et al., 2021). Several key factors are associated with SLE pathogenesis, including cytokine imbalance, oxidative stress, and apoptosis. Interleukin (IL-)17, IL-23, IL-21, and transforming growth factor beta 1 (TGF-β1) have only recently been distinguished for their pathogenic roles in SLE (Metawie et al., 2015; Schinocca et al., 2021).

Cytokines play a complex role in SLE pathogenesis. In patients with active SLE marked by extensive organ damage, IL-17 levels are high. The T helper (Th-)17 cell subset is the main producer of IL-17, wherein the retinoic acid-related orphan receptor gamma t (ROR-γt) is the signature transcriptional factor that primarily controls cell differentiation (Capone and Volpe, 2020). IL-17A and IL-17F both contribute to systemic inflammation associated with bone-cartilage destruction and generalized tissue damage, and the expanded population of Th-17 cells was defined in the peripheral blood of patients with SLE (Robert and Miossec, 2020).

The TGF-β1 isoform is the most potent immunosuppressant mediator that controls cell proliferation and fate via apoptosis. TGF-β1 is a substantial negative regulator of B-cell proliferation and differentiation, thereby dampening the production of immunoglobulins, with a distinctive role in T-cell proliferation, differentiation, and homeostasis (Oh and Li, 2013; Metawei et al., 2015). TGF-β1 production is reduced in patients with SLE, which could predispose them to autoreactive T-cell development and pathogenic autoantibody production (Metawei et al., 2015). A specific subset of TGF-β1-deficient mice showed early mortality, pointing to their crucial role in maintaining tolerance (Oh and Li, 2013). Both TGF-β and the transcription factor forkhead box-P3 (FOX-P3) act synergistically to promote T-reg cell differentiation. Conversely, the presence of TGF-β and IL-6 dampens T-reg cells and enhances Th-17 differentiation by inhibiting FOX-P3 and promoting RORc (Robert and Miossec, 2020).

T-reg cells produce IL-10, IL-35, and TGF-β; additionally, they stimulate IL-2 and TGF-β, which play a protective role in autoimmune diseases by inhibiting effector T-cell activity. However, in SLE, when IL-6 levels increase, T-reg cells are converted into Th-17 cells (Yuliasih et al., 2019). Immunotherapy agents have recorded more successful outcomes in inflammatory joint disorders than in SLE. This may be due to the complexity of the immunological profile of SLE (Becker-Merok et al., 2010).

To understand the abnormalities that lead to SLE development at the cytokine and cellular levels pertaining to the IL-17 and TGF-β1 axes, the aim of the present study was to reveal the immune balance between IL-17 and TGF-β1 and the gene-expression balance between ROR-γt and FOX-P3 in patients with SLE, and their relationship with disease pathogenicity and activity.

Material and Methods

This case-control study was conducted between December 2020 and March 2021. Eighty-eight patients visiting the Rheumatology Unit, Baghdad Teaching Hospital, Iraq, fulfilling the European League Against Rheumatism/American College of Rheumatology (EULAR/ACR) classification criteria for SLE (Petri et al., 2012) and 70 healthy age- and sex-matched controls were included. Participants aged <18 years, those with cancer, and those with other autoimmune and/or infectious diseases were excluded.

Data were collected through direct interviews and blood samples were collected. The SLE Disease Activity Index (SLEDAI) (Bombardier et al., 1992) was also evaluated. Disease activity was scored as follows: ≤ 3, no flare; score 3–12 indicating moderate disease activity; and > 12, severe flare (Gladman et al., 2000).

The study protocol was approved by the institutional review board of the College of Medicine/Al-Nahrain University (Approval No. 202011115). All the participants provided written informed consent.

Quantification of cytokines

Absolute serum levels of IL-17A and TGF-β were determined using the sandwich enzyme-linked immunosorbent assay (ELISA) technique (Human IL-17A and TGF-β kits, Abnova, Korea), according to the manufacturer's instructions. The results were expressed as optical density (OD), read at 450 nm, and calculated according to the OD of standards. As TGF-β is mostly present in an inactive form, activating reagents were used. The minimally detectable rate was 16.5 pg/ml for both IL-17A and TGF-β.

Quantitative mRNA expression

Quantitative mRNA expression of ROR-γt and FOX-P3 in peripheral mononuclear cells (PMNCs) was analysed using reverse-transcription polymerase chain reaction (RT-PCR). Blood samples were collected in ethylenediaminetetraacetic acid (EDTA) vacutainer tubes. Total RNA was extracted (Wizbio Solution, Korea) within 3 h of sample collection. The concentration and purity of the extracted RNA were further verified by measuring the absorption at 260 nm and 260/280 ratio, respectively (Nanodrop spectrophotometer/Thermo scientific). The eluted RNA was subjected to complementary DNA (cDNA) synthesis (Wizbio solutions/Korea) on the same day as the RNA extraction. Cycling conditions were as follows: 25 °C for 10 min, 42 °C for 30 min, and 4 °C for hold. Synthesized cDNA samples were stored

at –20 °C until use. For RT-PCR, glyceraldehyde 3-phosphate dehydrogenase (GADPH) was used as a housekeeping gene. Primers (Applied Biological Materials/ Canada) were as follows:

FOX-P3: forward (TACAGCACGGTATGCAAGCC);
reverse (GCAACCGATCTAGCTCACAGAG).
ROR-γt: forward (AGATTACTACAACCGATCCACCT);
reverse (GGGGACAGAGTTCATGTGGTA).
GADPH: forward (CATGTTCGTCATGGGTGTGAACCA);
reverse (AGTGATGGCATGGACTGTGCTCAT).

Two microliters cDNA, 10 µl mastermix-SYBR Green (KAPA SYBR Fast qPCR [2X]/USA), 2 µl primers were added to the reaction tube and completed to 20 µl RNase free water in an automated thermocycler (Sacace Biotechnologies/Italy) programmed as follows: enzyme activation 95 °C/5 min, denaturation 95 °C/20 s, annealing 60 °C/20 s (40 cycles), and extension at 72 °C for 20 s.

Statistical analysis

It was conducted using the Statistical Package for the Social Sciences (SPSS) software, version 23. Data are presented as mean ± SD (standard deviation), median and interquartile range (IQR), or n (%). The Mann-Whitney test was applied to compare the two groups. The receiver operating characteristic (ROC) curve was used to identify sensitivity and specificity. The area under the curve (AUC) was measured and discrimination considered premium > 0.9, excellent 0.7–0.8, agreeable 0.6–0.7. Statistical significance was set at $p \leq 0.05$.

Results

Clinical and laboratory characteristics of the participants

The age of the patients and controls ranged from to 18 to 50 years. The mean age of the patients was 30.96 ± 8.25 years, F:M 13.6:1, and matched with the control parameters (age 29.97 ± 8.06 years and F:M 10.6:1; p=0.45 and p=0.77, respectively). The body mass index (BMI) was also comparable (26.8 ± 4.38 vs. 26.04 ± 4.01; p=0.26). The controls had normal values of haemoglobin (11.79 ± 1.12 g/dl), platelets (235.7 ± 49.54×10^3/mm^3), erythrocyte sedimentation rate (ESR) (13.62 ± 5.3 mm/h), C-reactive protein (CRP) (1.45 ± 1.03 mg/dl), urea (18.24 ± 5.64 mg/dl), creatinine (0.51 ± 0.19 mg/dl), complement C3: 125.81 ± 19.45 mg/dl, complement C4: 35.71 ± 8.05 mg/dl, negative antinuclear antibodies (ANA) (125.81 ± 19.45 IU/ml), and anti-double-stranded deoxyribonucleic acid (anti-dsDNA) (2.29 ± 2.31 IU/ml). None of the participants were smokers. Ten (11.4%) patients and 2 (2.9%) controls had a family history of SLE (p=0.07). Regarding the SLEDAI, 10/88 (11.4%) patients had mild disease, while 78/88 (88.6%) had severe disease. Patient characteristics are presented in Table 1. The laboratory results are presented in Table 2.

Table 1 – Characteristics of the patients with systemic lupus erythematosus (SLE) and healthy controls

Variable		Patients (n=88)	Control (n=70)	p-value
Age (year), mean ± SD		30.96 ± 8.25	29.97 ± 8.06	0.453
BMI (kg/m^2), mean ± SD		26.80 ± 4.38	26.04 ± 4.01	0.261
Sex, n (%)	female male	82 (93.2%) 6 (6.8%)	64 (91.4%) 6 (8.6%)	0.767
Smoking, n (%)	negative positive	88 (100%) 0 (0.0%)	70 (100%) 0 (0.0%)	1.000
Family history, n (%)	absent present	78 (88.6%) 10 (11.4%)	68 (97.1%) 2 (2.9%)	0.067
Disease activity score, n (%)	no flare mild severe	0 (0.0%) 10 (11.4%) 78 (88.6%)		
Organ involvement				
Mucocutaneous	negative positive	20 (22.7%) 68 (77.3%)		
Musculoskeletal	negative positive	18 (20.5%) 70 (79.5%)		
Renal	negative positive	88 (100%) 0 (0.0%)		
Cardiovascular	negative positive	82 (93.2%) 6 (6.8%)		
Serositis	negative positive	88 (100%) 0 (0.0%)		
Neuropsychiatric	negative positive	52 (59.1%) 36 (40.9%)		
Hematological	negative positive	0 (0.0%) 88 (100%)		
Fever	negative positive	16 (18.2%) 72 (81.8%)		
Hair loss	negative positive	0 (0.0%) 88 (100%)		

BMI – body mass index; SD – standard deviation

Comparison of IL-17 and TGF-β levels between patients with SLE and healthy controls
The medians of IL-17 and TGF-β levels in patients with SLE (n=88) were compared to those of controls (n=70) using the Mann-Whitney test. Sandwich ELISA showed a significantly elevated level of circulating IL-17 in patients with SLE than in healthy controls, with a median of 594.61 pg/ml vs. 319.83 pg/ml ($p<0.001$). TGF-β1 levels

Table 2 – Comparison of laboratory markers between patients with systemic lupus erythematosus (SLE) and healthy controls

Variable	Patients (n=88)			Control (n=70)			p-value
	median	mean ± SD	IQR	median	mean ± SD	IQR	
dsDNA (IU/ml)	80.07	80.36 ± 55.48	77.0	1.89	2.29 ± 2.31	3.0	<0.001
ANA (IU/ml)	19.85	29.93 ± 38.40	37.0	0.32	0.36 ± 0.25	0.0	<0.001
C3 (mg/dl)	36.40	45.01 ± 38.15	36.0	122.45	125.81 ± 19.45	28.0	<0.001
C4 (mg/dl)	11.20	11.52 ± 7.58	8.0	36.00	35.71 ± 8.05	14.0	<0.001
ESR (mm/h)	45.00	54.32 ± 33.10	40.3	12.50	13.62 ± 5.3	7.0	<0.001
CRP (mg/dl)	2.70	2.92 ± 2.47	2.0	1.17	1.45 ± 1.03	2.0	<0.001
Hb (g/dl)	11.15	10.99 ± 1.72	2.0	11.85	11.79 ± 1.12	1.0	0.008
Platelet ($\times 10^3/mm^3$)	144.00	160.56 ± 87.77	106.0	230.00	235.7 ± 49.54	76.0	<0.001
Urea (mg/dl)	27.00	28.12 ± 13.16	19.0	17.50	18.24 ± 5.64	7.0	<0.001
Creatinine (mg/dl)	0.62	0.62 ± 0.24	0.0	0.50	0.51 ± 0.19	0.0	0.005

Hb – hemoglobin; CRP – C-reactive protein; C3 – complement 3; C4 – complement 4; ANA – antinuclear antibody; dsDNA – double-stranded deoxyribonucleic acid; ESR – erythrocyte sedimentation rate; IQR – interquartile range; SD – standard deviation

Table 3 – Comparison between patients with systemic lupus erythematosus (SLE) and healthy controls regarding interleukin-17 (IL-17), transforming growth factor beta 1 (TGF-β1), forkhead box-P3 (FOX-P3), and retinoic acid-related orphan receptor gamma t (ROR-γt)

Variable	Patients (n=88)		Control (n=70)		p-value
	median (IQR)	mean ± SD	median (IQR)	mean ± SD	
TGF-β1 (pg/ml)	76.4 (59.7)	70.2 ± 34.9	168.1 (69.6)	200.23 ± 124.77	<0.001
IL-17A (pg/ml)	594.6 (271.5)	614.7 ± 317.5	319.8 (191.9)	279.76 ± 110.65	<0.001
IL-17A/ TGF-β1	8.70 (14.5)	18.5 ± 30.1	1.60 (1.4)	1.66 ± 0.90	<0.001
FOX-P3*	0.28 (0.57)	0.6 ± 0.8	0.80 (5.1)	13.68 ± 39.35	0.001
ROR-γt*	3.01 (3.14)	3.9 ± 3.5	1.01 (2.8)	1.99 ± 2.09	<0.001
ROR/ FOX-P3	8.82 (18.2)	18.6 ± 21.1	0.90 (6.7)	7.63 ± 17.19	<0.001

IL-17 – interleukin-17; TGF-β1 – transforming growth factor beta 1; FOX-P3 – forkhead box-P3; ROR-γt – retinoic acid-related orphan receptor gamma t; IQR – interquartile range; SD – standard deviation; *the marker was determined by relative gene expression

were lower in patients with SLE than in controls (76.38 pg/ml vs. 168.13 pg/ml) (p<0.001). The IL-17/TGF-β ratio was significantly higher among patients with SLE (8.69), in comparison to that seen in controls (1.61%) (p<0.001). Comparisons of IL-17 and TGF-β levels and mRNA expression of FOX-P3 and ROR-γt between patients and controls are presented in Table 3.

Differential mRNA expression of FOX-P3 and ROR-γt in patients with SLE and healthy controls

The medians of FOX-P3 and ROR-γt of patients with SLE (n=88) were compared with those of controls (n=70) using the Mann-Whitney test. Quantitative measurement of mRNA expression of FOX-P3 using RT-PCR revealed that its relative gene expression in patients with SLE was 0.28 compared to 0.76 in healthy controls, which was significantly lower (p=0.001). However, the gene expression of ROR-γt in patients with SLE was 3.0, which was significantly higher than that in healthy controls (1.0) (p<0.001). Furthermore, the ROR-γt/FOX-P3 ratio was higher in patients with SLE (8.8) than in healthy controls (0.91) (p<0.001). Comparison of IL-17 and TGF-β levels and mRNA expression of FOX-P3 and ROR-γt in patients according to disease activity grade is shown in Table 4.

Table 4 – Comparison between patients with systemic lupus erythematosus (SLE) according to disease activity regarding interleukin-17 (IL-17), transforming growth factor beta 1 (TGF-β1), forkhead box-P3 (FOX-P3) and retinoic acid-related orphan receptor gamma t (ROR-γt)

Variable	Mild activity (n=10)		Severe activity (n=78)		p-value
	median (IQR)	mean ± SD	median (IQR)	mean ± SD	
TGF-β1 (pg/ml)	86.4 (56.3)	81.4 ± 28.8	72.8 (69)	68.8 ± 35.6	0.360
IL-17A (pg/ml)	555.7 (251.7)	582.6 ± 146.8	601.3 (256.7)	618.8 ± 333.5	0.730
IL-17A/ TGF-β1	8.90 (4.5)	7.9 ± 2.9	8.50 (15.4)	19.8 ± 31.7	0.490
FOX-P3*	0.41 (0.9)	0.7 ± 0.8	0.25 (0.5)	0.5 ± 0.8	0.510
ROR-γt*	6.23 (6.5)	7.4 ± 5.7	2.91 (2.6)	3.5 ± 2.9	0.003
ROR/ FOX-P3	17.60 (41.5)	29.7 ± 29.8	8.80 (17)	17.2 ± 19.5	0.150

IL-17 – interleukin-17; TGF-β1 – transforming growth factor beta 1; FOX-P3 – forkhead box-P3; ROR-γt – retinoic acid-related orphan receptor gamma t; IQR – interquartile range; SD – standard deviation; *the marker was determined by relative gene expression

The ROC analysis of IL-17, TGF-β1 and IL-17/TGF-β1 ratio

For differential diagnosis, ROC analysis showed that the AUC for TGF-β1 was 0.988, with 91.4% sensitivity and 97.9% specificity under a 116.7 cut-off value. For IL-17, the AUC was 0.918, with 81.8% sensitivity and 88.6% specificity under a 392.8 cut-off value. For IL-17/TGF-β, the AUC was 0.99, with 90.9% sensitivity and 97.1% specificity under a 3.38 cut-off value (Figure 1).

The ROC analysis of FOX-P3, ROR-γt, and ROR-γt/FOX-P3 ratio

For differential diagnosis, ROC analysis showed that FOX-P3 had an AUC of 0.661, with 54.3% sensitivity and 59.1% specificity, and 0.44 cut-off value. ROR-γt had an AUC of 0.710, with 68.2% sensitivity and 68.6% specificity, under a cut-off value of 2.23. Regarding ROR-γt/FOX-P3, it had an AUC of 0.797, with 72.7% sensitivity and 74.3% specificity, with 5.42 cut-off value (Figure 2).

Discussion

Systemic lupus erythematosus results from global self-tolerance collapse and is characterized by an aberrant innate immune response that contributes to tissue injury via the release of inflammatory mediators (Lee et al., 2016).

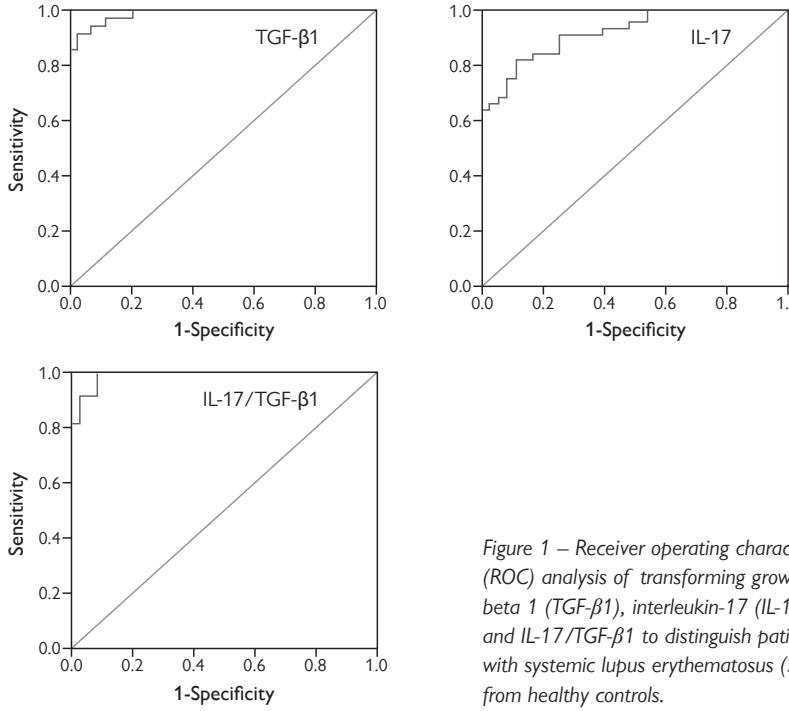

Figure 1 – Receiver operating characteristic (ROC) analysis of transforming growth factor beta 1 (TGF-β1), interleukin-17 (IL-17), and IL-17/TGF-β1 to distinguish patients with systemic lupus erythematosus (SLE) from healthy controls.

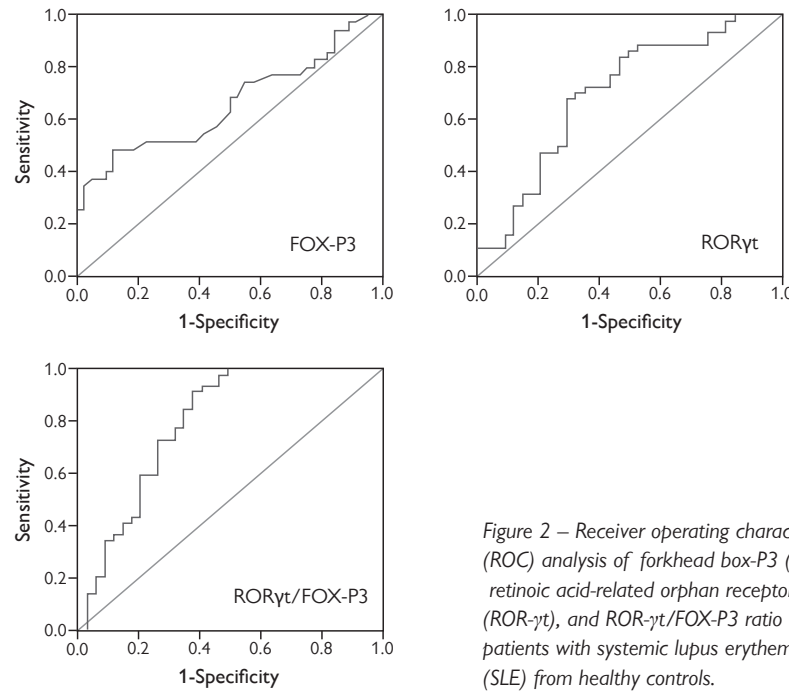

Figure 2 – Receiver operating characteristic (ROC) analysis of forkhead box-P3 (FOX-P3), retinoic acid-related orphan receptor gamma t (ROR-γt), and ROR-γt/FOX-P3 ratio to distinguish patients with systemic lupus erythematosus (SLE) from healthy controls.

The present study pointed to a significant female predominance (1:13.6 male:female ratio), which concurs with previous Iraqi and international studies (Al-Hattab and Al-Waiz, 2004). Notably, none of the patients were smokers, probably because most of them are women, and, by inference, non-smokers, due to pervasive cultural factors in Iraq. The most prevalent clinical manifestations were mucocutaneous (77.3%), musculoskeletal (79.5%), neuropsychiatric (40.9%), cardiovascular (6.8%), and fever (81.8%). None of the patients had renal or serositis involvement, which may be because the cases were newly diagnosed. It is likely that renal manifestations are observed on follow-up. Additionally, the cases were collected from a tertiary rheumatology center, and, possibly, cases with musculoskeletal manifestations were referred to, while those with renal manifestations were referred to the nephrology centers. Regarding the high percentage of neuropsychiatric manifestations, the occurrence of a particular neurological or psychiatric syndrome does not necessarily imply that SLE is the underlying cause, particularly with relatively common syndromes. Certain neurological symptoms may be coincidental, while others may arise from treatment complications or comorbidity. The present study recorded a disturbance in the serum levels of IL-17 and TGF-β1 in patients with SLE in comparison to control levels, and the IL-17/TGF-β ratio was significantly higher. IL-17, TGF-β, and their ratios were not significantly related to disease activity grade. In another study, IL-17 was found to be associated with disease activity (Chen et al., 2010). Concordantly, IL-17 family members are involved in several chronic inflammatory disorders, such as SLE, with an elevated serum concentration of IL-17 (Chen et al., 2010) and the number of Th-17 cells (Xing et al., 2012). Other studies have reported increased circulating levels of IL-17 in patients with SLE, with no association with disease activity (Zhao et al., 2010; Vincent et al., 2013). Conversely, comparable serum levels of IL-17 in patients with SLE and controls without a clear link to disease activity have been reported (Schinocca et al., 2021).

The pathogenic action of IL-17 is an essential attribute of acute inflammation; it is involved in neutrophil infiltration via a pathway distinct from that of IL-1 and TNF-α (Liu et al., 2016). Elevated circulating IL-17 levels have also been recorded in other autoimmune disorders, psoriasis, and ankylosing spondylitis, and its antagonists have been potentially successful (Schinocca et al., 2021). IL-17 is also capable of inducing inflammation through mediators, such as matrix metalloproteinases and nitric oxide, which is being implemented in patients with SLE, it is associated with disease activity and renal injury (Adamidis et al., 2019). The pathologic role of IL-17 in the development of rheumatic diseases such as SLE has led to the emergence of novel anti-IL-17 drugs, such as secukinumab (Rafael-Vidal et al., 2020).

TGF-β1 levels are significantly lower in patients with SLE than in healthy controls and are not associated with disease activity (El Menyawi et al., 2018). Another Egyptian study reported a significantly reduced level of TGF-β1 in patients with SLE in comparison to the control level; in contrast, they emphasized that low plasma

TGF-β1 levels are associated with high disease activity and severe renal damage (Metawie et al., 2015). Abnormal levels of TGF-β have been reported in patients with SLE, associated with both disease activity and renal damage (Becker-Merok et al., 2010). It is speculated that the reduction in serum TGF-β1 is associated with SLE through its role in abrogating T-reg cell function and differentiation (Joshi et al., 2014). Another proposed mechanism for TGF-β implementation in immunoregulation is through the induction of naive $CD4^+$ T cell differentiation into Th-3 cells, which are found to play a remarkable role in inducing peripheral tolerance through elevated TGF-β secretion, with low amounts of IL-10 and IL-4 (Carrier et al., 2007). Patients with SLE who reported reduced plasma TGF-β levels showed autoreactive T-cell activation and differentiation, in addition to pathogenic autoantibody production. Simultaneously, TGF-β1 upregulation may worsen outcomes. Although TGF-β plays a pivotal role in maintaining immune tolerance, direct signalling blockade may result in critical adverse effects, owing to its pleiotropic effect. This represents an obstacle in the development of direct TGF-β1 therapy or neutralizing antibodies (Komai et al., 2018).

Notably, disturbances in IL-17 and TGF-β levels may be driven by polymorphisms in the genes encoding these two cytokines or their receptors, which may culminate in the development of SLE (Hristova et al., 2021).

In a prior *in vivo* study, the IL-17/TGF-β1 ratio was increased in comparison to that seen in the control (Poeranto, 2019). A previous study conducted in India highlighted the association between cytokine imbalance and autoimmune diseases; they recorded an increase in INF-γ/IL-10 in patients with vitiligo in comparison to the ratio in healthy individuals (Ala et al., 2015).

In the present study, the gene-expression level of FOX-P3 was lower in patients than in controls, and the ROR-γt and ROR-γt/FOX-P3 levels were higher. However, ROR-γt levels were significantly higher in patients with mild activity than in those with severe activity. An increase in peripheral ROR-γt gene expression indicates an increase in activation and proliferation of Th-17 cells. As ROR-γt is the master regulator gene in Th-17 cells, it controls differentiation and induces IL-17A and IL-17F expression. Furthermore, naive $CD4^+$ helper cells require ROR-γt to respond to IL-6 and TGF-β, which are required for Th-17 differentiation (Lamb et al., 2021). Concordant with the findings of the current study, an increase in the number of Th-17 cells in patients with SLE in comparison to that seen in controls has been reported, which is significantly correlated with disease activity and renal injury (Narani, 2019).

Th-17 cells are implicated in the pathogenesis of autoimmune diseases not only for their critical role in producing IL-17; these cells also produce IL-21, which has been implicated in autoimmune diseases, including SLE, and its mRNA expression is associated with disease severity (Liu and King, 2013). Th-17 cells produce a wide range of inflammatory mediators, including IL-22, IL-26, IL6, TNF-α, GM-CSF, and chemokines (Schinocca et al., 2021). Th-17 cells profoundly express IL-23 receptors,

thereby conditioning them for IL-23 stimulation, considering that IL-23-induced Th-17 cells are more pathogenic compared with IL-12-induced Th-17 cells (Ouyang et al., 2008).

Reduced FOX-P3 gene expression in patients is also concordant with the results of other studies (Miyara et al., 2005; Álvarez-Rodríguez et al., 2019; Yuliasih et al., 2019). In contrast, other researchers have reported an association between FOX-P3 and disease manifestations (Miyara et al., 2005). FOX-P3 is a master controller of T-reg cell gene expression. The suppressive effect of T-reg cells is mediated by CTLA-4, which is a highly expressed molecule on the surface of T-regs. It is involved in the suppression of T-reg cells through two mechanisms: their interaction with CD80/86 co-stimulatory molecules on antigen-presenting cells (APCs) inhibits their expression. Additionally, CTLA-4 interaction with CD80/86 induces "indoleamine 2,3 dioxygenase", which controls the synthesis of pro-apoptotic metabolites, thereby inhibiting the activation of effector T-cells (Rowshanravan et al., 2018).

Both TGF-β and T-reg cells may be involved in autoimmunity via a B cell-dependent pathway. When autoantigens are expressed at low levels, they are presented by B cells, which produce autoantibodies in addition to various cytokines, primarily TGF-β, which modulates the conversion of $CD4^+$ T cells to T-reg (Rowshanravan et al., 2018). It has been found that IL-2 plays a crucial role in limiting $CD8^+$ T cell activation; however, simultaneously, it shows a potential role in improving T-reg suppression function through STAT5, highlighting the importance of IL-2 agonists as therapeutic agents for SLE, mainly because T-regs extensively express IL-2 receptors (Chinen et al., 2016).

The present study shows molecular evidence for a peripheral Th-17/T-reg (ROR-γt/FOX-P3) imbalance with no association with disease activity. The role of effector/regulatory cell imbalance in SLE pathogenicity was first recorded *in vivo* and further confirmed by others, from T-reg cells isolated from patients with active SLE (Lee et al., 2008). In agreement, it was reported that Th-17/T-reg was higher among patients with SLE with no link to disease activity (Kleczynska et al., 2011). Another study reported a significantly higher Th-17/T-reg ratio in SLE and in patients with primary antiphospholipid syndrome (Álvarez-Rodríguez et al., 2019). Other studies have reported an increase in Th-17/T-reg among patients with SLE; however, the number of Th-17 cells is still within the normal range, which indicates that the imbalance is the primary independent driving factor of SLE, and not Th-17 solely (Kleczynska et al., 2011). A similar study also reported an increase in Th-17/T-regs in patients with SLE and a significant association with disease activity (Yuliasih et al., 2019). It has been speculated that these two cell subsets consort and frustrate each other's activities to maintain immune homeostasis (Yang et al., 2008). The ROR-γt/FOX-P3 ratio could be applied as an indicator of the immune balance of Th-17/T-regs and is anticipated to be an excellent disease target in patients with SLE. In contrast, TGF-β promotes the generation of T-regs by activating FOX-P3

expression. An imbalance in these cytokines is reflected in the Th-17/T-regs (Mitra et al., 2015).

Circulating cytokines (IL-17, TGF-β1, and IL-17/TGF-β1) showed higher sensitivity and specificity than the peripheral molecular markers (ROR-γt, FOX-P3, and ROR-γt/FOX-P3), making them more suitable for SLE diagnosis and monitoring. Patients with SLE demonstrated disturbance in the Th-17 and T-reg axes compared with controls, with no significant contribution to disease activity. Circulatory cytokine levels are more valuable than the molecular signatures of immune cell subsets for SLE diagnosis.

A limitation of the present study is that a larger number of participants should be analysed, including those receiving various treatment regimens. In addition, more extensive cytokine, chemokine, and immune cell profiles, such as B-cell profiles, should be verified to fully recognize the immune mechanisms underlying disease pathogenesis. Assessment of the cytokine profile at the early onset stage and follow-up is warranted.

Conclusion

IL-17/Th-17 and TGF-β1/T-regs axes and their balance are skewed during SLE manifestation; therefore, immune disturbance is substantially implicated in SLE pathogenicity. Identifying the axes that are abnormal in each patient may pave the way for a precise therapeutic target, especially among those who do not respond to conventional therapy.

References

Adamidis, K. N., Kopaka, M. E., Petraki, C., Charitaki, E., Apostolou, T., Christodoulidou, C., Nikolopoulou, N., Giatromanolaki, A., Vargemesis, V., Passadakis, P. (2019) Glomerular expression of matrix metalloproteinases in systemic lupus erythematosus in association with activity index and renal function. *Ren. Fail*. **41(1)**, 229–237.

Ala, Y., Pasha, M. K., Rao, R. N., Komaravalli, P. L., Jahan, P. (2015) Association of IFN-γ: IL-10 cytokine ratio with nonsegmental vitiligo pathogenesis. *Autoimmune Dis*. **2015**, 8.

Al-Hattab, M. K., Al-Waiz, M. (2004) Discoid lupus erythematosus in Iraqi patients: A clinical and histopathological study. *Ann. Saudi Med*. **24(4)**, 289–292.

Álvarez-Rodríguez, L., Martínez-Taboada, V., Calvo-Alén, J., Beares, I., Villa, I., López-Hoyos, M. (2019) Altered Th17/Treg ratio in peripheral blood of systemic lupus erythematosus but not primary antiphospholipid syndrome. *Front. Immunol*. **10**, 391.

Becker-Merok, A., Eilertsen, G. Ø., Nossent, J. C. (2010) Levels of transforming growth factor-β are low in systemic lupus erythematosus patients with active disease. *J. Rheumatol*. **37(10)**, 2039–2045.

Bombardier, C., Gladman, D. D., Urowitz, M. B., Caron, D., Chang, C. H., Austin, A., Bell, A., Bloch, D. A., Corey, P. N., Decker, J. L., Esdaile, J., Fries, J. F., Ginzler, E. M., Goldsmith, C. H., Hochberg, M. C., Jones, J. V., Le Riche, N. G. H., Liang, M. H., Lockshin, M. D., Muenz, L. R., Sackett, D. L., Schur, P. H. (1992) Derivation of the SLEDAI. A disease activity index for lupus patients. *Arthritis Rheum*. **35(6)**, 630–640.

Capone, A., Volpe, E. (2020) Transcriptional regulators of T helper 17 cell differentiation in health and autoimmune diseases. *Front. Immunol*. **11**, 348.

Carrier, Y., Yuan, J., Kuchroo, V. K., Weiner, H. L. (2007) Th3 cells in peripheral tolerance. I. Induction of Foxp3-positive regulatory T cells by Th3 cells derived from TGF-β T cell-transgenic mice. *J. Immunol*. **178(1)**, 179–185.

Chen, X. Q., Yu, Y. C., Deng, H. H., Sun, J. Z., Dai, Z., Wu, Y. W., Yang, M. (2010) Plasma IL-17A is increased in new-onset SLE patients and associated with disease activity. *J. Clin. Immunol*. **30(2)**, 221–225.

Chinen, T., Kannan, A., Levine, A., Fan, X., Klein, U., Zheng, Y., Gasteiger, G., Feng, Y., Fontenot, J., Rudensky, A. (2016) An essential role for IL-2 receptor in regulatory T cell function. *Nat. Immunol*. **17(11)**, 1322–1333.

El Menyawi, M., Fawzy, M., Habib, M., Shaker, O. (2018) Serum transforming growth factor-beta 1 level in Egyptian systemic lupus erythematosus patients. *Arch. Rheumatol*. **33(3)**, 358–366.

Gladman, D. D., Urowitz, M. B., Kagal, A., Hallett, D. (2000) Accurately describing changes in disease activity in systemic lupus erythematosus. *J. Rheumatol*. **27(2)**, 377–379.

Hristova, M., Kamenarska, Z., Dzhebir, G., Nikolova, S., Hristova, R., Mihova, K., Vinkov, A., Georgiev, T., Pozharashka, J., Kaneva, R., Savov, A., Koundurdjiev, A., Dourmishev, L. (2021) The role of IL-17 rs2275913, IL-17RC rs708567 and TGFB1 rs1800469 SNPs and IL-17A serum levels in patients with lupus nephritis. *Rheumatol. Int*. **41(12)**, 2205–2213.

Joshi, N., Minz, R. W., Anand, S., Parmar, N. V., Kanwar, A. J. (2014) Vitamin D deficiency and lower TGF-β/IL-17 ratio in a North Indian cohort of pemphigus vulgaris. *BMC Res. Notes* **7(1)**, 1–6.

Kleczynska, W., Jakiela, B., Plutecka, H., Milewski, M., Sanak, M., Musial, J. (2011) Imbalance between Th17 and regulatory T-cells in systemic lupus erythematosus. *Folia Histochem. Cytobiol*. **49(4)**, 646–653.

Komai, T., Inoue, M., Okamura, T., Morita, K., Iwasaki, Y., Sumitomo, S., Shoda, H., Yamamoto, K., Fujio, K. (2018) Transforming growth factor-β and interleukin-10 synergistically regulate humoral immunity via modulating metabolic signals. *Front. Immunol*. **9**, 1364.

Lamb, D., De Sousa, D., Quast, K., Fundel-Clemens, K., Erjefält, J. S., Sandén, C., Hoffmann, H. J., Kästle, M., Schmid, R., Menden, K., Delic, D. (2021) RORγt inhibitors block both IL-17 and IL-22 conferring a potential advantage over anti-IL-17 alone to treat severe asthma. *Respir. Res*. **22(1)**, 1–14.

Lee, H. T., Wu, T. H., Lin, C. S., Lee, C. S., Wei, Y. H., Tsai, C. Y., Chang, D. M. (2016) The pathogenesis of systemic lupus erythematosus – From the viewpoint of oxidative stress and mitochondrial dysfunction. *Mitochondrion* **30**, 1–7.

Lee, H. Y., Hong, Y. K., Yun, H. J., Kim, Y. M., Kim, J. R., Yoo, W. H. (2008) Altered frequency and migration capacity of $CD4^+$ $CD25^+$ regulatory T cells in systemic lupus erythematosus. *Rheumatology* **47(6)**, 789–794.

Liu, R., Lauridsen, H. M., Amezquita, R. A., Pierce, R. W., Jane-Wit, D., Fang, C., Pellowe, A. S., Kirkiles-Smith, N. C., Gonzalez, A. L., Pober, J. S. (2016) IL-17 promotes neutrophil-mediated immunity by activating microvascular pericytes and not endothelium. *J. Immunol*. **197(6)**, 2400–2408.

Liu, S. M., King, C. (2013) IL-21-producing Th cells in immunity and autoimmunity. *J. Immunol*. **191(7)**, 3501–3506.

Metawie, S. A., ElRefai, R. M., ElAdle, S. S., Shahin, R. M. H. (2015) Transforming growth factor-β1 in systemic lupus erythematosus patients and its relation to organ damage and disease activity. *Egyptian Rheumatologist* **37(4)**, S49–S54.

Mitra, S., Anand, S., Das, A., Thapa, B., Chawla, Y. K., Minz, R. W. (2015) A molecular marker of disease activity in autoimmune liver diseases with histopathological correlation; FoXp3/RORγt ratio. *APMIS* **123(11)**, 935–944.

Miyara, M., Amoura, Z., Parizot, C., Badoual, C., Dorgham, K., Trad, S., Nochy, D., Debré, P., Piette, J. C.,

Gorochov, G. (2005) Global natural regulatory T cell depletion in active systemic lupus erythematosus. *J. Immunol*. **175(12)**, 8392–8400.

Narani, A. (2019) Systemic lupus erythematosus (SLE) – A review of clinical approach for diagnosis and current treatment strategies. *Jaffna Medical Journal* **31(2)**, 9–13.

Oh, S. A., Li, M. O. (2013) TGF-β: Guardian of T cell function. *J Immunol*. **191(8)**, 3973–3979.

Ouyang, W., Kolls, J. K., Zheng, Y. (2008) The biological functions of T helper 17 cell effector cytokines in inflammation. *Immunity* **28(4)**, 454–467.

Petri, M., Orbai, A. M., Alarcon, G. S., Gordon, C., Merrill, J. T., Fortin, P. R., Bruce, I. N., Isenberg, D., Wallace, D. J., Nived, O., Sturfelt, G., Ramsey-Goldman, R., Bae, S. C., Hanly, J. G., Sánchez-Guerrero, J., Clarke, A., Aranow, C., Manzi, S., Urowitz, M., Gladman, D., Kalunian, K., Costner, M., Werth, V. P., Zoma, A., Bernatsky, S., Ruiz-Irastorza, G., Khamashta, M. A., Jacobsen, S., Buyon, J. P., Maddison, P., Dooley, M. A., van Vollenhoven, R. F., Ginzler, E., Stoll, T., Peschken, C., Jorizzo, J. L., Callen, J. P., Lim, S. S., Fessler, B. J., Inance, M., Kamen, D. L., Rahman, A., Steinsson, K., Franks, A. G. Jr., Sigler, L., Hameed, S., Fang, H., Pham, N., Brey, R., Weisman, M. H., McGwin, G. Jr., Magder, L. S. (2012) Derivation and validation of the Systemic Lupus International Collaborating Clinics classification criteria for systemic lupus erythematosus. *Arthritis Rheum*. **64(8)**, 2677–2686.

Poeranto, S. (2019) Escalating dose antigen specific therapy with dsDNA injection regulate inflammatory cells in pristane-induced lupus mice model. *Journal of Stem Cell Research and Tissue Engineering* **3(1)**, 22–33.

Rafael-Vidal, C., Perez, N., Altabas, I., Garcia, S., Pego-Reigosa, J. (2020) Blocking IL-17: A promising strategy in the treatment of systemic rheumatic diseases. *Int. J. Mol. Sci*. **21**, 7100.

Robert, M., Miossec, P. (2020) Interleukin-17 and lupus: Enough to be a target? For which patients? *Lupus* **29(1)**, 6–14.

Rowshanravan, B., Halliday, N., Sansom, D. M. (2018) CTLA-4: A moving target in immunotherapy. *Blood* **131(1)**, 58–67.

Schinocca, C., Rizzo, C., Fasano, S., Grasso, G., La Barbera, L., Ciccia, F., Guggino, G. (2021) Role of the IL-23/IL-17 pathway in rheumatic diseases: an overview. *Front. Immunol*. **12**, 637829.

Vincent, F. B., Northcott, M., Hoi, A., Mackay, F., Morand, E. (2013) Clinical association of serum interleukin-17 in systemic lupus erythematosus. *Arthritis Res. Ther*. **15**, R97.

Xing, Q., Wang, B., Su, H., Cui, J., Li, J. (2012) Elevated Th17 cells are accompanied by FoxP3+ Treg cells decrease in patients with lupus nephritis. *Rheumatol. Int*. **32(4)**, 949–958.

Yang, X. O., Nurieva, R., Martinez, G. J., Kang, H. S., Chung, Y., Pappu, B. P., Shah, B., Chang, S. H., Schluns, K. S., Watowich, S. S., Feng, X. H., Jetten, A. M., Dong, C. (2008) Molecular antagonism and plasticity of regulatory and inflammatory T cell programs. *Immunity* **29(1)**, 44–56.

Yuliasih, Y., Rahmawati, L. D., Putri, R. M. (2019) Th17/Treg ratio and disease activity in systemic lupus erythematosus. *Caspian J. Intern. Med*. **10(1)**, 65–72.

Zhao, X. F., Pan, H. F., Yuan, H., Zhang, W. H., Li, X. P., Wang, G. H., Wu, G. C., Su, H., Pan, F. M., Li, W. X., Li, L. H., Chen, G. P., Ye, D. Q. (2010) Increased serum interleukin 17 in patients with systemic lupus erythematosus. *Mol. Biol. Rep*. **37(1)**, 81–85.

Impact of Hemorrhagic Stroke on Molar Bite Force: A Prospective Study

Gabriel Pádua da Silva[1,2], Edson Donizetti Verri[1,3], Marcelo Palinkas[1,4,5], Camila Roza Gonçalves[1,6], Paula Napolitano Gonçalves[1], Robson Felipe Tosta Lopes[1,2], Guilherme Gallo Costa Gomes[1], Isabela Hallak Regalo[1], Selma Siéssere[1,5], Simone Cecilio Hallak Regalo[1,5]

[1]School of Dentistry of Ribeirão Preto, University of São Paulo, São Paulo, Brazil;
[2]UNIFAFIBE, Bebedouro, Brazil;
[3]Claretiano, University Center of Batatais, Batatais, Brazil;
[4]Faculty Anhanguera, Ribeirão Preto, São Paulo, Brazil;
[5]National Institute for Translational Medicine (INCT-TM), Ribeirão Preto, Brazil;
[6]Hospital do Amor, Barretos, Brazil

Received February 25, 2022; Accepted August 2, 2022.

Key words: Cerebrovascular disorders – Stroke – Bite force – Record – Stomatognathic system

Abstract: Stroke is a neurological deficit of cerebrovascular origin that promotes physical impairments of adult individuals. The present study is aimed to demonstrate whether hemorrhagic stroke affects the maximum molar bite force. The prospective study carried in Centro Universitario Claretiano de Batatais, Brazil, determined the distribution of the sample into two groups: hemorrhagic stroke group (n=18, median age, 62.5 years) and disease-free group (n=18, median age, 62.0 years), with 10 men and 8 women in each group. Subjects were paired one-to-one (age and body mass index). The dynamometer was used to measure the maximum molar bite force (right and left). All analyses were performed with a significance level of 5% (Student's *t*-test). Differences were found on the right (p=0.048) and left (p=0.042) molar bite force, with lower bite force (both sides) in hemorrhagic stroke group. The study suggests that hemorrhagic stroke negatively affects the maximum molar bite force and necessitates changes in food intake to nutritious and softer consistency foods.

This study was supported by the Fundação de Amparo a Pesquisa do Estado de São Paulo (FAPESP, Brazil), and National Institute and Technology – Translational Medicine (INCT.TM), São Paulo.

Mailing Address: Prof. Marcelo Palinkas, PhD., School of Dentistry of Ribeirão Preto, University of São Paulo, Avenida do Café s/n, Bairro Monte Alegre CEP 14040-904, Ribeirão Preto, São Paulo, Brazil; e-mail: palinkas@usp.br

https://doi.org/10.14712/23362936.2022.16
© 2022 The Authors. This is an open-access article distributed under the terms of the Creative Commons Attribution License (http://creativecommons.org/licenses/by/4.0).

Introduction

Stroke is a pathology of the central nervous system, with important implications on global health, characterized by sudden neurological changes resulting from vascular injuries (Markus and Brainin, 2020). It is classified into two subtypes: ischemic, due to a clot that blocks the flow of blood to the brain, and hemorrhagic, due to the rupture of a blood vessel leading to hemorrhage (Tsai et al., 2018).

When there is an injury to the central nervous system, contraction and relaxation of the skeletal striated muscles may be compromised (Ludwig et al., 2020). This pathology can trigger complications in affected individuals, such as motor deficit, reduced balance, and changes in muscle strength, also affecting the stomatognathic system (Umay et al., 2019).

Muscle hypotonia, associated with weakness of all or some reflexes of the human body, is a characteristic stroke sequel. This hypotonia leads to a progressive and slow decrease in muscle tone, causing a reduction in strength (Al-Hassnan et al., 2008). With functional changes in the musculature, the stomatognathic system, which is an extremely complex system consisting of interdependent static and dynamic structures, can be affected, impacting the quality of life of individuals with stroke (Yılmaz et al., 2020).

The masticatory performance of individuals with stroke is compromised due to the reduced strength of orofacial structures such as tongue, lips and muscles, in addition to molar bite force even though there is no significant difference between the ipsi- and contralesional sides (Schimmel et al., 2017).

This study aimed to determine the maximum molar bite force in individuals with hemorrhagic stroke in order to understand the functional dynamics of the stomatognathic system. The null hypothesis of this study was that the hemorrhagic stroke group would not present changes in relation to the maximum molar bite force when compared to the disease-free group.

Material and Methods

Study design

All procedures followed this prospective and observational study were in accordance with the ethical standards of the responsible committee on human experimentation (School of Dentistry of Ribeirão Preto, University of São Paulo, process # 92222318.8.0000.5419). The informed consent form was signed by the individuals selected to participate in the sample.

Post hoc test (α=0.05) was applied to confirm the sample size of the groups. Sample size calculation indicated that the required number of individuals was 18 for each group (power of 84% and effect size of 0.68). We used the G* Power program (Franz Faul, Kiel, Germany) to validate the sample data.

Following the inclusion and exclusion criteria, eighteen individuals (mean age [SD – standard deviation], 62.5 [3.2] years), out of a total of 40 individuals evaluated, with hemorrhagic stroke that provided problems in the right side of body,

Table 1 – Depicting inter group comparison of anthropometric measurements

Variables	Group	Mean ± std. error	P-value
Body mass index	hemorrhagic stroke disease-free	27.69 ± 0.91 26.91 ± 0.57	0.477
Age	hemorrhagic stroke disease-free	62.5 ± 3.2 62.0 ± 3.2	0.923

diagnosed over a period of more than five years by neurologists at the Centro Universitário Claretiano de Batatais were selected in the case group. The case and disease-free groups (mean age [SD], 62.0 [3.2] years), with 10 men and 8 women in each group, were paired one-to-one by sex, age, and body mass index (Table 1).

The inclusion criteria were individuals with all teeth except the third molars, normal occlusion, and absence of temporomandibular dysfunction according to the Research Diagnostic Criteria for Temporomandibular Disorders. The exclusion criteria were completely and partially edentulous patients, those with a complete and partial prosthesis; diagnosis period of hemorrhagic stroke less than five years; not undergoing clinical treatment; having ulcerations, wounds, or skin hypersensitivity; having cognitive problems; and the presence of chronic-degenerative diseases. Five years of time span were considered because of the available sample, through the survey.

Individuals with hemorrhagic stroke were staged by modified ranking (Wilson et al., 2002), being distributed into degrees 2 and 3 of disability. In addition, all the individuals in the sample presented sensorimotor alterations related to disorders in the somesthetic and primary motor areas.

Bite force analysis

A digital dynamometer (IDDK, Kratos, Cotia, São Paulo, Brazil) with a force load of up to 980.66 N determined the maximum molar bite force. The biosafety protocol was employed for the apparatus using 70% alcohol and latex fingers in rods with Teflon discs (Waripe, São Paulo).

The measurements were made in the region of the right and left permanent first molars. The individual positioned his head in a relaxed and erect, way looking into the horizon, with the Frankfort Horizontal plane kept parallel to the floor. The individual was asked to bite the device three times, with maximum strength, with a two-minute interval between each measurement while alternating the side. This was supervised by a qualified professional (Palinkas et al., 2010; Righetti et al., 2020; Gomes et al., 2022).

Table 2 – Depicting inter group comparison of maximum molar bite force

Molar bite force	Group	Mean ± std. error (N)	P-value
Right	hemorrhagic stroke disease-free	207.9 ± 33.5 310.7 ± 37.3	0.048
Left	hemorrhagic stroke disease-free	192.4 ± 29.7 313.8 ± 49.2	0.042

Method error

Dahlberg's formula was used to calculate the error in the study's methodology with a sample of ten individuals. The interval between two sessions in a week was sufficient to determine the maximum molar bite force error, which was 6.68%.

Statistics

The Shapiro-Wilk test was used to determine the normal distribution of the data. SPSS version 22.0. (SPSS Inc., Chicago, USA) was used to analyse the data obtained (Student's *t*-test, $p<0.05$).

Results

There was significant difference in the right ($p=0.048$) and left ($p=0.042$) maximum molar bite force, between the hemorrhagic stroke and disease-free groups. The hemorrhagic stroke group showed had lower maximum molar bite force (both sides) when compared to the group without the disease (Table 2).

Discussion

The null hypothesis of this study was rejected because there were significant differences between groups for maximum molar bite force. The human body undergoes continuous transformations due to extrinsic and intrinsic factors. This makes it impossible for the motor response to function properly in posture control and body balance, which in turn causes functional impairments (Feger et al., 2019).

Global assessment has shown that the population is increasingly aging, presenting commodities with risk factors for stroke; therefore, knowledge regarding the dynamics of the stomatognathic system and the characteristics of the molar bite force is important in understanding the functional changes resulting from hemorrhagic stroke (Ramírez-Moreno et al., 2015).

In the current study, the null hypothesis was not rejected because the disease had a negative influence on the maximum molar bite force. Individuals with hemorrhagic stroke had a lower bite force than those in the disease-free control group, showing the interaction between the brain and muscle strength after brain injury (Rawson et al., 2018).

Motor sensory disturbances in the stomatognathic system after a hemorrhagic stroke affect the masticatory muscles and the head and neck muscles leading to a decrease in the bite force (Schimmel et al., 2011). When the cells of the nervous system die as a result of a stroke, the individual loses the skills controlled by the affected brain area such as body movement (Stinear et al., 2020).

A hypothesis that could explain the reduction in bite strength in individuals with hemorrhagic stroke would be that the damage and/or injury of the brain resulting from the disease promotes a functional change in the control of voluntary movement. This is because the spasticity, characterized by the interruption of important signals between the nervous system and skeletal striated muscles, promotes functional imbalance with increased muscle activity and muscle tone leading to the appearance of recurrent spasms (Gupta et al., 2018).

These clinical signs favor the weakening of the muscular system, including the muscles used in mastication, triggering a decrease in muscle strength. Literature shows that the masseter muscle is affected by the generalized spasticity in stroke, limiting mouth opening due to trismus (Seo et al., 2012). In this study, the sensation of the resistance of the masticatory muscles or head and neck muscles to passive stretching in individuals with hemorrhagic stroke was not evaluated.

Other factors that could have influenced the decrease in the bite force of individuals with hemorrhagic stroke in this study could be the loss of muscle tone and decreased aerobic capacity, which can increase energy expenditure in daily activities, reducing body strength (Stinear et al., 2020).

Dorsch et al. (2016) evaluated the strength of the lower limbs in individuals with stroke and found a reduction of 48% in strength when compared to that in the disease-free group. The findings of this study demonstrated a reduction in the bite force in the hemorrhagic stroke group. Further, when we transformed the results into percentage data, we observed that the hemorrhagic stroke group experienced a 66.7% reduction in the maximum molar bite force on the right side and 62.3% on the left side when compared to the disease-free group.

Authors report that any disharmony, such as those occurring in the muscle tone in individuals with stroke, may have a negative impact on the dynamics, function, and strength of the human body, resulting in the reduced performance of the skeletal striated muscle, which is responsible for these dynamics (Bovonsunthonchai et al., 2011).

Therefore, the factors reported also have a direct link with poor posture. Often, positioning the head and neck forward affects the functionality of the stomatognathic system structures, especially mandibular movement that involves combined action of the musculature of the neck and cervical spine (Zafar et al., 2000).

Poor posture of the head and neck promotes muscle fatigue because it stimulates the fascia muscle fibers (rapid contraction) that are used for movement, strength, and activity instead of the static muscle fibers that maintain body position (Moccia et al., 2016).

Over time, poor posture causes weakening of the deeper muscles due to lack of use, impairing the functional capacity of the cranio-cervical system. This hypothesis should help clarify the reduction in maximum molar bite force in the group with hemorrhagic stroke. In this study, the postural condition of individuals with hemorrhagic stroke was not assessed.

One of the biggest problems for stroke patients is the difficulty in feeding and swallowing (Nakamori et al., 2021), which can lead to changes in food choices, leading patients to malnutrition. This study proves that even a few years after the hemorrhagic stroke, the stomatognathic system, especially the maximum molar bite force, is still functionally compromised, which is an important clinical report for the knowledge of physicians, nutritionists and speech therapists who work with these patients, seeking an adequate power diet, providing a better nutritional status and quality of life for patients.

Although there are some limitations to this study, such as the inability to evaluate the sensation of resistance of the muscles to passive stretching and the postural position of the head showing a possible increase in muscle tone, a functional change in the stomatognathic system was demonstrated using the maximum molar bite force in the hemorrhagic stroke group.

Conclusion

The results suggest that individuals with hemorrhagic stroke may show a decrease in the maximum molar bite force. Therefore, this study provides basis for future research to improve the function of the stomatognathic system in individuals with hemorrhagic stroke, in addition to confirming our results. Further, there is a need to assess changes in the pattern of food intake, with selection of nutritious and softer consistency foods in such individuals.

References

Al-Hassnan, Z. N., Rashed, M. S., Al-Dirbashi, O. Y., Patay, Z., Rahbeeni, Z., Abu-Amero, K. K. (2008) Hyperornithinemia-hyperammonemia-homocitrullinuria syndrome with stroke-like imaging presentation: Clinical, biochemical and molecular analysis. *J. Neurol. Sci*. **264**, 187–194.

Bovonsunthonchai, S., Hiengkaew, V., Vachalathiti, R., Vongsirinavarat, M. (2011) Gait symmetrical indexes and their relationships to muscle tone, lower extremity function, and postural balance in mild to moderate stroke. *J. Med. Assoc. Thai*. **94**, 476–484.

Dorsch, S., Ada, L., Canning, C. G. (2016) Lower limb strength is significantly impaired in all muscle groups in ambulatory people with chronic stroke: a cross-sectional study. *Arch. Phys. Med. Rehabil*. **97**, 522–527.

Feger, M. A., Donovan, L., Herb, C. C., Handsfield, G. G., Blemker, S. S., Hart, J. M., Saliba, S. A., Abel, M. F., Park, J. S., Hertel, J. (2019) Effect of impairment-based rehabilitation on lower leg muscle volumes and strength in patients with chronic ankle instability: a preliminary study. *J. Sport Rehabil*. **28**, 450–458.

Gomes, G. G. C., Palinkas, M., da Silva, G. P., Gonçalves, C. R., Lopes, R. F. T., Verri, E. D., Fabrin, S. C. V., Fioco, E. M., Siéssere, S., Regalo, S. C. H. (2022) Bite force, thickness, and thermographic patterns of masticatory muscles post-hemorrhagic stroke. *J. Stroke Cerebrovasc. Dis*. **31**, 106173.

Gupta, A. D., Chu, W. H., Howell, S., Chakraborty, S., Koblar, S., Visvanathan, R., Cameron, I., Wilson, D.

(2018) A systematic review: Efficacy of botulinum toxin in walking and quality of life in post-stroke lower limb spasticity. *Syst. Rev*. **7**, 1.

Ludwig, P. E., Reddy, V., Varacallo, M. (2020) Neuroanatomy, Central Nervous System (CNS). *StatPearls [Internet]*.

Markus, H. S., Brainin, M. (2020) COVID-19 and stroke – A global World Stroke Organization perspective. *Int. J. Stroke* **15**, 361–364.

Moccia, D., Nackashi, A. A., Schilling, R., Ward, P. J. (2016) Fascial bundles of the infraspinatus fascia: Anatomy, function, and clinical considerations. *J. Anat*. **228**, 176–183.

Nakamori, M., Hosomi, N., Imamura, E., Matsushima, H., Maetani, Y., Yoshida, M., Yoshikawa, M., Takeda, C., Nagasaki, T., Masuda, S., Kayashita, J., Tsuga, K., Tanimoto, K., Wakabayashi, S., Maruyama, H. (2021) Association between stroke lesions and videofluoroscopic findings in acute stroke patients. *J. Neurol*. **268**, 1025–1035.

Palinkas, M., Nassar, M. S., Cecílio, F. A., Siéssere, S., Semprini, M., Machado-de-Sousa, J. P., Hallak, J. E., Regalo, S. C. (2010) Age and gender influence on maximal bite force and masticatory muscles thickness. *Arch. Oral Biol*. **55**, 797–802.

Ramírez-Moreno, J. M., Alonso-González, R., Peral-Pacheco, D., Millán-Núñez, M. V., Aguirre-Sánchez, J. J. (2015) Stroke awareness is worse among the old and poorly educated: A population-based survey. *J. Stroke Cerebrovasc. Dis*. **24**, 1038–1046.

Rawson, E. S., Miles, M. P., Larson-Meyer, D. E. (2018) Dietary supplements for health, adaptation, and recovery in athletes. *Int. J. Sport Nutr. Exerc. Metab*. **28**, 188–199.

Righetti, M. A., Taube, O. L. S., Palinkas, M., Gonçalves, L. M. N., Esposto, D. S., de Mello, E. C., Regalo, I. H., Regalo, S. C. H., Siéssere, S. (2020) Osteoarthrosis: Analyze of the molar bite force, thickness and masticatory efficiency. *Prague Med. Rep*. **121**, 87–95.

Schimmel, M., Leemann, B., Christou, P., Kiliaridis, S., Schnider, A., Herrmann, F. R., Müller, F. (2011) Oral health-related quality of life in hospitalised stroke patients. *Gerodontology* **28**, 3–11.

Schimmel, M., Ono, T., Lam, O. L., Müller, F. (2017) Oro-facial impairment in stroke patients. *J. Oral Rehabil*. **44**, 313–326.

Seo, J. H., Kim, D. K., Kang, S. H., Seo, K. M., Seok, J. W. (2012) Severe spastic trismus without generalized spasticity after unilateral brain stem stroke. *Ann. Rehabil. Med*. **36**, 154–158.

Stinear, C. M., Lang, C. E., Zeiler, S., Byblow, W. D. (2020) Advances and challenges in stroke rehabilitation. *Lancet Neurol*. **19**, 348–360.

Tsai, H. H., Kim, J. S., Jouvent, E., Gurol, M. E. (2018) Updates on prevention of hemorrhagic and lacunar strokes. *J. Stroke* **20**, 167–179.

Umay, E. K., Yilmaz, V., Gundogdu, I., Ozturk, E., Gurcay, E., Karaahmet, O., Saylam, G., Ceylan, T., Cakci, A. (2019) What happens to swallowing muscles after stroke? A prospective randomized controlled electrophysiological study. *Neurol. India* **67**, 1459–1466.

Wilson, J. T. L., Harendran, A., Grant, M., Baird, T., Schulz, U. G. R., Muir, K. W., Bone, I. (2002) Improving the assessment of outcomes in stroke: Use off a structured interview to assign grades on the modified rankin scale. *Stroke* **33**, 2243–2246.

Yılmaz, V., Aras, B., Umay, E. (2020) Temporomandibular joint dysfunction and impaired stomatognathic alignment: A problem beyond swallowing in patients with stroke. *Indian J. Otolaryngol. Head Neck Surg*. **72**, 329–334.

Zafar, H., Nordh, E., Eriksson, P. O. (2000) Temporal coordination between mandibular and head-neck movements during jaw opening-closing tasks in man. *Arch. Oral Biol*. **45**, 675–682.

 Prague Medical Report / Vol. 123 (2022) No. 3, p. 188–192

A New Mystery: Phantosmia after COVID-19 Infection

Banu Atalay Erdogan[1], Anas Eldahshan[2]
[1]Department of Ear Nose Throat, Istinye University, VM Medical Park Pendik Hospital, Istanbul, Turkey;
[2]Rotherham NHS Foundation Trust, London, United Kingdom

Received April 14, 2022; Accepted August 2, 2022.

Key words: COVID-19 – Anosmia – Olfactory disorders – Phantosmia

Abstract: Coronavirus disease 2019 (COVID-19) has developed as a pandemic and has caused millions of deaths worldwide. Multiple studies have implicated anosmia and ageusia as symptoms associated with COVID-19. In this case report we present the cases who suffer from phantosmia after COVID-19 infection. As the prevalence of the virus increases, the symptomatology profile continues to be updated. More studies are needed to better understand this disease.

Mailing Address: Prof. Dr. Banu Atalay Erdogan, MD., Faculty of Medicine, Istinye University, Topkapı Kampüs – 125, Maltepe Mah., Teyyareci Sami Sk., No.3 Zeytinburnu, Istanbul 34010, Turkey; e-mail: banuatalay81@gmail.com

https://doi.org/10.14712/23362936.2022.17
© 2022 The Authors. This is an open-access article distributed under the terms of the Creative Commons Attribution License (http://creativecommons.org/licenses/by/4.0).

Introduction

The 2019 coronavirus disease outbreak (COVID-19) originated in Wuhan, China, and quickly became a global pandemic. COVID-19, also known as coronavirus 2 of acute respiratory syndrome (SARS-CoV-2), infected 116,874,912 people worldwide by March 2021 and caused 2,597,381 deaths. The disease is mainly transmitted through the upper respiratory tract by inhalation of droplets. Patients with COVID-19 may experience cough, shortness of breath, fever, chills, myalgia, headache, new loss of taste or smell, nasal congestion and runny nose, vomiting and diarrhoea. These symptoms can range from mild to severe (Neto et al., 2021).

In May 2020, the Ear, Nose, and Throat Societies warned physicians about olfactory and gustatory disorders that occur before common symptoms develop. Odour and taste disturbances are not uncommon in viral upper respiratory tract infections. They are observed in more than 30% of patients (Dalton, 2004). Some studies have shown that COVID-19 may have an interest or tropism for certain olfactory sensors (Beltrán-Corbellini et al., 2020; Hopkins et al., 2020). The frequency of olfactory and gustatory disturbances ranged from 11 to 86% in COVID-19 positive patients (Lechien et al., 2020; Mao et al., 2020). It usually lasts for a period of 7 to 14 days, in most cases after two weeks (Klopfenstein et al., 2020; Yan et al., 2020). Parosmia is a disorder of the sense of smell. Phantosmia is a term for olfactory hallucinations or ghostly odours that occur in the absence of any odour. We presented two cases of phantosmia after recovery from COVID-19 infection.

Case 1

A 30-year-old female patient presented with one week of phantosmia and described a persistent cigarette tobacco odour. She did not smoke and there were no smokers in her family. She had an COVID-19 infection two months ago. She had no nasal obstruction or rhinitis, and no abnormalities were noted in her nasal or nasopharyngeal mucosa on medical examination. Complete blood count and biochemistry tests were normal. The patient underwent magnetic resonance imaging (MRI) of the brain, with and without contrast, to measure the volume of the olfactory bulb (OBV). Images were acquired with 1.5T MRI with a cranial coil (Philips Ingenia 1.5T, Eindhoven, The Netherlands). T2-weighted images in the coronal plane were obtained as a 1 mm notch at 5 mm slice thickness. The repetition time/time echo was 4833/100 (milliseconds/milliseconds), field of view was 220×183 mm and matrix was 356×209 mm. 22 coronal sections were acquired. Standard OBV measurements were obtained from coronal T2-weighted images. The volumes of the olfactory bulb were 64 mm^3 (left) and 65 mm^3 (right). These values were accepted as normal based on the limits in the study by Buschhüter et al. (2008). There is no abnormal signal intensity on T2 and FLAIR (fluid-attenuated inversion recovery) images at the primary olfactory cortex and visualized olfactory pathways.

Case 2

A 26-year-old female patient presented with one week of phantosmia and described a persistent odour of burnt plastic. She had an COVID-19 infection two months ago. Her otolaryngologic examination was normal except for septal deviation. She has a history of allergic rhinitis and urticaria. Routine laboratory tests were normal limits. SARS-CoV-2 IgM was 1.25 (reference range: 0–0.99) and SARS-CoV-2 IgG was 3.28 (reference range: 0–1.4). This patient underwent MRI like the other patient and was examined by the same radiologist. The volumes of the olfactory bulb were 70 mm^3 (left) and 68 mm^3 (right).

Oxymetazoline hydrochloride nasal spray for 5 days and daily saline nasal irrigation were recommended for both patients. The complaint of the first patient disappeared 4 weeks after admission to the hospital, but the resolution of the second patient's complaint took 12 weeks.

Discussion

Many studies have shown that acute anosmia and ageusia seem to be among the important symptoms and signs for the diagnosis of COVID-19 infection, especially in the early stage of the disease (Lee et al., 2020). Initially, mechanical obstruction due to overproduction of mucus during active infection was thought to be the cause of anosmia. But patients suffering from persistent anosmia with normal acoustic rhinometry after infection suggest a different pathophysiology leading to more permanent damage (Netland et al., 2008).

Viral damage to the olfactory epithelium causes acute onset anosmia or ageusia. Viruses such as influenza A, parainfluenza, herpes viruses, adenoviruses, polioviruses, rabies viruses, and Japanese encephalitis reach the central nervous system via the olfactory nerve (Netland et al., 2008). Studies from the 1960s have shown us that coronaviruses are neuroinvasive and neurotropic. In mouse models, SARS-CoV showed transneuronal access through the olfactory bulb in mice after intranasal inoculation (Netland et al., 2008). Recent studies demonstrated that ACE2 and TMPRSS2 are critical for SARS-CoV and SARS-CoV-2 entry into host cells (Dong et al., 2020). In addition, a recent study has shown that ACE2 and TMPRSS2 are found in nasal respiratory tissue, olfactory neuroepithelium, central nervous system and lymphoid tissues (Fodoulian et al., 2020). This information supports the occurrence of neurologic symptoms such as headache, nausea, and vomiting in some patients with COVID-19.

Phantom odour perception is an olfactory disorder in which people perceive an odour in the absence of a stimulus. While perceived odours vary from person to person, they are usually described as burnt bread, metallic or chemical odours.

Phantosmia has been documented in various conditions such as chronic rhinosinusitis, viral upper respiratory tract infections, intracranial hemorrhage, tumours, epilepsy, psychiatric disorders, Parkinson's disease, radiation therapy, and head trauma. In most cases, however, phantosmia has no identifiable origin and is diagnosed as idiopathic phantosmia (Morosanu et al., 2020). The cause of phantosmia is not fully understood.

The phantom sense of smell may be caused by a neuronal signal imbalance that causes non-sensory olfactory signals to achieve the central nervous system. The sense of smell may arise from the peripheral nervous system at the level of olfactory sensory neurons or may arise from the central brain. Also it may be due to damage to the olfactory nerve (Patel and Pinto, 2014). Many viruses can cause parosmia and phantosmia, either as part of the first deficit or when the nerves make abnormal connections as they try to heal. Based on this information, we can say that COVID-19 virus causes olfactory phantosmia with a mechanism similar to other viruses.

Diagnostic work-up should start a standard head and neck examination. Nasal endoscopy is indicated to examine the olfactory pathways in the nose. A dental examination should be included for the oral diseases that may produce a foul odour. At the same time, magnetic resonance imaging should be the modality of choice to rule out neoplasm, cerebrovascular or sinus disease and malignancies.

MRI is of great importance in demonstrating olfactory bulb abnormalities in patients with olfactory dysfunction after trauma and upper respiratory tract infection. Findings may indicate that olfactory deficiency both after trauma and after upper respiratory tract infection causes decreased sensory input in olfactory bulbs, leading to structural changes at the bulbus level and formation of parosmia. As correlational analyses show, olfactory bulb volumes decrease in parallel with olfactory function. Therefore, damage to peripheral olfactory structures was associated with the presence of olfactory dysfunction and reduced olfactory bulb volumes (Cummings et al., 1997). Therefore, we looked at the changes in olfactory bulb volume in our patients with MRI, but we could not find a significant change.

The treatment of phantosmia can be divided into medical treatment and surgical methods, and treatment is determined by the underlying cause, which is usually determined by the diagnostic workup.

Our article has several limitations. First, only two cases were presented in this study. Second, a formal quantitative chemosensory test was lacking. The olfactory problem is not precisely diagnosed neither by objective (olfactometry, rhinomanometry) nor by subjective examination (sniffing test). We performed only MRI examination for rolling out the other pathologies. We diagnosed phantosmia based on the patients' medical history. Phantosmia related with COVID-19 is an interesting topic that could be explored in further studies.

References

Beltrán-Corbellini, Á., Chico-García, J. L., Martínez-Poles, J., Rodríguez-Jorge, F., Natera-Villalba, E., Gómez-Corral, J., Gómez-López, A., Monreal, E., Parra-Díaz, P., Cortés-Cuevas, J. L., Galán, J. C., Fragola-Arnau, C., Porta-Etessam, J., Masjuan, J., Alonso-Cánovas, A. (2020) Acute-onset smell and taste disorders in the context of COVID-19: A pilot multicentre polymerase chain reaction based case-control study. *Eur. J. Neurol*. **27(9)**, 1738–1741.

Buschhüter, D., Smitka, M., Puschmann, S., Gerber, J. C., Witt, M., Abolmaali, N. D., Hummel, T. (2008) Correlation between olfactory bulb volume and olfactory function. *Neuroimage* **42(2)**, 498–502.

Cummings, D. M., Knab, B. R., Brunjes, P. C. (1997) Effects of unilateral olfactory deprivation in the developing opossum, *Monodelphis domestica*. *J. Neurobiol*. **33**, 429–438.

Dalton, P. (2004) Olfaction and anosmia in rhinosinusitis. *Curr. Allergy Asthma Rep*. **4(3)**, 230–236.

Dong, M., Zhang, J., Ma, X., Tan, J., Chen, L., Liu, S., Xin, Y., Zhuang, L. (2020) ACE2, TMPRSS2 distribution and extrapulmonary organ injury in patients with COVID-19. *Biomed. Pharmacother*. **131**, 110678.

Fodoulian, L., Tuberosa, J., Rossier, D., Boillat, M., Kan, C., Pauli, V., Egervari, K., Lobrinus, J. A., Landis, B. N., Carleton, A., Rodriguez, I. (2020) SARS-CoV-2 receptors and entry genes are expressed in the human olfactory neuroepithelium and brain. *iScience* **23(12)**, 101839.

Hopkins, C., Surda, P., Whitehead, E., Kumar, B. N. (2020) Early recovery following new onset anosmia during the COVID-19 pandemic – An observational cohort study. *J. Otolaryngol. Head Neck Surg*. **49(1)**, 26.

Klopfenstein, T., Kadiane-Oussou, N. J., Toko, L., Royer, P. Y., Lepiller, Q., Gendrin, V., Zayet, S. (2020) Features of anosmia in COVID-19. *Med. Mal. Infect*. **50(5)**, 436–439.

Lechien, J. R., Chiesa-Estomba, C. M., De Siati, D. R., Horoi, M., Le Bon, S. D., Rodriguez, A., Dequanter, D., Blecic, S., El Afia, F., Distinguin, L., Chekkoury-Idrissi, Y., Hans, S., Delgado, I. L., Calvo-Henriquez, C., Lavigne, P., Falanga, C., Barillari, M. R., Cammaroto, G., Khalife, M., Leich, P., Souchay, C., Rossi, C., Journe, F., Hsieh, J., Edjlali, M., Carlier, R., Ris, L., Lovato, A., De Filippis, C., Coppee, F., Fakhry, N., Ayad, T., Saussez, S. (2020) Olfactory and gustatory dysfunctions as a clinical presentation of mild-to-moderate forms of the coronavirus disease (COVID-19): A multicenter European study. *Eur. Arch. Otorhinolaryngol*. **277(8)**, 2251–2261.

Lee, Y., Min, P., Lee, S., Kim, S. W. (2020) Prevalence and duration of acute loss of smell or taste in COVID-19 patients. *J. Korean Med. Sci*. **35(18)**, e174.

Mao, L., Jin, H., Wang, M., Hu, Y., Chen, S., He, Q., Chang, J., Hong, C., Zhou, Y., Wang, D., Miao, X., Li, Y., Hu, B. (2020) Neurologic manifestations of hospitalized patients with coronavirus disease 2019 in Wuhan, China. *JAMA Neurol*. **77(6)**, 1–9.

Morosanu, C. O., Clamp, P. J., Teo, M. K. (2020) Phantosmia as the first presentation of a cavernous sinus – Clinoidal meningioma. *Br. J. Neurosurg*. **2020**, 1–7.

Netland, J., Meyerholz, D. K., Moore, S., Cassell, M., Perlman, S. (2008) Severe acute respiratory syndrome coronavirus infection causes neuronal death in the absence of encephalitis in mice transgenic for human ACE2. *J. Virol*. **82(15)**, 7264–7275.

Neto, A. R. de S., Carvalho, A. R. B. de, Oliveira, E. M. N. de, Magalhães, R. de L. B., Moura, M. E. B., Freitas, D. R. J. de (2021) Symptomatic manifestations of the disease caused by coronavirus (COVID-19) in adults: Systematic review. *Rev. Gaucha Enferm*. **42(spe)**, e20200205.

Patel, R. M., Pinto, J. M. (2014) Olfaction: Anatomy, physiology, and disease. *Clin. Anat*. **27(1)**, 54–60.

Yan, C. H., Faraji, F., Prajapati, D. P., Boone, C. E., DeConde, A. S. (2020) Association of chemosensory dysfunction and COVID-19 in patients presenting with influenza-like symptoms. *Int. Forum Allergy Rhinol*. **10(7)**, 806–813.

Rare Location of a Dermoid Cyst in the Parotid Gland: A Case Report

Michal Vavro[1], Samuel Horák[2], Bronislava Dvoranová[1], Zuzana Čierna[2,3], Pavel Babál[2], Daniela Kobzová[2], Dušan Hirjak[1], Ladislav Czakó[1]

[1]Department of Oral and Maxillofacial Surgery, Comenius University in Bratislava and University Hospital Ružinov, Bratislava, Slovakia;
[2]Institute of Pathological Anatomy, Faculty of Medicine, Comenius University in Bratislava and University Hospital Bratislava, Bratislava, Slovakia;
[3]Department of Pathology, University Hospital, Trnava, Slovakia

Received April 16, 2022; Accepted August 2, 2022.

Key words: Dermoid cyst – Cyst of parotid gland – Parotid gland disease

Abstract: Dermoid cyst of the parotid gland is a lesion composed of benign tissues of ectodermal and mesodermal origin. Although a dermoid cyst can be encountered across nearly all sites of the body, its location in the head and neck area is quite uncommon and even more unusual inside the parotid gland. We present a case of a patient with gradually enlarging tumour in her right parotid gland who underwent surgical removal of the tumour histologically corresponding to a dermoid cyst.

Mailing Address: MDDr. Bronislava Dvoranová, Department of Oral and Maxillofacial Surgery, Comenius University in Bratislava, University Hospital Ružinov, Ružinovská 6, Bratislava 826 06, Slovakia; Phone: +421 248 234 865; e-mail: lencuchova.bronislava@gmail.com

https://doi.org/10.14712/23362936.2022.18
© 2022 The Authors. This is an open-access article distributed under the terms of the Creative Commons Attribution License (http://creativecommons.org/licenses/by/4.0).

Introduction

Dermoid cyst inside the parotid gland is a rare finding with only a few cases reported (Moody et al., 1998; Naujoks et al., 2007; Islam and Hoffman, 2009; Tas et al., 2010; Gonzalez-Perez and Crespo-Torres, 2013; Damar et al., 2015; Glaas et al., 2017; Dwivedi et al., 2019; Yang, et al., 2020). This benign lesion comprises of epidermal and dermal elements entrapped ectopically in deeper tissues. It typically manifests as a painless tumour that generally poses a problem only due to its enlarging volume. In the management of patients with dermoid cysts, multiple diagnostic approaches are available, such as ultrasonography, computed tomography and magnetic resonance imaging (USG, CT, MRI) (Morón et al., 2004; Sabhalok et al., 2016). The curative method is surgical removal of the cyst. We present a case of a woman who was treated by right extracapsular dissection of the parotid gland with a brief discussion on the management of patients with this condition.

Material and Methods

A 40-year-old female noticed a gradually enlarging tumour in the area of her right parotid gland in the course of 2 months. She has never had trauma, nor underwent any surgical procedure in the area of head or neck, had no fever, other swellings, salivatory or neurological disorders. The patient had a medical history of subclinical hypothyroidism in Hashimoto thyreoiditis and chronic venous disease of lower extremities, without any prescribed medication.

On palpation, there was a soft, painless, sharply demarcated tumour of 4×2 cm in the caudal part of the right parotideomasseteric region, without pathological changes on the overlying skin. On USG examination, a slightly lobed, hypoechogenic, homogenous, intraparotid formation with dimensions up to 5×2.5 cm was detected,

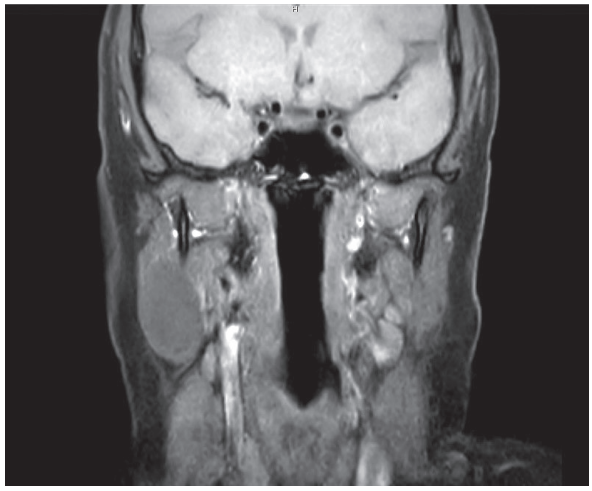

Figure 1 – Coronal magnetic resonance imaging view of the lesion in T1.

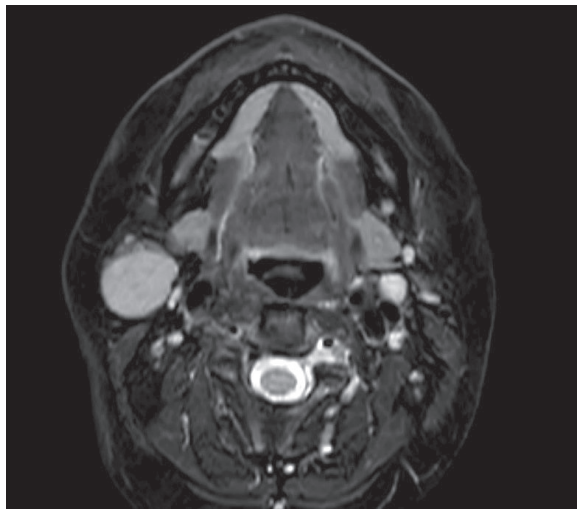

Figure 2 – Axial magnetic resonance imaging view of the lesion in T2.

without obvious signs of vascularization. Additionally, there was a single enlarged lymph node underneath the right parotid gland. Other visualized lymph nodes were of normal size. The thyroid gland was of normal size, without conspicuous pathological findings. The patient had an MRI scan which showed an oval, slightly irregular, T1 hypointense and T2 hyperintense structure of a relatively homogenous signal in the central part of the right parotid gland (Figures 1 and 2), with size of 26×25×40 mm, sharply demarcated from the surrounding tissues. In the caudal part ventrally, there was a small zone of hyperintensity. Other salivary glands were without significant findings.

Results

The patient underwent surgery under general anesthesia – right extracapsular dissection of the parotid gland, level II. The tumour was of semi-soft consistency, on cut section with a thin capsule and pale yellow, soft, dough-like content (Figures 3 and 4). On histology, the cyst was embedded in fat tissue of the parotid gland, its capsule was composed of connective tissue with sparse to moderate lymphocytic infiltrate and scarce capillaries. The lumen was lined by regular, focally atrophic squamous epithelium with keratinization on the luminal side and with numerous sebaceous glands inside the epithelial layer (Figure 5), with keratin-like material inside the lumen of the cyst, which is consistent with the diagnosis of a dermoid cyst.

After the surgery, the patient had mild transient signs of weakness of muscles innervated by ramus marginalis mandibulae of the facial nerve. Otherwise, the postoperative period was uneventful.

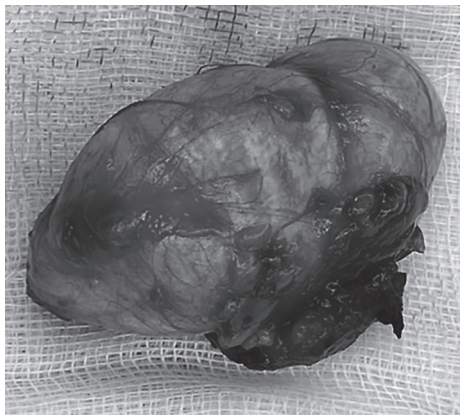

Figure 3 – The intact dermoid cyst postoperatively.

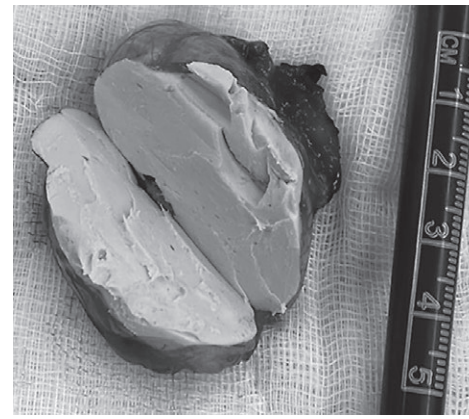

Figure 4 – The dermoid cyst cut in the longitudinal axis.

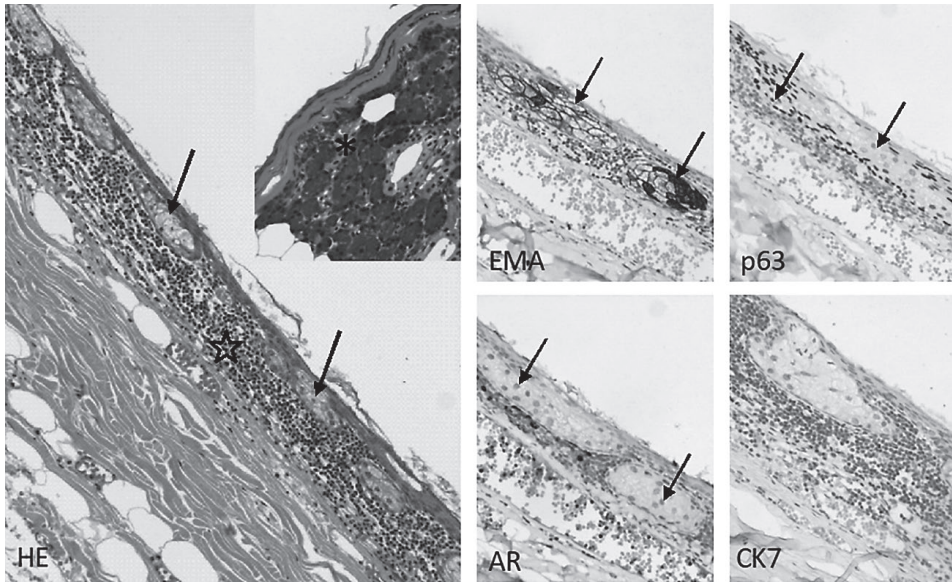

Figure 5 – Histological findings of a cyst in glandula parotis (*) lined with regular squamous epithelium, focally atrophic (insertion), elsewhere with sebaceous differentiation (arrow) and subepithelial lymphocytic infiltration (star). Sebaceous gland differentiation shows positivity of epithelial membrane antigen (EMA), androgen receptor (AR) and partially p63; cytokeratin 7 (CK7) is not expressed. Hematoxylin and eosin (HE); immunoperoxidase, diaminobenzidine, 100×.

Discussion

Dermoid cyst is a benign lesion that can occur in virtually any part of the body with adjacency to the skin. These cysts are composed of cells of ectodermal and mesodermal origin that are entrapped in deeper tissues either during the embryonic

or fetal development (congenital cysts), or in postnatal life (acquired cysts). In the parotid gland, they are believed to form due to either entrapment of cells during closure of embryonic branchial arches, or as a result of impacted epidermal and dermal cells into deeper layers of tissues. When fully developed, they contain squamous cells, often with keratin, and dermal structures such as hair follicles, sebaceous or sweat glands. The distribution of occurrence across the body is diverse with only approximately 7% of them being reported in the head and neck region (Sabhalok et al., 2016). The frequency of incidence in the head and neck area is 49.5% in the orbit, 23% in submental and submaxillar region, 12.6% in the nose and 14.6% in other locations (Yigit et al., 2015). However, the presence of a dermoid cyst in the parotid gland is uncommon, with only several cases published in the literature (Shakeel et al., 2014; Yigit et al., 2015; Glaas et al., 2017; Dwivedi et al., 2019; Yang et al., 2020).

In the process of diagnostics, there are several modalities that can be used in order to ensure the correct management of the patient. Ultrasonography is the most accessible, cheap and non-invasive method and is mainly used in distinguishing between solid and cystic lesions and evaluation of the presence of blood vessels. Both CT and MRI can visualize the content of the cyst and are used to give a complex detailed overview of the terrain of the lesion. The CT attenuation varies depending on the composition of the content of the cyst, typically showing fat attenuation in the dermoid cysts. On MRI, the dermoid cyst content shows hypointensity on T1-weighted images and hyperintensity on T2-weighted images, and hence these cysts can be misdiagnosed as a lipoma (Morón et al., 2004; Dwivedi et al., 2019). Another approach is the use of fine-needle aspiration cytology (FNAC), although its results can be deceptive and opinions on its use are controversial. In context with all other diagnostic methods, it can provide helpful information leading towards the correct diagnosis (Baschinsky et al., 1999). Commonly the aspirated material contains keratin, squamous cells and occasionally hair (presence of which discerns it from epidermoid cyst on FNAC).

Despite their crucial importance in the process of diagnostics, none of the mentioned methods can identify a dermoid cyst with absolute certainty, as all mentioned structures and appearances can be seen in other types of teratomas and even in malignant tumours, such as well differentiated squamous cell carcinoma and carcinomas with squamous metaplasia (Yigit et al., 2015). Thus, the definitive diagnosis should always be made by histopathological examination of the resected specimen.

For the surgery, the recommended approach is partial or total parotidectomy with complete resection of the cyst, with sparing of nerves where possible. In the case of an incomplete resection, there is a high chance of recurrence of the cyst. From all the reported cases of dermoid cysts inside a parotid gland, only a few (Damar et al., 2015; Dwivedi et al., 2019; Yang et al., 2020) were treated by isolated excision of the cyst, in the rest of the cases either partial or total parotidectomy was performed

(Yigit et al., 2015; Glaas et al., 2017; Yang et al., 2020). In this case, the patient was treated by right extracapsular dissection of the parotid gland, level II.

Conclusion

Despite the paucity of reported cases, the diagnostics of dermoid cyst of the parotid gland has been well established, with all modalities bringing valuable information for the surgical plan. All authors of the articles regarding the dermoid cysts of the parotid gland agree on the importance of the final histopathological examination of the resected specimen in order to provide the correct diagnosis.

References

Baschinsky, D., Hameed, A., Keyhani-Rofagha, S. (1999) Fine-needle aspiration cytological features of dermoid cyst of the parotid gland: A report of two cases. *Diagn. Cytopathol*. **20(6)**, 387–388.

Damar, M., Erdem, D., Dinç, A. E., Bişkin, S., Bahadır, B. (2015) Dermoid cyst of the parotid gland. *ENTCase* **1(3)**, 191–194.

Dwivedi, G., Gupta, V., Patnaik, U., Kumar, M., Sood, A., Upadhyay, M. (2019) Dermoid cyst of the parotid gland: A rare entity. *Indian J. Otolaryngol. Head Neck Surg*. **71(1)**, 809–812.

Glaas, M. F., Schipper, J., Kajasi, N., Albrecht, A. (2017) The youngest reported and successfully treated patient with a dermoid cyst of the parotid gland: A rare pediatric case. *Case Rep. Otolaryngol*. **2017**, 4187030.

Gonzalez-Perez, L. M., Crespo-Torres, S. (2013) Dermoid cyst of the parotid gland. *Oral Radiol*. **29(1)**, 92–95.

Islam, S., Hoffman, G. R. (2009) Parotid dermoid cyst: A rare entity. *J. Laryngol. Otol*. **123(2)**, e7.

Moody, A. B., Avery, C. M. E., Harrison, J. D. (1998) Dermoid cyst of the parotid gland. *Int. J. Oral Surg*. **27(6)**, 461–462.

Morón, F. E., Morriss, M. C., Jones, J. J., Hunter, J. V. (2004) Lumps and bumps on the head in children: Use of CT and MR imaging in solving the clinical diagnostic dilemma. *Radiographics* **24(6)**, 1655–1674.

Naujoks, C., Handschel, J., Braunstein, S., Emaetig, F., Depprich, R., Meyer, U., Kübler, N. (2007) Dermoid cyst of the parotid gland – A case report and brief review of the literature. *Int. J. Oral Surg*. **36(9)**, 861–863.

Sabhalok, S. S., Shetty, L. S., Sarve, P. H., Setiya, S. V., Bharadwaj, S. R. (2016) Epidermoid and dermoid cysts of the head and neck region. *Plast. Aesthet. Res*. **3**, 347–350.

Shakeel, M., Keh, S. M., Chapman, A., Hussain, A. (2014) Intra-parotid dermoid cyst: Excision through a face lift incision. *J. Coll. Physicians Surg. Pak*. **24**, S238–S239 (Suppl. 3).

Tas, A., Yagiz, R., Altaner, S., Karasalihoğlu, A. R. (2010) Dermoid cyst of the parotid gland: First pediatric case. *Int. J. Pediatr. Otorhinolaryngol*. **74(2)**, 216–217.

Yang, C., Wang, X., Zhang, S., Wu, D. (2020) Dermoid cyst of the parotid gland location. *J. Craniofac. Surg*. **31(7)**, e698–e699.

Yigit, N., Karslioglu, Y., Yildizoglu, U., Karakoc, O. (2015) Dermoid cyst of the parotid gland: Report of a rare entity with literature review. *Head Neck Pathol*. **9(2)**, 286–292.

Primary Epithelioid Angiomyolipoma of Adrenal Gland: Case Report and Literature Review

Muhammet Cicek[1], Huseyin Ozgur Kazan[2], Ramazan Gokhan Atis[1], Asif Yildirim[1]

[1]Department of Urology, Istanbul Medeniyet University, Goztepe Training and Research Hospital, Istanbul, Turkey;
[2]Department of Urology, Kocaeli State Hospital, Izmit, Turkey

Received April 10, 2022; Accepted August 6, 2022.

Key words: Epithelioid angiomyolipoma – PEComa – Adrenal angiomyolipoma – Laparoscopic adrenalectomy

Abstract: Angiomyolipomas (AMLs) are mesenchymal tumours derived from perivascular epithelioid cells. Although AMLs are generally known as benign and extremely rare epithelioid variants of AML, they may be potentially aggressive. Here we present an adrenal epithelioid AML and the literature review. A 64-year-old female patient was diagnosed with a left adrenal mass detected incidentally on ultrasonography. Preoperative abdominal CT (computed tomography) showed a 95×68 mm heterogeneous contrast enhancement mass lesion in the left adrenal gland. The lesion was hormone inactive in the endocrinological evaluation, and left laparoscopic adrenalectomy was performed. The patient was discharged on the 2nd postoperative day. Pathology was reported as epithelioid subtype AML. The patient has no local recurrence or metastasis in the 18-month follow-up period and imaging. Adrenal epithelioid AML is an extremely rare and potentially aggressive variant. According to the literature, open or laparoscopic adrenalectomy seems to be suitable option for disease management.

Mailing Address: Muhammet Cicek, MD., Department of Urology, Istanbul Medeniyet University, Goztepe Training and Research Hospital, Eğitim Mahallesi, Dr. Erkin Cd., 34722 Kadıköy, Istanbul, Turkey; Phone: +90 552 993 672; Fax: +90 216 566 66 14; e-mail: muhammetcicekk@gmail.com

https://doi.org/10.14712/23362936.2022.19
© 2022 The Authors. This is an open-access article distributed under the terms of the Creative Commons Attribution License (http://creativecommons.org/licenses/by/4.0).

Introduction

Angiomyolipomas (AMLs) are benign mesenchymal tumours which originate from perivascular epithelioid cells with the substance of mature fat cells, blood vessels, and smooth muscle cells. General prevalence is 4–5/1000 and female to male ratio is approximately 1.5. AMLs are most commonly found in the kidney (Aydin et al., 2009; Li et al., 2015). Extrarenally located AMLs are rare in the literature. To our knowledge, 28 cases of adrenal AML have been reported in the literature up to date. With the present report, 5 were reported as epithelioid angiomyolipoma (eAML). While they are usually diagnosed on incidental imaging, larger AMLs may cause bleeding and pain. The growth rate of AMLs is slow, and the probability of morbidity is very low.

Epithelioid subtype AMLs are distinguished from other AMLs by their potential to display malignant character. In this extremely rare variant of AML, immunoreactivity for myelocytic markers such as human melanoma black 45 (HMB-45), predominance of epithelioid cells, and absence of mature adipocytes are characteristic diagnostic features (Konosu-Fukaya et al., 2014). The renal eAML has limited clinical data in the literature. Likewise adrenal localized eAML is very rare. In this manuscript, we report a case with adrenal eAML who was successfully treated with surgical resection and English-language literature reviewed by scanning the publications up to date. This report has been prepared in accordance with the current CARE checklist.

Case report

A 64-year-old female patient was admitted to our clinic due to microscopic hematuria. Patient had no family history of malignancy, no smoking or alcohol addiction. She had a history of hysterectomy due to premalignant cervical lesion and previous subtotal thyroidectomy. The patient was on regular medical therapy due to the diagnosis of hypertension and hypothyroidism and had no other chronic diseases. An incidental left adrenal mass was detected on urinary system ultrasonography. Preoperative contrast-enhanced abdominal CT (computed tomography) showed a 95×68 mm heterogeneous, spherical-shaped mass lesion in the left adrenal gland with smooth borders. The Hounsfield unit (HU) of the lesion was measured as 66 ± 12 to 79 ± 9 on non-contrast and contrast sections respectively (Figure 1). Furthermore, there was a second lesion with a diameter of 14 mm compatible with AML in the right kidney posterior middle zone. During physical examination, there was no finding other than the scar of the hysterectomy in the pelvis. The lesion was hormone inactive in the endocrinological evaluation, and left laparoscopic adrenalectomy was performed. There were no postoperative complications. The patient was discharged on the 2nd postoperative day. Gross examination revealed a grey-orange 8.5 cm diameter solid lesion with hemorrhagic foci reaching 1 cm in some areas and including adipose adrenal tissue with the largest diameter of 2 cm (Figure 2). In the microscopic examination, vimentin, calretinin,

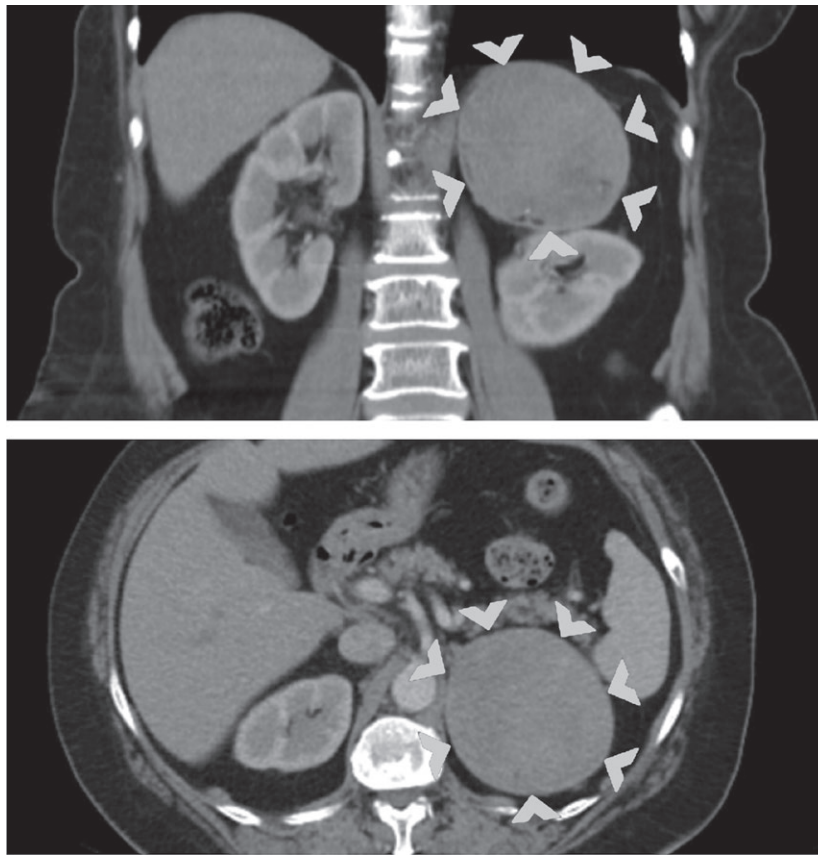

Figure 1 – Axial and sagittal computed tomography section of 95×68 mm heterogeneous, spherical-shaped mass lesion in the left adrenal gland with smooth borders.

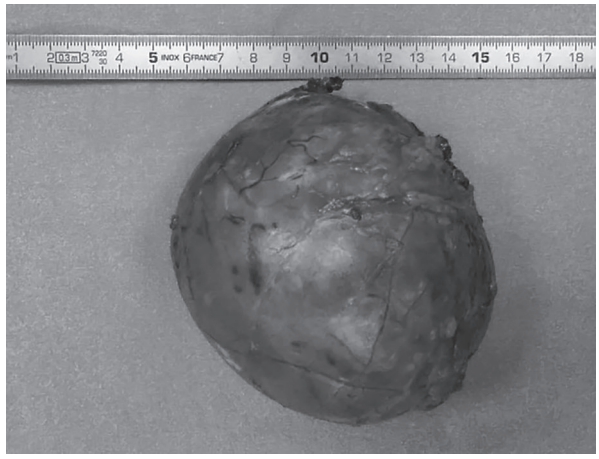

Figure 2 – Macroscopic aspect of the adrenalectomy specimen.

and Melan A were positive, and the findings were evaluated in favour of epithelioid angiomyolipoma. No histomorphological risk factor was observed in favour of an aggressive clinical course, except for the large diameter of the lesion. There was no local recurrence or metastasis in the 18-month follow-up period and imaging. Preoperatively diagnosed 14 mm AML in the right kidney persisted.

Discussion

We reported a rare case of epithelioid AML of adrenal gland. The PubMed, Medline, Web of Science databases were searched for case reports and case series of adrenal angiomyolipoma published in English language between January 1, 1980, and December 31, 2021. The following key words were used: (Adrenal Glands or Adrenal Gland or Gland Adrenal or Glands Adrenal) and (Angiomyolipoma or Angiomyolipomas or epithelioid angiomyolipoma).

The most common extrarenal site for angiomyolipomas is the liver. AML also may be encountered in retroperitoneum, adrenal, breast, genital tract, pancreas, colon, and several other locations (Lam and Lo, 2001; Godara et al., 2007). According to our literature search, 28 cases have been reported for adrenal localized AML with the presented case. Only 5 of these cases are eAML (Table 1). AML is more common in the 5th decade and approximately two times more often diagnosed in women. In this present report the mean age of diagnosis of adrenal AML is 47 and female to male ratio is 4:3. It is known that the frequency of AML increases in hereditary diseases such as tuberous sclerosis (TSC) and lymphangiomyomatosis. Tuberous sclerosis has been reported in approximately 20% of patients in recent AML case series (Aydin et al., 2009). Three of the patients with adrenal AML reported in this review had a history of TSC (11%). Sporadic lymphangioleiomyomatosis was reported in 1 patient. Two of 5 patients with eAML have a history of TSC. Although the limited case number restricts for consequences, history of TSC may be related with increased risk of epithelioid subtype likelihood on adrenal AMLs.

Urgent surgical procedures may be required due to bleeding, which can result in organ loss or mortality (D'Antonio et al., 2009). D'Antonio et al. (2009) reported a case of adrenal eAML with kidney loss resulting in hemorrhagic shock due to spontaneous retroperitoneal hemorrhage. The most important risk factor associated with bleeding is the size of the lesion. Patients who have large AMLs with increased bleeding risk and are not suitable for surgical intervention or unwilling to undergo surgical intervention, selective arterial embolization is an eligible option. Antar et al. (2017) reported an unsuccessful attempt for selective arterial embolization in a case of adrenal AML, with the thought that the lesion might originate from the kidney. Then, they reported that the adrenalectomy procedure was performed. Our literature search revealed that the data related to the successful use of selective arterial embolization in adrenal localized AML does not exist. The use of mTOR (mammalian target of rapamycin) inhibitors in large or symptomatic

Table 1 – Demographic, imaging, and pathological characteristic of epithelioid angiomyolipoma in the literature

Author name (publication date)	Age	Sex	Laterality (left or right)	Largest diameter (cm)	Imaging features	Surgery	Open or laparo-scopic	Histo-pathological features	Follow--up (years)
D'Antonio et al. (2009)	42	M	L	6	Heterogeneous contrast enhancement with a lipidic struma and sign of haemorrhage	Nephrectomy and adrenalectomy	open	Focally seen adipose tissue, HMB-45+, cyto-keratin–, sign of haemorrhage	1
Komarowska et al. (2015)	39	M	R	16	Large retroperitoneal tumour with uncertain origin	Nephrectomy and adrenalectomy	open	HMB-45+, Me-lan A+, SMA+, tumour was infil-trated capsule of right kidney	0.5
Valeshabad et al. (2019)	33	F	L	7.3	Solid and enhancing soft-tissue density mass in the left adrenal gland, which enlarged from 1.5 cm to 7.3×6.9 cm over approximately 21 months	Adrenalectomy and partial nephrectomy (for renal AML)	–	Melan A+ cytoke-ratin and largely PAX8 negative	–
Torres Luna et al. (2020)	32	M	R	20	Areas of necrosis, hemorrhage, and parenchymal calcification	Nephrectomy and adrenalectomy	open	Melan A+, MART-1+, HMB-45+	–
Present case	64	F	L	9.5	Round mass lesion with heterogen contrast enhancement. Additional 14 mm right sided AML	Adrenalectomy	laparo-scopic	Melan A+, vimen-tin+, calretinin+	1.5

M – male; F – female; R – right; L – left; AML – angiomyolipoma; HMB-45 – human melanoma black 45; SMA – smooth muscle actin

AMLs is spreading in recent years especially in patients who have TSC. There is no information in the literature regarding its use in adrenal localized AMLs.

Classical fat-predominant AMLs may be detected by the typical diagnostic features of the fat density on imaging. Negative HU measurement in non-contrast CT imaging gives an important clue for diagnosis. In eAML located in the kidney, the decision to surgery is usually taken with the preliminary diagnosis of RCC (renal cell carcinoma). It seems difficult to diagnose with the typical imaging finding for eAML in preoperative imaging. For the adrenal eAMLs reported in this review, the mean diameter on preoperative imaging was calculated as 11.8 cm (6–20 cm). Only D'Antonio et al. (2009) defined a lesion with significant fat density on preoperative CT. In other eAML cases, the presence of an area of fat density was not reported on imaging. Surgery indications are usually made by the suspicion of adrenocortical carcinoma (D'Antonio et al., 2009; Komarowska et al., 2015; Valeshabad et al., 2019; Torres Luna et al., 2020).

In pathological classification, AMLs are evaluated within the group of perivascular epithelioid cell (PEComa) tumours. Angiomyolipomas, clear cell "sugar" tumour (CCST), pulmonary lymphangioleiomyomatosis, clear cell myomelanocytic tumour of the falciform ligament, and rare clear cell tumours of other anatomical regions are included in this group. In the WHO (World Health Organization) 2002 classification, PEComa was defined as "a mesenchymal tumour composed of histologically and immuno-histochemically distinctive perivascular epithelioid cells". In epithelioid AML, the lesion is microscopically composed of pure or dominant large epithelioid cells. These cells are characterized by large hyperchromatic nuclei with a clear or eosinophilic cytoplasm. Varying degrees of nuclear atypia may be observed. The size of the lesion, growth pattern, nuclear grade determined by microscopic examination, mitotic activity, necrosis and vascular invasion are poor prognostic indicators. In our case, only increased size of lesion existed as a poor prognostic factor. Myelocytic marker positivity in epithelioid cells is one of the characteristic features for diagnosis. Desmin and smooth muscle actin (SMA) positivity were other immunohistochemical markers indicating the presence of smooth muscle components in the tissue.

The data on prognosis and malignancy potential in eAML are controversial in the literature due to limited number of the cases. In general, an aggressive course has been reported in approximately one third of the cases. However, Aydin et al. (2009) reported no recurrence or metastasis in a large case series of 15 patients with renal eAML and an overall follow-up time of 5.1 years. Since the literature data usually consists of case reports of a single or several patients, the authors' tendency to report tumours with an aggressive course may overestimate the potential for an aggressive course (Aydin et al., 2009). Aggressive course and local recurrence were reported in 1 of 5 eAML cases reviewed in this report. However, except for our case, the postoperative follow-up period was not longer than 1 year in any of the 4 cases presented.

In conclusion, adrenal epithelioid AML is an extremely rare and potentially aggressive variant. According to the literature, open or laparoscopic adrenalectomy seems to be suitable options for disease management. There is insufficient data on arterial embolization and the use of mTOR inhibitors in case of adrenal AML.

References

Antar, A., Boyle, A., Patel, T. (2017) Angiomyolipoma of the adrenal gland: A case presentation and a review of adrenal lipomatous tumors. *Urol. Case Rep.* **12**, 59–61.

Aydin, H., Magi-Galluzzi, C., Lane, B. R., Sercia, L., Lopez, J. I., Rini, B. I., Zhou, M. (2009) Renal angiomyolipoma: Clinicopathologic study of 194 cases with emphasis on the epithelioid histology and tuberous sclerosis association. *Am. J. Surg. Pathol.* **33(2)**, 289–297.

D'Antonio, A., Caleo, A., Caleo, O., De Dominicis, G., Boscaino, A. (2009) Monotypic epithelioid angiomyolipoma of the adrenal gland: An unusual site for a rare extrarenal tumor. *Ann. Diagn. Pathol.* **13(5)**, 347–350.

Godara, R., Vashist, M. G., Singla, S. L., Garg, P., Sen, J., Mathur, S. K., Gupta, A. (2007) Adrenal angiomyolipoma: A rare entity. *Indian J. Urol.* **23(3)**, 319.

Komarowska, H., Bednarek-Rajewska, K., Kański, M., Janicka-Jedyńska, M., Gut, P., Ruchała, M. (2015) Epithelioid angiomyolipoma mimicking adrenal cortical carcinoma: A diagnostic pitfall. *Oncol. Lett.* **10(4)**, 2130–2134.

Konosu-Fukaya, S., Nakamura, Y., Fujishima, F., Kasajima, A., McNamara, K. M., Takahashi, Y., Joh, K., Saito, H., Ioritani, N., Ikeda, Y., Arai, Y., Watanabe, M., Sasano, H. (2014) Renal epithelioid angiomyolipoma with malignant features: Histological evaluation and novel immunohistochemical findings. *Pathol. Int.* **64(3)**, 133–141.

Lam, K. Y., Lo, C. Y. (2001) Adrenal lipomatous tumours: A 30 year clinicopathological experience at a single institution. *J. Clin. Pathol.* **54(9)**, 707–712.

Li, W., Pang, H., Cao, Y., Guan, L., Chen, J. (2015) High ^{18}F-fluorodeoxyglucose uptake in adrenal angiomyolipoma: Case report and review of literature. *Medicine (Baltimore)* **94(22)**, e900.

Torres Luna, N., Mosquera, J. E., Comba, I. Y., Kinaan, M., Otoya, J. (2020) A primary adrenal epithelioid angiomyolipoma (PEComa) in a patient with tuberous sclerosis complex: Report of a case and review of the literature. *Case Rep. Med.* **2020**, 5131736.

Valeshabad, A. K., Kravis, B., Bremer, W., Alsadi, A., Xie, K. L. (2019) Angiomyolipoma of the adrenal glands. *Clin. Genitourin. Cancer* **17(3)**, e553–e555.

 Prague Medical Report / Vol. 123 (2022) No. 3, p. 206–209

Instructions to Authors

Prague Medical Report is an English multidisciplinary biomedical journal published quarterly by the First Faculty of Medicine of the Charles University. Prague Medical Report (Prague Med Rep) is indexed and abstracted by Index-medicus, MEDLINE, PubMed, EuroPub, CNKI, DOAJ, EBSCO, and Scopus.

Articles issued in the journal

a) Primary scientific studies on the medical topics (not exceeding 30 pages in standardized A4 format – i.e. 30 lines and 60–65 characters per line – including tables, graphs or illustrations)
b) Short communications
c) Case reports
d) Reviews
e) Lectures or discourses of great interest
f) Information about activities of the First Faculty of Medicine and other associated medical or biological organizations

Layout of the manuscript

a) Title of the study (brief and concise, without abbreviations)
b) Information about the author(s) in the following form:
   - first name and surname of the author(s) (without scientific titles)
   - institution(s) represented by the author(s)
   - full corresponding (mailing) author's reference address (including first name, surname and scientific titles, postal code, phone/fax number and e-mail)
c) Abstract (maximum 250 words)
d) Key words (4–6 terms)
e) Running title (reduced title of the article that will appear at the footer (page break), not more than 50 typewritten characters including spaces)
f) Introduction
   - The use of abbreviations should be restricted to SI symbols and those recommended by the IUPAC-IUB. Abbreviations should be defined in brackets on first appearance in the text. Standard units of measurements and chemical symbols of elements may be used without definition.
g) Material and Methods
h) Results
i) Discussion

j) Conclusion
k) References
   - All the sources of relevant information for the study should be cited in the text (citations such as "personal communication" or "confidential data" are not accepted).
   - It is not permitted to cite any abstract in the References list.
   - References should be listed alphabetically at the end of the paper and typed double-spaced on separate pages. First and last page numbers must be given. Journal names should be abbreviated according to the Chemical Abstract Service Source Index. All co-authors should be listed in each reference (et al. cannot be used).
   - Examples of the style to be used are:
     Yokoyama, K., Gachelin, G. (1991) An Abnormal signal transduction pathway in CD4–CD8– double-negative lymph node cells of MRL *lpr/lpr* mice. *Eur. J. Immunol.* **21**, 2987–2992.
     Loyd, D., Poole, R. K., Edwards, S. W. (1992) *The Cell Division Cycle. Temporal Organization and Control of Cellular Growth and Reproduction.* Academic Press, London.
     Teich, N. (1984) Taxonomy of retroviruses. In: *RNA Tumor Viruses,* eds. Weiss, R., Teich, N., Varmus, H., Coffin, J., pp. 25–207, Cold Spring Harbor Laboratory, Cold Spring Harbor, New York.
     References in the text should be cited as follows: two authors, Smith and Brown (1984) or (Smith and Brown, 1984); three or more authors, Smith et al. (1984) or (Smith et al., 1984). Reference to papers by the same author(s) in the same year should be distinguished in the text and in the reference list by lower-case letters, e.g. 1980a, or 1980a, b.
l) tables, figures, illustrations, graphs, diagrams, photographs, etc. (incl. legends)

Technical instructions

a) Manuscripts (in UK English only) must be delivered in the electronic form via Online Manuscript Submission and Tracking system (http://www.praguemedicalreport.org/). In case of problems, contact the Prague Medical Report Office (medical.report@lf1.cuni.cz). The online submission has to include the complete version of the article in PDF format, separately the manuscript as a MS Word file and a cover letter. The detailed version of the Instructions to Authors can be found at: http://www.praguemedicalreport.org/download/instructions_to_authors.pdf.
b) Text should be written in MS WORD only. We accept only documents that have been spell-checked with UK English as a default language.
c) Please, write your text in Times New Roman script, size 12, and line spacing 1.5.
d) Text should be justified to the left, with no paragraph indent (use Enter key only); do not centre any headings or subheadings.

e) Document must be paginated-numbered beginning with the title page.
f) Tables and graphs should represent extra files, and must be paginated too.
g) Edit tables in the following way: Make a plain text, indent by Tab (arrow key) all the data belonging to a line and finish the line by Enter key. For all the notes in table, use letter x, not *.
h) Make your graphs only in black-and-white. Deliver them in electronic form in TIFF or JPG format only.
i) Deliver illustrations and pictures (in black-and-white) in TIFF or JPG format only. The coloured print is possible and paid after agreement with the Prague Medical Report Office.
j) Mark all the pictures with numbers; corresponding legend(s) should be delivered in an extra file. Mark the position of every picture (photo) in the manuscript by the corresponding number, keep the order 1, 2, 3...

Authors' Declaration

The corresponding (or first author) of the manuscript must print, fill and sign by his/her own hand the Authors Declaration and fax it (or send by post) to the Prague Medical Report Office. Manuscript without this Declaration cannot be published. The Authors' Declaration can be found by visiting our web pages: http://pmr.lf1.cuni.cz or web pages of Prague Medical Report Online Manuscript Submission and Tracking system: http://www.praguemedicalreport.org/.

Editorial procedure

Each manuscript is evaluated by the editorial board and by a standard referee (at least two expert reviews are required). After the assessment the author is informed about the result. In the case the referee requires major revision of the manuscript, it will be sent back to the author to make the changes. The final version of the manuscript undergoes language revision and together with other manuscripts, it is processed for printing.

Concurrently, proofs are electronically sent (in PDF format) to the corresponding (mailing) author. Author is to make the proofs in PDF paper copy and deliver it back to the editorial office by fax or as a scanned file by e-mail. Everything should be done in the required time. Only corrections of serious errors, grammatical mistakes and misprints can be accepted. More extensive changes of the manuscript, inscriptions or overwriting cannot be accepted and will be disregarded. Proofs that are not delivered back in time cannot be accepted.

Article processing charge

Authors do not pay any article processing charge.

Open Access Statement

This is an open access journal which means that all content is freely available without charge to the user or his/her institution. Users are allowed to read, download, copy,

distribute, print, search, or link to the full texts of the articles, or use them for any other lawful purpose, without asking prior permission from the publisher or the author. This is in accordance with the BOAI definition of open access.

Copyright Statement
The journal applies the Creative Commons Attribution 4.0 International License to articles and other works we publish. If you submit your paper for publication by Prague Medical Report, you agree to have the CC BY license applied to your work. The journal allows the author(s) to hold the copyright without restrictions.

Editorial Office
Prague Medical Report
Kateřinská 32, 121 08 Prague 2, Czech Republic
e-mail: medical.report@lf1.cuni.cz
Phone: +420 224 964 570. Fax: +420 224 964 574

Prague Medical REPORT

(Sborník lékařský)

Published by the First Faculty of Medicine, Charles University, Karolinum Press,
Ovocný trh 560/5, 116 36 Praha 1 – Staré Město, Czech Republic, www.karolinum.cz

Editorial Office: Prague Medical Report, Kateřinská 32, 121 08 Prague 2, Czech Republic,
Phone: +420 224 964 570, Fax: +420 224 964 574,
e-mail: medical.report@lf1.cuni.cz
Editor in Chief: Kateřina Jandová, MD., PhD.
Foreign Language Editor: Prof. Jaroslav Pokorný, MD., DSc.
Executive Editor: Mgr. Lucie Šulcová
Editorial Board: Prof. Jan Betka, MD., DSc.; Zdeněk Kostrouch, MD., PhD.;
Prof. Emanuel Nečas, MD., DSc.; Prof. Karel Smetana, MD., DSc.;
Prof. Karel Šonka, MD., DSc.; Assoc. Prof. Jan Tošovský, MD., PhD.;
Prof. Jiří Zeman, MD., DSc.

Published as quarterly journal. Typeset and printed by Karolinum Press.
Annual subscription (4 issues) EUR 60,–. Single copy EUR 20,–.
Distribution: Karolinum Press, Ovocný trh 560/5,
116 36 Praha 1, Czech Republic, e-mail: journals@karolinum.cz

ISSN 1214-6994 (Print)
ISSN 2336-2936 (Online)

Reg. No. MK ČR E 796